Nuclear Heat Transfer and Passive Cooling

Volume 5: **Liquid Metal Thermal Hydraulics**

FRAZER-NASH CONSULTANCY

Introduction to the Technical Volumes and Case Studies

Convection, Radiation and Conjugate Heat Transfer

Natural Convection and Passive Cooling

Confidence and Uncertainty

Liquid Metal Thermal Hydraulics

Molten Salt Thermal Hydraulics

Liquid Metal CFD Modelling of the TALL-3D Test Facility

Fuel Assembly CFD and UQ for a Molten Salt Reactor

Reactor Scale CFD for Decay Heat Removal in a Lead-cooled Fast Reactor

System Code and CFD Analysis for a Light Water Small Modular Reactor

Authors:	Carolyn Howlett	Frazer-Nash Consultancy
	Richard Underhill	Frazer-Nash Consultancy
Contributors:	Graham Macpherson	Frazer-Nash Consultancy
	Hector Iacovides	The University of Manchester
	Janne Wallenius	LeadCold
	Milorad Dzodzo	Westinghouse Electric Company
	Paolo Ferroni	Westinghouse Electric Company
	Shuisheng He	The University of Sheffield
	Steve Graham	National Nuclear Laboratory
Technical Volumes Lead:	Tim Houghton	Frazer-Nash Consultancy
Approver:	Graham Macpherson	Frazer-Nash Consultancy

Document Number: FNC 60148/49312R

Issue and Date: Issue 1, December 2021

Legal Statement

Preface

Nuclear thermal hydraulics is the application of thermofluid mechanics within the nuclear industry. Thermal hydraulic analysis is an important tool in addressing the global challenge to reduce the cost of advanced nuclear technologies. An improved predictive capability and understanding supports the development, optimisation and safety substantiation of nuclear power plants.

This document is part of *Nuclear Heat Transfer and Passive Cooling: Technical Volumes and Case Studies*, a set of six technical volumes and four case studies providing information and guidance on aspects of nuclear thermal hydraulic analysis. This document set has been delivered by Frazer-Nash Consultancy, with support from a number of academic and industrial partners, as part of the UK Government *Nuclear Innovation Programme: Advanced Reactor Design*, funded by the Department for Business, Energy and Industrial Strategy (BEIS).

Each technical volume outlines the technical challenges, latest analysis methods and future direction for a specific area of nuclear thermal hydraulics. The case studies illustrate the use of a subset of these methods in representative nuclear industry examples. The document set is designed for technical users with some prior knowledge of thermofluid mechanics, who wish to know more about nuclear thermal hydraulics.

The work promotes a consistent methodology for thermal hydraulic analysis of single-phase heat transfer and passive cooling, to inform the link between academic research and end-user needs, and to provide a high-quality, peer-reviewed document set suitable for use across the nuclear industry.

The document set is not intended to be exhaustive or provide a set of standard engineering ‘guidelines’ and it is strongly recommended that nuclear thermal hydraulic analyses are undertaken by Suitably Qualified and Experienced Personnel.

The first edition of this document set has been authored by Frazer-Nash Consultancy, with the support of the individuals and organisations noted in each. Please acknowledge these documents in any work where they are used:

> Frazer-Nash Consultancy (2021) Nuclear Heat Transfer and Passive Cooling,
> Volume 5: Liquid Metal Thermal Hydraulics.

Contents

1 Introduction

This technical volume considers the fluid flow and heat transfer within Liquid Metal-cooled Fast Reactors (LMFRs). This is primarily of relevance to the design of next generation reactors employing sodium, lead or Lead-Bismuth Eutectic (LBE) as a primary circuit fluid.

The primary motivation is to inform the use of thermal hydraulic modelling in a liquid metal reactor context with an understanding of how this differs from the modelling of other coolants employed in fission reactors. Therefore, it is recommended that Volume 2 (Convection, Radiation and Conjugate Heat Transfer) and Volume 3 (Natural Convection and Passive Cooling) are read before reading this volume, because it builds on and emphasises areas of contrast with the descriptions of phenomena and methods applied in more conventional fluids.

LMFRs are less familiar to nuclear engineers than Light Water Reactors (LWRs) and (in the UK) Advanced Gas-cooled Reactors (AGRs), so this section provides introduction and context for considerations relevant to their thermal hydraulic modelling:

- An introduction to the use of liquid metal as a reactor coolant.
- A brief description of the history of LMFRs from a UK perspective.
- An overview of the main features of the design of a typical LMFR.
- Some specific examples of modern LMFR designs.

1.1 The Use of Liquid Metal as a Coolant in Nuclear Reactors

The use of liquid metals as coolants in nuclear reactors dates back to the early experimental reactors of the 1940s and 1950s. The low neutron absorption and moderation of liquid metals makes them suited for fast spectrum reactors, which is the intention for liquid metal reactor designs that are currently being pursued by several developers worldwide.

As well as generating electricity, fast spectrum reactors have the capability to play an important role in enhancing the sustainability of the nuclear fuel cycle, whose importance is anticipated to further increase should the installed nuclear capacity increase globally. Depending on the core and fuel cycle design adopted, they can enable a more efficient use of the world's finite uranium resources by converting commonly found (fertile) isotopes into the fissile isotopes needed for a sustained neutron chain reaction. They are also potentially capable of producing far less nuclear waste per unit of electricity generation and can be configured to convert the long lived radioactive isotopes in LWR waste into more benign products with much shorter half-lives (transmutation)[1].

[1] Realising the full potential of fast reactors requires suitable fuel reprocessing infrastructure and a closed fuel cycle. As these may be longer-term goals for countries interested in the deployment of LMFRs, in the meantime these reactors can operate in a once-through fuel cycle similar to traditional Nuclear Power Plants (NPPs).

In addition to its neutronic properties, a liquid metal coolant is also appealing for a number of thermal hydraulic reasons, for example:

- The high thermal conductivity of metal coolants enables heat to be transferred from the surface of the fuel to the coolant and from the coolant to heat exchangers very effectively. It also enables transport of heat within the coolant, even under very low flow conditions, reducing the potential for local high temperatures.
- The high thermal mass[2] typically associated with LMFR primary coolants increases the time available for operator action in the event of fault.
- The high boiling point of liquid metals enables the reactors to be operated at high temperatures (compared with water), resulting in a high thermal efficiency for electricity generation and the potential to provide heat for industrial processes (such as chemical processes or hydrogen generation). These high operating temperatures are possible without the need to pressurise the reactor's primary system, thereby providing opportunities for reduction in capital cost of certain components and, by reducing the risk of a loss of coolant accident, improve safety.

However, the use of a liquid metal is not without its challenges, such as:

- Inspection of reactor components is more challenging in a visually opaque coolant.
- The chemical reactivity of some liquid metals (specifically alkali metals such as sodium) when exposed to water or air can lead to fire and/or hydrogen generation with consequent explosion risks.
- The high operating temperatures required and the corrosive properties of lead (and LBE) can result in a high rate of damage to traditional structural materials such as conventional steels.
- The fast neutron spectrum increases irradiation damage to core structures, thereby requiring the use of irradiation-resistant materials.
- The large differences in thermophysical properties of liquid metals compared with more conventional fluids, and lack of detailed experimental databases of material properties, requires special consideration in the use of thermal hydraulic analysis tools.

1.2 History of Liquid Metal Cooled Reactors

Although the earliest liquid metal reactor was mercury cooled[3], subsequent reactor development has been focused on the use of either sodium (especially, including sodium-potassium eutectic; NaK) or lead (including lead-bismuth eutectic). Of these coolants, sodium was historically chosen for civil nuclear applications and the first electricity generating NPP in the world was the sodium-cooled Experimental Breeder Reactor I (EBR-I) in the United States in 1951. Fast breeder reactor programmes were also initiated in the UK, France, Italy, Germany and the (former) Soviet Union throughout the 1950s and 1960s and in Japan in the 1970s. These programmes included the development of a number of experimental and demonstration reactors (Figure 1.1) which are the

[2] Thermal mass (or heat capacity) refers to the product of mass and specific heat capacity of a body (mc_p) and is a measure of its ability to absorb energy.

[3] The Los Alamos 'Clementine' reactor achieved criticality in 1946.

source of much of the world's current knowledge and experience with liquid metal cooled reactors (IAEA, 2008).

In the UK the fast reactor programme was initiated after World War II. The Dounreay Fast Reactor (DFR) was a 60 MWth, sodium-potassium eutectic cooled, experimental reactor which achieved criticality in 1959. This was then succeeded by the more powerful, sodium-cooled, Prototype Fast Reactor (PFR) and work was undertaken to design a Commercial Fast Reactor (CFR) as the next stage. However, in the late 1970s fast reactors fell out of political favour in the UK and plans for the CFR were halted. In 1981, an improved design for a new UK Commercial Demonstration Fast Reactor (CDFR) was presented and formed the starting point for the UK to collaborate with Europe (France and Germany in particular) on fast reactor development.

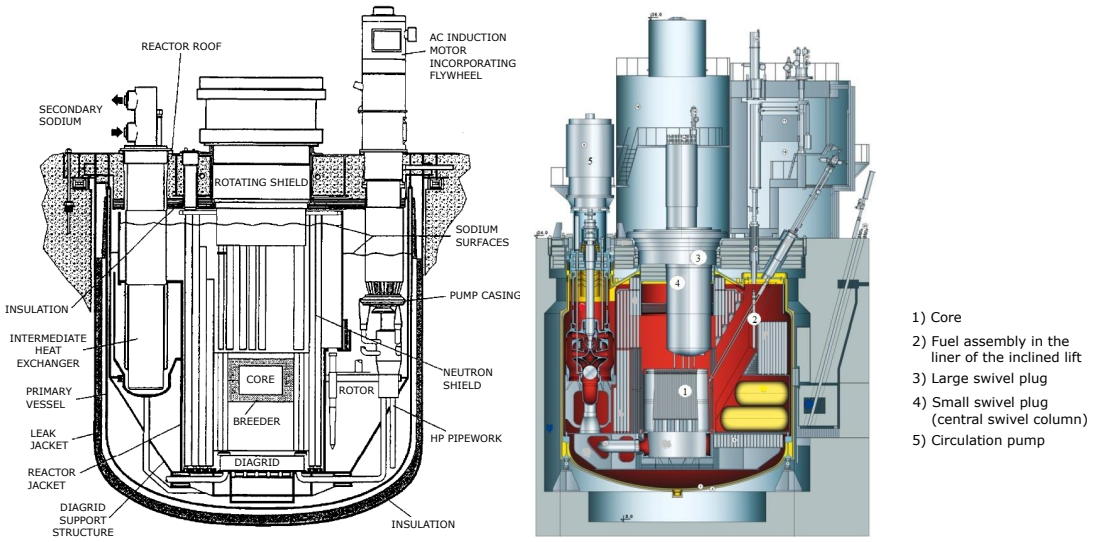

a: PFR, Dounreay, UK (IAEA, 2013c)

b: BN-600 reactor, Russia (Tashlykov *et al.*, 2021)

Figure 1.1: Cross-sectional diagrams of two historic LMFRs.

Throughout Europe, the United States, the (former) Soviet Union and Japan the development of LMFRs progressed in parallel with UK efforts. Notable reactors that came into operation prior to 1980 include: the Rapsodie and Phénix reactors in France; the BOR-60 and BN-350 reactors in the former Soviet Union[4]; the EBR-I, EBR-II and Fast Flux Test Facility (FFTF) in the United States; the KNK-II reactor in Germany; and the Joyo reactor in Japan. A more comprehensive list and a summary of reactor operation is given in IAEA, 2013c.

After 1981, the UK entered into talks with Europe with a view to engaging in a European Fast Reactor (EFR) project and independent work on this technology in the UK was largely stopped. However, it was not until 1989 that agreements were reached that allowed a truly collaborative project to begin. Meanwhile (and relevant to the collaboration), the Superphénix (SPX) reactor started operating in France in 1986. Independently, Russia's BN-600 reactor began operation in 1980, India's Fast Breeder Test Reactor (FBTR) achieved criticality in 1985 and the Monju reactor began construction in Japan in 1986. In the USA, the Clinch River Breeder Reactor project was cancelled in 1983, although work continued on the Integral Fast Reactor (IFR) design.

[4] The BN-350 reactor was operated to generate electricity and desalinate water for over 25 years in what is now Kazakhstan.

In addition to the loss of life and the health and environmental impacts, the accident at Chernobyl in April 1986 had a significant negative impact on the public perception of nuclear power. Although the RBMK-1000 reactor involved in the incident was water-cooled and substantially different from any LWR (and LMFR) in design, governments world-wide were under pressure to reduce investment in, and dependence on, nuclear power in general.

The EFR project was phased out in the early 1990s, as the UK and German governments withdrew funding. In the UK the PFR was finally shut down in 1994. In France, fast reactor technology continued to receive government support with a reduced budget. Superphénix was operated (intermittently) until 1996 and Phénix until 2010.

Marth (1993) provides a more detailed description of fast reactor development within Europe up to 1993, including both a high level technical description of key reactors and projects and the history of the collaboration between vendors, utilities and research organisations. It also documents the political decisions and their impact on reactor development activities.

The majority of the reactors mentioned above have now been permanently shut down and several of the countries (notably the UK, US and Germany) that had led the way in early LMFR development stopped, or greatly reduced, their fast reactor programmes in the 1990s, at the prototype stage or before. In Asia (China, India, Korea and Japan) and in Russia, fast reactor development activities continued, although the Fukushima-Daiichi incident in 2011 caused further political unease, especially in Japan.

Russia has the only 'commercial' LMFRs currently in operation for the purpose of electricity generation, with the sodium-cooled BN-600 having provided electricity since the 1980s and the BN-800 since 2016. A number of potentially useful publications relating to work carried out in support of the Russian fast reactor programme are only available in Russian (making them less accessible for UK engineers). However, IAEA (2008) and IAEA (2013c) contain descriptions of, and operational experience with, many historic LMFRs and includes the BN-350 and BN-600 reactors.

A large part of the original historic motivation behind developing LMFRs (and fast spectrum reactors in general) was related to plutonium production. However, in the context of the fight against climate change and growing world energy demands, LMFRs have again gained support over the past decade and new designs are underway in Europe, North America and Asia (led by potential vendors as well as national organisations). The higher potential operating temperatures of LMFRs compared with LWRs results in heat that can be used in industrial processes. Promoters of this technology also consider that the ability of the reactor designs to be simple, low pressure and passively safe and potentially to produce less nuclear waste (compared with LWRs), could be key to gaining public support for nuclear power.

The Generation IV International Forum (GIF), which was established in 2001, currently forms a framework for international research and development in the next generation of NPPs, with a number of demonstration and prototype reactors under development. Although the UK was a founder member, its participation in LMFR activities has been limited. However, the UK recently signed the GIF framework agreement and became a full member in 2018 with Sodium-cooled Fast Reactors (SFRs) named as one of the key systems for initial UK participation.

From a nuclear engineering perspective, the work undertaken on previous LMFRs programmes is

very relevant. Considerable advances in inspection, instrumentation and reactor repair were made during the operational life of the reactors. In many cases, decommissioning has enabled detailed inspection of components and increased knowledge of the performance of materials in a liquid metal environment. From a thermal hydraulics perspective, extensive plant instrumentation and end of life reactor tests investigating aspects such as sodium boiling and passive cooling provide vital data for future designs.

It should be noted that all of the prototype civil reactors built and operated anywhere in the world have used sodium (or NaK) as a coolant. Research and development efforts on heavy liquid metal cooled reactors has historically been more limited than for sodium-cooled reactors. However, the development of LBE-cooled reactors for the purposes of submarine propulsion started in the 1950s in the former Soviet Union, resulting in approximately 70 years of reactor operating experience.

Some operational experience with LBE from the Russian Federation is published in IAEA, 2008 and a useful summary, including the learning captured from a number of accidents, is discussed by Zrodnikov *et al.* (2000). However, information regarding this experience is more limited due to its military application. Leveraging this operating experience, but now using pure lead instead of LBE, Russia has continued development of Lead-cooled Fast Reactor (LFR) technology and in 2021 started construction of the 300 MWe BREST-OD-300 LFR, whose completion is expected by 2026. Moreover, currently there are a number of lead- and LBE-cooled commercial and national prototype designs in progress, supported by the development of a large number of test facilities worldwide. However, it is inevitable that the experience with these coolants lags behind sodium.

1.3 Design Features of Liquid Metal Cooled Reactors

Since the earliest designs, most LMFR reactor designs have followed one of two concepts; pool type and loop type. In simple terms, pool type reactors are those where all of the main primary system components, including the core, pumps and heat exchangers are located inside the main reactor vessel, immersed in a single ‘pool’ of coolant. In loop type designs, the core of the reactor is located in a similar smaller pool, but the pumps and heat exchangers are located outside of the main reactor vessel and connected to it via pipework. A simple illustration of the differences between pool and loop type designs is shown in Figure 1.2.

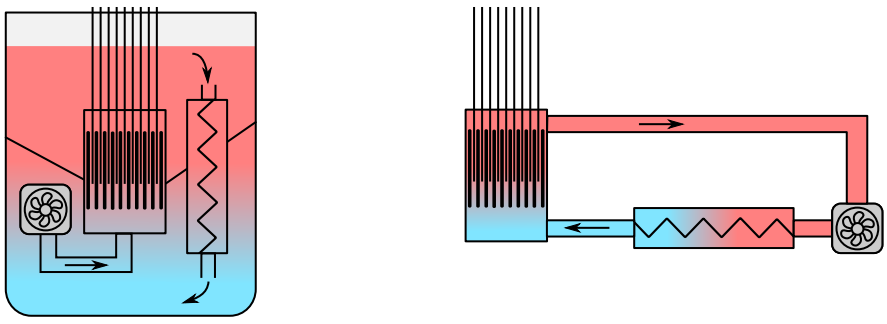

(a) Pool type (b) Loop type

Figure 1.2: Concept of (a) Pool type and (b) Loop type reactor designs.

There are advantages and disadvantages associated with both concepts. The loop type design requires a smaller reactor vessel and the pumps and heat exchangers are, in principle, easier

to access for maintenance. Experience has also shown that loop type designs are cheaper and quicker to construct than pool type designs (IAEA, 2008). However, the pipework connections increase the risk of a primary circuit breach and therefore introduce additional safety challenges. Pool type designs eliminate this problem but require a larger vessel and careful thought to be given to the removal of major components from the pool for inspection and repair. In turn, this larger vessel is generally accompanied by a larger coolant inventory and thus thermal mass, which is favourable during fault transients.

In general, the loop type design has been favoured for smaller, experimental reactors. However, with the increasing importance of demonstrating safety, and the technical challenges of designing large, loop type reactors (i.e. relating to large diameter piping required and the need to accommodate large, heavy valves), a pool type concept has been chosen for almost all commercial designs currently under development. This document therefore focuses primarily on the thermal hydraulics of pool type designs (although many aspects will be common to both).

The shape and layout varies between specific reactor designs, however, the operational concept and most major components are similar. The coolant flow path is usually up through the core into the 'upper plenum' (or upper pool) before passing through the heat exchangers into a cool, 'lower plenum' (or lower pool). An important part of a pool type reactor design is the presence of an internal vessel or core barrel, which separates the hot and cold liquid metal plena to ensure uniform flow through the core and around the primary circuit.

Movement of the primary circuit fluid is achieved by pumps (either mechanical or electromagnetic pumps can be used). The location of the pumps varies with reactor design, but they are generally located in the cold plenum, to minimise the operating temperatures. Figure 1.3 illustrates an indicative LMFR reactor layout to aid understanding of the basic primary circuit flow path and function of the major components.

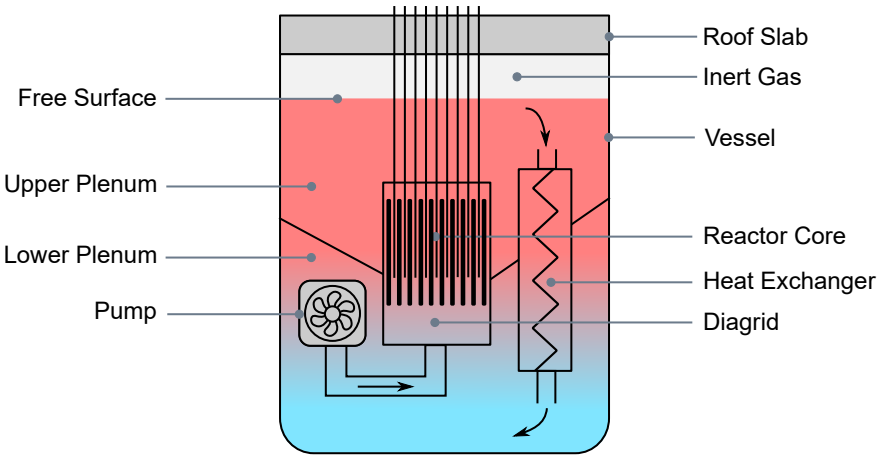

Figure 1.3: Simplified diagram of a pool type reactor design.

Heat transfer between the primary coolant and the secondary (power) circuit is by immersed heat exchangers located between the hot and cold plena. Sodium-cooled designs generally include an intermediate loop separating the primary system coolant from the power conversion system, as the immersion of a water filled component in the sodium pool would not be acceptable from a safety perspective. However, in reactors containing lead or LBE, because of the lack of exothermic reac-

tion between these coolants and power conversion fluids, it is possible to locate steam generators within the pool.

In addition to electrical power and process heat generation, an LMFR may be configured to act as a 'burner' of transuranic waste (TRU) or plutonium or as a breeder of fissile elements. The fuel may be either ceramic (most often oxide, but carbide and nitride have been used) or metallic and the specific fuel used varies between designs (in some cases concepts envisage the use of different fuel at different stages in the design evolution). The role that a reactor plays in the nuclear fuel cycle changes its core design, performance and a number of safety considerations. However, there are a number of more general aspects of the core and fuel assembly design that can be considered from a thermal hydraulic perspective.

For the same power output, the core of an LMFR can be quite compact compared with an LWR, especially if a sodium coolant is employed. The fuel pins in an SFR are often arranged in a tight triangular (also called hexagonal) lattice within the fuel assemblies to enable a high ratio of fuel area to flow area (important for certain fast reactor performance indicators), whilst maintaining sufficient gaps between adjacent pins.

The fuel pins are held in position and prevented from touching each other by either spacer grids or, in tighter lattices, by spacer wires wrapped helically around each pin (as shown in Figure 1.4). Each fuel assembly is generally encased within a duct or 'wrapper' providing structural support to the assembly and preventing transverse flow between fuel assemblies. The small spaces between each assembly are open for coolant flow (the 'inter-wrapper' flow).

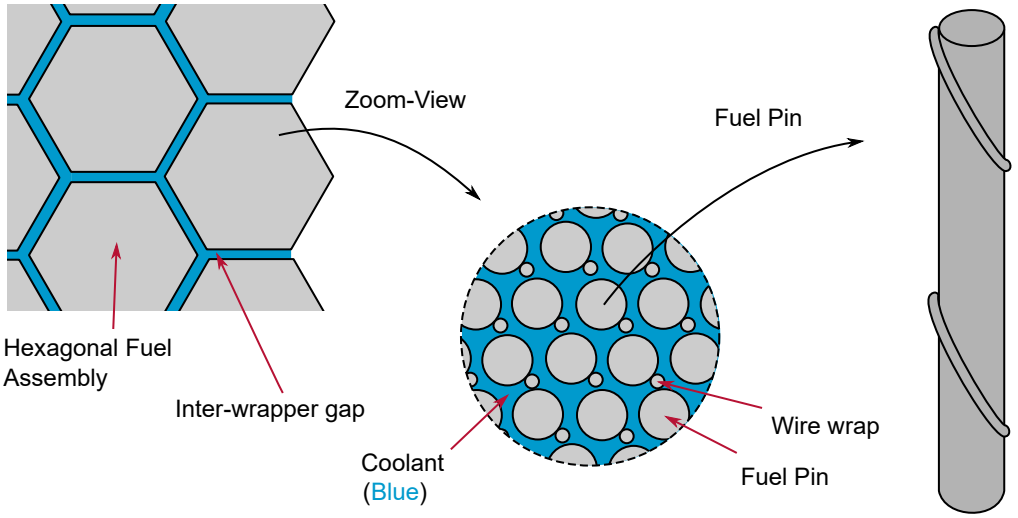

Figure 1.4: Typical SFR Fuel Layout.

Although a tight hexagonal lattice arrangement is most common for the fuel in SFRs, some LFR core designs take advantage of the very low neutron absorption of lead (even lower than sodium) to adopt a more open lattice. By doing so, the core flow velocity and pressure drop is reduced without appreciably affecting the neutron spectrum or neutron economy, thus reducing erosion/corrosion and favouring natural circulation[5].

[5] Lower flow velocities are an advantage with regard to reducing damage by erosion (and erosion/corrosion) mechanisms. Low pressure drops help to promote natural circulation in the event of a loss of forced flow.

As with other reactor designs, channels within the core are also allocated to control rods and instrumentation. Shielding is included at the top of the active core and around the outside. If a reactor design aims at increasing breeding[6], then 'blanket' regions of fertile material are included around and, usually, within the core (the location of breeding blankets varies with core design). These are often made up of blanket assemblies of similar design to the fuel assemblies such that the flow paths are broadly the same.

Other components located within the pools vary with the design and include above core structures to support refuelling, control rods (if inserted from above) and instrumentation. A structure is usually located below the core and may include provision for 'catching' molten fuel or displaced structural components in the event of a severe accident (although in lead or LBE many components will float). Separate 'decay heat removal' heat exchangers, also known as dip-coolers, are sometimes included within the reactor vessel to cool the primary circuit under conditions where the primary circuit pumps and primary heat exchangers are not operating. In some other designs, this function is performed by a Reactor Vessel Auxiliary Cooling System (RVACS), which transfers heat through the reactor vessel walls to external heat sink(s).

For all 'pool type' LMFRs, it is necessary to cover the surface of the pool with an inert gas (e.g. argon) which allows for the pool to thermally expand and prevents the coolant from oxidising in contact with air.

The vessel itself is usually sealed at the top with a roof slab. All vessel penetrations (for the secondary or intermediate circuit, refuelling equipment, the pump, coolant purification, decay heat removal etc.) generally pass through this roof slab. The vessel is then surrounded by additional safety structures such as a guard vessel, concrete shielding and protective structures.

As with all NPPs, there is a significant amount of ancillary equipment located outside of the reactor vessel. However, as much of this is design specific, detailed information cannot be included here.

Due to the degree of variation in LMFR design, the description given in this section is generic. IAEA (2013c) contains descriptions and images of both historic and current LMFR designs, illustrating this variation and a number of different of design innovations. Some examples of modern reactor designs currently being progressed are included in Section 1.4.

1.4 Modern Liquid Metal Cooled Reactors

In the past, LMFRs have primarily been developed as part of national research and demonstration programmes, but more recently these designs are now being developed by commercial organisations. These advanced reactor designs aim to offer the potential for safe, cheap electricity generation with the opportunity for industrial heat and hydrogen production. A full list of LMFRs under development is detailed in the International Atomic Energy Agency (IAEA) Advanced Reactor Information System (ARIS) database[7]. However, a few examples are briefly described below to highlight the variety and ingenuity of next generation LMFRs. Further information on all of these designs is available from the organisations involved in their development.

[6] Breeding in this context is the process of producing additional fissile material from fertile material for use in future fuel.
[7] aris.iaea.org

1.4.1 Natrium

The Natrium™ 345 MWe sodium-cooled reactor is being co-developed by TerraPower and GE Hitachi Nuclear Energy and builds on both GE Hitachi's PRISM reactor and TerraPower's Travelling Wave Reactor (TWR)[8]. TerraPower was awarded $80m in 2020 under the US Department of Energy's Advanced Reactor Demonstration Program (ARDP) to contribute to building a reactor that can be operational within the next five to seven years. The Natrium reactor project will therefore bring together public and private investment to develop a commercial SFR.

Notably, the Natrium design includes an integrated molten salt thermal energy storage system that supports load following, energy storage and industrial process heat applications. This feature makes it particularly suitable to complement other forms of power generation, such as renewables. Like many modern LMFRs, the system incorporates a compact, pool type reactor system at atmospheric pressure with passive vessel cooling to reduce the size and cost of the nuclear island.

1.4.2 MYRRHA

The Multipurpose hYbrid Research Reactor for High-tech Applications (MYRRHA) 100 MWth fast reactor is being developed by SCK CEN with €588m committed in 2018 by the Belgian Federal Government and commissioning scheduled for 2036[9]. This 16 m high and 10 m wide double-walled pool type reactor is cooled by LBE with a water filled secondary system and air-cooled tertiary system (Figure 1.5). The cooling systems use forced circulation during normal operation but, as for other LMFRs, have been designed to remove the decay heat using natural circulation under loss of power scenarios.

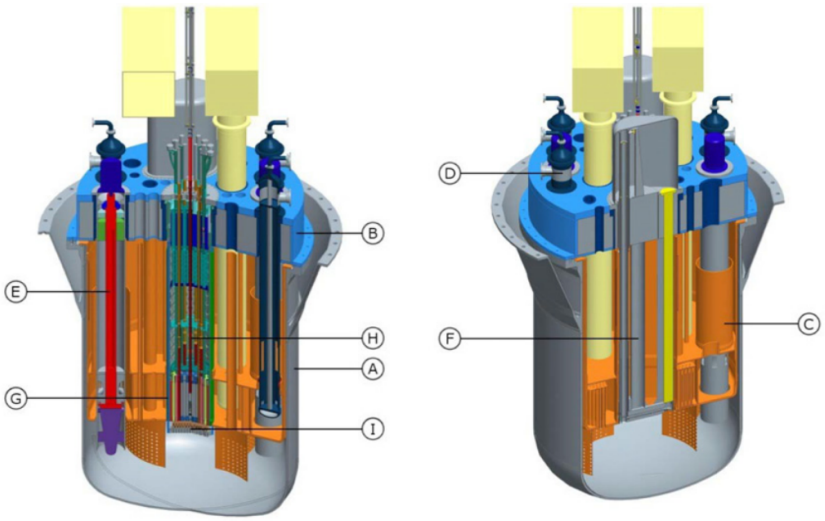

Figure 1.5: Section of the MYRRHA reactor (De Bruyn *et al.*, 2015).

[8] natriumpower.com
[9] www.myrrha.be

The MYRRHA reactor is intended to be the world's first large scale accelerator driven reactor system[10]. This means that the core has a sub-critical design and does not contain enough fissile material to maintain the chain reaction on its own. This multipurpose research reactor will be used to support research into nuclear medicine, nuclear waste treatment, fundamental physics and fusion technology.

1.4.3 Westinghouse LFR

The Westinghouse LFR (Figure 1.6) is a 450 MWe lead-cooled reactor that operates at high temperatures (up to 650 °C) in a pool type configuration with an air-cooled supercritical water (replacing an older design which adopted supercritical CO_2) power conversion system and a thermal energy storage system[11]. The reactor's primary missions are competitive flexible electricity, achieved through plant simplification and high thermodynamic efficiencies, and market versatility through high-temperature heat.

The compact, atmospheric pressure design includes a passive heat removal system that, under fault conditions, transfers heat from the reactor vessel to a pool of water surrounding the guard vessel which, once depleted, allows transition to natural circulation of air. The natural circulation in the primary circuit and heat loss through the vessel has been analysed in Study C: Reactor Scale CFD for Decay Heat Removal in a Lead-cooled Fast Reactor. Westinghouse was awarded £10m in 2020 under the UK Government's Advanced Modular Reactor (AMR) Feasibility and Development project Phase 2 to undertake development activities.

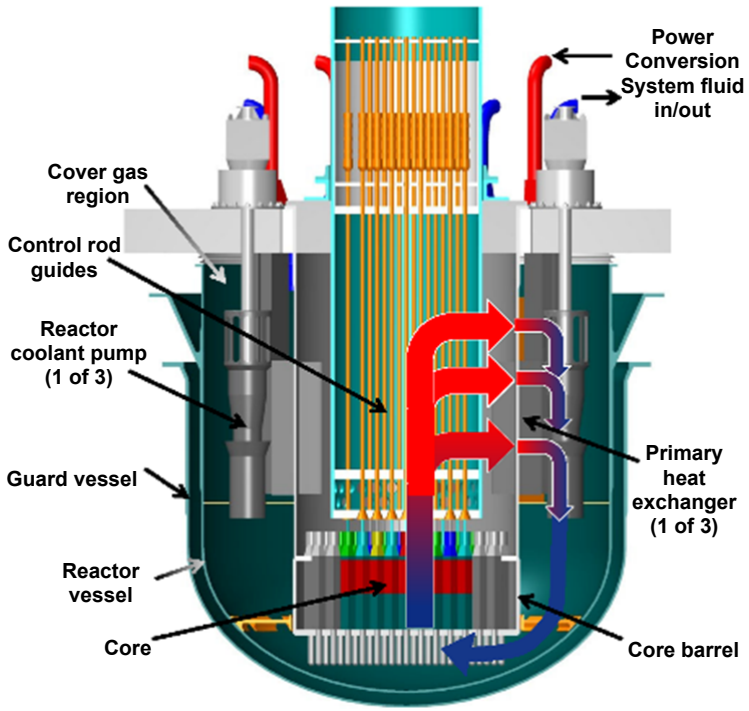

Figure 1.6: Cross-section of the Westinghouse LFR.

[10] High energy protons are provided to a spallation target, which in turn creates primary neutrons to feed the core.
[11] www.westinghousenuclear.com/new-plants/lead-cooled-fast-reactor

1.4.4 SEALER

The Swedish Advanced Lead Reactor (SEALER) is being developed by LeadCold[12] with 10 MWe and 55 MWe (Figure 1.7) versions for off-grid (arctic) and on-grid applications respectively. Power generation is via steam turbines and the off-grid design is small enough to be transported to the site by ship, ice-road or aircraft. The design includes a single use reactor core to minimise the cost of fuel management.

In common with other modern lead-cooled reactors, protective oxide films on the surfaces of structural materials are intended to reduce corrosion. During loss of power, decay heat is removed using either activated dip-coolers or air cooling on the outside of the reactor guard vessel. The passive heat removal system is driven by natural circulation in the primary circuit as the coolant temperature increases.

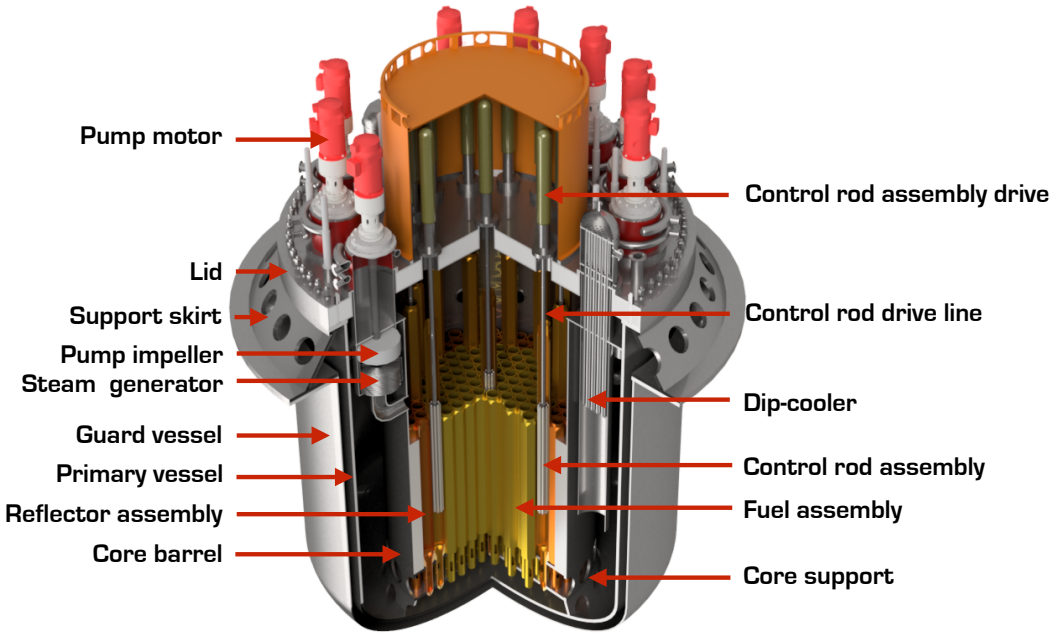

Figure 1.7: Cross-section of the primary system of SEALER on-grid design.

[12] www.leadcold.com

2 Technical Context

From a thermal hydraulic perspective, the differences in the challenges within a liquid metal cooled reactor, when compared with other reactor technologies, stem from two sources: the material properties of the fluid, and the design of the reactor.

The thermophysical properties of the liquid metals deployed in next generation reactors differ from each other but, from the perspective of reactor thermal hydraulics, there are significant similarities in their behaviour. Section 2.1 discusses the fluid material properties and their implications for reactor thermal hydraulics generally and turbulent heat transfer specifically.

As discussed in Section 1, most of the LMFRs under development in recent times use a 'pool type' layout. Due to this similarity in design, it is useful to consider the relevant thermal hydraulic phenomena in the context of the regions of the reactor where they are most important. Section 2.2 describes some important differences compared to the thermal hydraulic phenomena described by Volumes 2 and 3. Section 2.3 discusses more design specific thermal hydraulic challenges and associated phenomena in the context of three regions of interest within the reactor:

- The fuel assemblies and reactor core.
- The region above the core.
- The reactor plena.

The purpose of this volume is to provide information regarding the modelling of liquid metals in the context of an overarching objective to guide the analysis of single-phase convective flow and heat transfer. However, these are not the only thermal hydraulic topics of relevance to the development of a LMFR. For completeness, Section 2.3.4 briefly describes other topics and cites a number of references for those wishing to learn more.

2.1 Material Properties

Table 2.1 shows representative thermophysical material properties for a number of liquid metals at relevant temperatures. In addition, water, helium, carbon dioxide (used in current UK AGR reactors) and FLiBe (a molten salt) properties at representative temperatures and pressures are also included for comparison. The references given at the end of this section included more accurate properties, information such as temperature and pressure dependencies and additional properties such as surface tension, latent heat, vapour pressure and coefficient of thermal expansion.

As could be anticipated, the variation in some properties between the different materials in Table 2.1 is several orders of magnitude. Of particular relevance to the thermal hydraulics of nuclear reactors is the high thermal conductivity of liquid metals, with sodium being the highest. This gives

	T °C	P MPa	k W/m K	ρ kg/m^3	c_p J/kg K	μ mPa s	Pr	ρc_p kJ/m^3 K
Lead	450	0.1	17.15	10516	145.9	2.00	0.017	1534
Sodium	450	0.1	69.21	844.1	1272	0.254	0.0047	1074
LBE	450	0.1	13.77	10130	142.0	1.40	0.014	1438
Water	300	15.5	0.564	726.5	5458	0.0885	0.86	3965
Carbon Dioxide	500	4.0	0.055	27.3	1174	0.0344	0.73	32
Helium	550	6.0	0.318	3.48	5190	0.0403	0.66	18
FLiBe	650	0.1	1.1	1963	2386	6.78	14.7	4683

Table 2.1: Thermophysical material properties of reactor coolants at representative temperatures and pressures: thermal conductivity (k), density (ρ), specific heat capacity (c_p), dynamic viscosity (μ), Prandtl number (Pr) and volumetric specific heat capacity ρc_p.
Data sources: Pb and LBE (NSC, 2015); Na (Sobolev, 2011); FLiBe (Romatoski and Hu, 2017); Water (IAPWS, Wagner *et al.*, 2000); CO_2 and He (NIST Chemistry WebBook, webbook.nist.gov).

liquid metals the ability to transfer heat effectively under low flow conditions and leads to high surface-to-fluid Heat Transfer Coefficients (HTCs) and compact design.

Lead and LBE have a higher density and a lower specific heat capacity than sodium. However, the similar magnitude of these differences results in all three metals having a volumetric specific heat capacity (ρc_p) of a similar magnitude (with sodium being a little lower) and therefore a similar ability to transport heat via the movement of the fluid within a given size of vessel fluid. However, it is noted that all these metals have a lower volumetric heat capacity than water and molten salt at representative reactor pressures and temperatures. The higher density and lower specific heat capacity of heavy liquid metals would result in a higher pressure drop over the core (and therefore a greater demand on reactor pumps) compared with sodium, if other aspects of the design were the same. To reduce this pressure drop, a larger, more open core design and lower flow velocities are often used for LFRs than SFRs.

The higher density of the heavy liquid metals is also of note regarding the potential for higher mechanical loads to be experienced by structural components, including the reactor vessel, and a higher potential for the erosion of reactor components subject to high shear stresses with the coolant, particularly the reactor coolant pumps. In practice this results in the need for structurally stronger internal components and places a limitation on the size of heavy liquid metal cooled reactors due to the need to accommodate seismic events. Additionally, the high density causes most other materials (including steel and oxide reactor fuel) to float if not held in place (Roelofs, 2019 and Waltar *et al.*, 2012).

The melting and boiling points of all of the proposed liquid metal coolants are above those of water. Due to the high boiling point of liquid metals, LMFRs can be designed to operate at atmospheric pressure without boiling. The boiling temperature of sodium at atmospheric pressure is 883 °C. For lead and LBE the boiling temperatures are 1748 °C and 1654 °C respectively. In the case of lead or LBE, the boiling point is at such a high temperature that boiling of the coolant is considered extremely unlikely (melting of the structural steel would be likely to happen at a lower temperature). For sodium, boiling is a credible scenario, and needs to be considered in the context of some faults.

The reactors must operate above the melting point of the liquid metal coolant and the working fluid

must be heated to a liquid at start up. The melting temperature of sodium and LBE at atmospheric pressure are 98 °C and 125 °C respectively and the melting temperature of lead is 327 °C. The design implications of the melting point are particularly significant in the case of lead, meaning that activities such as inspection and refuelling need to be carried out at temperatures of around 370 °C to 400 °C, to provide sufficient margin above the freezing point. For sodium and LBE a value of closer to 200 °C is likely to be adequate.

All liquid metals are opaque to visible (infrared or ultraviolet) wavelength light. This makes visual inspection of the reactor impossible once the primary circuit is filled and other techniques (for example ultrasonic inspection) need to be used.

The chemical properties of a reactor coolant (although not the focus of this document) are also important for the design and a number of aspects of importance are mentioned briefly in Section 2.3.4. The control of impurities in liquid metal coolants and the implications for the design are discussed in more detail in IAEA (2002) and IAEA (2012).

There are a number of sources of data for the thermophysical material properties of liquid metals. However, there is a smaller body of data available than for more conventional engineering fluids, with less independent duplication of experiments. Users should, therefore, be cautious regarding the level of confidence they place in published data. Even data that appears to be from a number of sources, may all be based on the same single set of experimental measurements. If a high level of accuracy or confidence is needed, it is worth investigating the data source in detail and determining if any recent work has been carried out to corroborate the values of high importance.

The following references are presented as examples of well respected and commonly used sources of material property data. More detailed information on the origins of the properties presented can be found within these references:

- **NSC** (2015) Handbook on Lead-Bismuth Eutectic Alloy and Lead Properties, Materials Compatibility, Thermal-Hydraulics and Technologies. 7268, OECD NEA Nuclear Science Committee.
- **Sobolev V** (2011) Database of Thermophysical Properties of Liquid Metal Coolants for GEN-IV. SCK-CEN-BLG-1069, Belgian Nuclear Research Center SCK CEN.
- **Fink J, Leibowitz L** (1995) Thermodynamic and Transport Properties of Sodium Liquid and Vapor. ANL/RE–95/2, 94649, Argonne National Laboratory, dx.doi.org/10.2172/94649.
- **IAEA** (2013b) Challenges Related to the Use of Liquid Metal and Molten Salt Coolants in Advanced Reactors. IAEA-TECDOC-1696, International Atomic Energy Agency.

Jaeger (2017b) contains a helpful example of using correlations for the material properties of various liquid metals for implementation into a system code (in this case TRACE). The author includes references to the original sources so that potential users can check the origins of the data.

The differences in the material properties of liquid metals compared with water and gases is well known, but the implications of this for reactor thermal hydraulics and the ability to perform calculations require careful consideration. Sections 2.1.1 to 2.1.3 discuss the effect of liquid metal material properties on the values and application of a number of important thermal hydraulic parameters that have an impact on the modelling of liquid metals.

2.1.1 Prandtl Number

The Prandtl number (Pr) is a dimensionless property representing the ratio of the momentum diffusivity of a fluid to its thermal diffusivity. It is a function of the thermal conductivity (k), the dynamic viscosity (μ) and the specific heat capacity (c_p):

$$Pr = \frac{c_p \mu}{k}$$

Unlike many other dimensionless numbers used in thermal hydraulics, the Prandtl number is a property of the fluid alone, independent of length scale or flow parameters. Largely as a consequence of their high thermal conductivity, liquid metals have a much lower Prandtl number ($Pr \ll 1$) than more commonly used fluids such as gases or water.

A low Pr means that the molecular heat transport through a fluid is much greater than the momentum transport. A consequence of the low Prandtl number is, therefore, that the velocity and temperature fields are not similar in a liquid metal.

One of the easiest ways to illustrate this is by considering a boundary layer for a fluid flow adjacent to a cold wall. Figure 2.1 shows that for fluids with Pr of close to 1 (such as air or water[1]) the thickness of the hydrodynamic and thermal boundary layers is similar. For a liquid metal, the transport of thermal energy is greater and so the thermal boundary layer is much thicker.

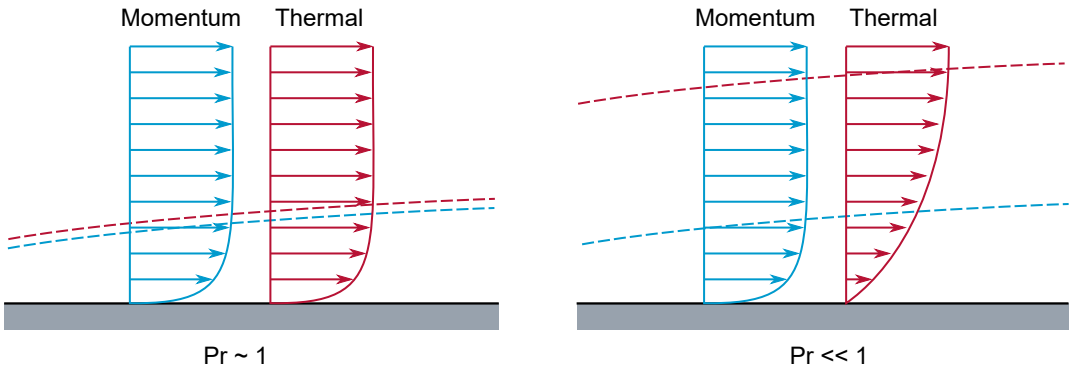

Figure 2.1: A diagram to show the difference in the momentum and thermal profiles normal to a cold wall. The dashed lines indicate the location of the boundary layer thickness (δ_{99}), where the quantity (either velocity or temperature) reaches 99% of its freestream value. The momentum profile is shown in blue and the thermal profile in red.

This is true under both laminar and turbulent flow conditions. Whilst the convective heat transfer in all fluids is strongly dependent on conduction under laminar flow conditions, in fluids with a Pr of close to 1 or greater, the transfer of both momentum and heat becomes dominated by the turbulent eddies (outside of the laminar sublayer) once the flow becomes turbulent. However, for liquid metals, the transfer of heat continues to be dominated by conduction up to much higher Reynolds numbers. For example, Grötzbach (2013) shows that the eddy transport of heat does not exceed that by molecular diffusivity[2] until $Re > 214{,}000$ in a channel for a fluid with $Pr = 0.007$. As

[1] $Pr \approx 1$ for water at LWR conditions, but not at room temperature, where Pr varies from approximately 11 to 3 over the range 5 to 60°C.

[2] The qualifier 'molecular' is being used here to distinguish it from 'turbulent' – for the remainder of this volume, the term 'conduction' will be used with the 'molecular' implied.

a result, even at fully turbulent Reynolds numbers, the influence of the thermal boundary layer can extend well outside the momentum boundary layer into the main flow.

For example, the temperature and velocity profiles across a pipe containing fully developed turbulent liquid metal flow (at say Re = 10,000) would be characterised by a classic 'turbulent' velocity profile, but may have a temperature profile that looks similar to that expected under laminar flow conditions (Figure 2.2).

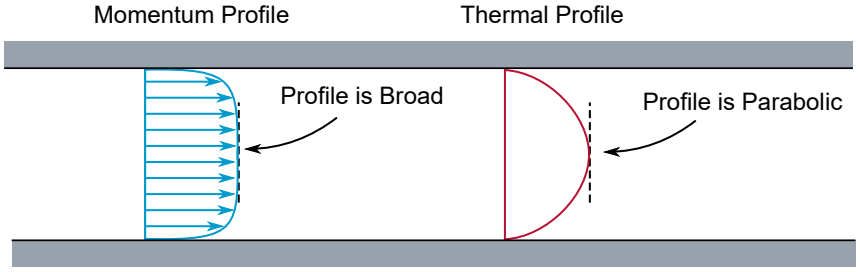

Figure 2.2: The difference in the momentum and thermal profiles of a fluid with $Pr \ll 1$, either in a pipe or between two parallel plates. The flow is fully developed and turbulent at a moderate Re ($\approx$ 10,000).

At much higher Reynolds numbers (e.g. Re > 214,000 for a fluid with Pr = 0.007) the influence of turbulence on the dissipation of heat becomes more significant. Under these conditions, it is expected that the temperature profile would start to flatten in the centre of the channel, appearing more similar to that of a fluid with a moderate Pr. However, evidence of this is hard to obtain as experimental measurement of the flow temperatures in liquid metals is very challenging and Direct Numerical Simulation (DNS) analysis is less practicable at higher Re due to its higher computational cost.

2.1.2 Reynolds Analogy

The Reynolds analogy is commonly used to relate the transfer of momentum, mass and heat through a fluid and relies on similarity between the hydrodynamic, concentration and thermal flow fields (Rogers and Mayhew, 1992). Since this similarity cannot be assumed for liquid metals, the analogy is invalid. Unfortunately, in thermal hydraulics, extensive use is made of this analogy and its underlying assumptions in the development of heat transfer correlations and fluid modelling techniques, which limit the applicability of many of these to liquid metals.

For example, a modified form of the Reynolds analogy (the Chilton-Colburn analogy) is used to to determine the equation for local Nusselt number (Nu_x) for laminar flow over a flat plate at a distance x downstream from the edge of the plate:

$$Nu_x = 0.332 Re_x^{1/2} Pr^{1/3} \quad \text{for } Pr > 0.6$$

At first glance it can be seen that this equation includes the Prandtl number and therefore might be assumed to be valid for liquid metals. However, a closer look at the derivation reveals that the surface temperature gradient can only be correlated to $Pr^{1/3}$ when Pr > 0.6 and therefore it is not applicable. Many more complex correlations (for turbulent flow) also make use of the Reynolds analogy in their derivation and this is not always apparent from just looking at the final equation (the range of validity should always be checked). Heat transfer correlations are discussed further

in Section 3.1. Assumptions relating to the Reynolds analogy are also embedded in numerous modelling tools. For example, use of the simplest form of the Reynolds analogy yields a turbulent Prandtl number of 1 and values of between 0.7 and 1 are often used as a default in Computational Fluid Dynamics (CFD) codes. Therefore, care needs to be taken when using Reynolds-Averaged Navier-Stokes (RANS) turbulence models for low-Prandtl number fluids, and methods to address this issue are discussed in Section 3.3.2.

Due to the dissimilarity of the momentum and thermal flow fields, it is advised that care is taken when using any correlations and/or parameters for heat transfer that have been developed for $Pr \approx 1$ fluids. For example, the use of hydraulic diameter for the scaling of heat transfer correlations between differently shaped channels may be found to work well for specific cases with a fluid of $Pr \approx 1$, but this cannot be assumed to be the case at much lower Prandtl numbers. The importance of conduction, even at fully turbulent Reynolds numbers, results in the specific geometry and the thermal boundary conditions having greater influence on the heat transfer than for fluids with a higher Pr.

2.1.3 Reynolds Number and Péclet Number

Reynolds number (Re) is one of the most commonly used dimensionless parameters in fluid mechanics. It is defined as the ratio of the momentum (or inertial) forces to viscous forces:

$$Re = \frac{\rho U L}{\mu}$$

where U is the flow velocity and L is an appropriate length scale.

Reynolds number is often used to determine the onset of turbulence under specific flow conditions (the critical Reynolds number). For example, fully developed forced flow in a smooth pipe (of diameter L) is found to transition from laminar to turbulent when $Re > 2300$.

The density and dynamic viscosity of liquid metals means that this critical Re can occur at low velocities. For example, for flow in a 5 cm diameter pipe, critical Re is reached at just 0.01 m/s for lead. In practice this means that the flow is likely to remain turbulent within an LMFR, even under very low flow conditions, which is beneficial in terms of heat transfer.

For calculations of heat transfer in liquid metals, the Péclet number (Pe) is often found to be a more relevant dimensionless parameter than the Reynolds number alone. The Péclet number is defined as

$$Pe = RePr$$

thereby taking account of the low Prandtl number of the fluid (and therefore the high thermal conductivity). The Péclet number can be thought of as the ratio between the thermal energy transported by convection and that transported by conduction.

2.2 Generic Liquid Metal Reactor Phenomena

As discussed in the introduction to Section 2, a detailed description of many of the thermal hydraulic challenges within a liquid metal cooled reactor are most usefully considered in the context of the reactor design. However, this section briefly describes some generic thermal hydraulic phenomena (that are relevant to all areas of the reactor) and their similarities and differences with those seen in reactors with other coolants.

2.2.1 Turbulent Heat Transfer

Turbulent heat transfer describes the transport of thermal energy by a moving fluid under turbulent flow conditions. In engineering systems the main focus is often the exchange of thermal energy between the fluid and the solid surface it is in contact with. Despite its engineering importance across a range of industries, this is not entirely straightforward to predict in any fluid. In particular, the modelling of turbulence is still a challenge (as discussed in Volume 1) especially in regions with complex flow patterns (e.g. impinging jets or flow recirculation). Although modelling solutions do exist that can predict these conditions, they are not generally suitable for extensive deployment in an industrial context (Section 3.3.1).

Most of the additional challenges posed by turbulent heat transfer in liquid metals are due to their material properties (as described in Section 2.1) and the dissimilarity between the thermal and momentum flow fields. The level of knowledge and experience with liquid metals, especially in the context of modern modelling methods, is lower than with more commonly used fluids. This means that development of, for example, appropriate RANS turbulence models is behind those that are suitable for water and gases.

2.2.2 Buoyancy Influenced Flow Phenomena

Volume 3 describes buoyancy influenced phenomena relevant to NPPs. In common with many next generation plants, LMFRs currently under design intend to make extensive use of passive systems, including passive decay heat removal systems and naturally driven primary circuit circulation under various fault scenarios. Additionally, the low flow velocities present in parts of the reactor plena may result in the influence of buoyancy being important even under nominally forced circulation conditions (mixed convection). Therefore, much of contents of Volume 3 is equally applicable to LMFRs. In particular the following topics of relevance are described in Volume 3:

- The forces associated with the buoyant movement of fluid.
- Natural, forced and mixed convection and circulation.
- Plumes.
- Stratification.
- The influence of buoyancy on transition to turbulence.
- Additional dimensionless parameters including Grashof number and Rayleigh number.

There are, however, a number of differences in the behaviour of a low Pr fluid under the influence of buoyancy, when compared to more common reactor coolants, that need to be taken into account.

2.2.2.1 Influence of Buoyancy on the Velocity Field

In theory, buoyancy can have an influence on any forced convective flow where there are temperature and therefore density differences within the fluid. In practice, however, there are many occasions where the influence of buoyancy can be ignored. Volume 3, Section 2.2.1 describes the dimensionless group (Richardson number)

$$\frac{Gr}{Re^2}$$

where Gr is the Grashof number and Re is the Reynolds number. This can be used (especially in environmental fluid mechanics) to indicate the relative magnitude of forced and natural convection effects, and therefore when the influence of buoyancy needs to be considered[3]. In LMFRs, evaluation of this parameter in plena can indicate whether buoyancy will be important.

Even in simple 'forced flow', the high thermal conductivity of liquid metals generally results in lower near-wall temperature gradients, but temperature differences that extend further into the fluid domain than in higher Pr fluids. As described in Section 2.1.1, for flow adjacent to a heated wall, the thermal boundary layer (and therefore the potential for varying body forces acting on the flow velocity due to buoyancy) extends well beyond the hydrodynamic boundary layer into the bulk flow. In practice this results in liquid metal flows being affected by buoyancy over a wider range of flow parameters.

NSC (2015) refers to experimental studies with vertical, circular pipes where distortion of the velocity field due to buoyancy has been observed at Reynolds numbers of up to 10^5 which is higher than the expected range for 'mixed convection' based on conventional flow 'regime maps' (for example, that presented in Chapter 15 of Kakaç *et al.*, 1987).

2.2.2.2 Surface Heat Transfer in Mixed Convection

Volume 3 describes the reduction and enhancement in surface heat transfer observed in vertical heated channels with mixed convection, due to the influence of buoyancy on the fluid near the wall. It is found that in some buoyancy assisted flows (heated flow in an upward direction), buoyancy acts to reduce the shear stress and, therefore, the turbulence generation in the boundary layer, resulting in a reduction in the surface heat transfer (Kakaç *et al.*, 1987)[4]. When the heated flow is in a downward direction, buoyancy acts to enhance the turbulence by opposing the flow and therefore the heat transfer is increased.

In liquid metals, the turbulence generation in the boundary layer is thought to be influenced by buoyancy in a similar way. However, in low Prandtl number fluids, the dominant heat transfer mechanism remains that of conduction, up to quite high Reynolds numbers (see Section 2.1.1). Under these conditions, a local reduction or increase in turbulence due to the action of buoyancy within the boundary layer would be expected to have less effect on the overall heat transfer (Jackson, 1983).

[3] It should be noted that the Richardson number is strictly only recommended for the consideration of stratification and external flows. More general parameters Gr/Re^n or Ra/Re^n can be calibrated to be more appropriate for internal flow, as described in Kakaç *et al.* (1987).

[4] The high strain rate layer is pushed closer to the wall, which reduces the generation rate of turbulence and leads to an increase in the thickness of wall-adjacent viscous sublayer.

Interestingly, a number of experimental investigations of vertical liquid metal pipe flow have observed considerable inconsistency in the effect of buoyancy on the surface heat transfer in liquid metals. In an experimental study of vertical pipes using liquid sodium (Jackson *et al.*, 1994) the surface heat transfer is seen to be enhanced by buoyancy in upward flow across the range where the previous analysis (Jackson, 1983) predicted that it would be suppressed.

At the current time, there is insufficient data to offer definitive guidance, but it is clear that care should be used when basing calculations on criteria or regime maps developed primarily for fluids with higher Prandtl numbers.

2.2.3 Conjugate Heat Transfer

Volume 2 describes Conjugate Heat Transfer (CHT) – heat transfer between fluids and solid structures – which is of significant importance to the structural integrity of NPPs. For example, areas of unsteady high temperature gradient within the primary circuit coolant can be found in many types of reactors. These can arise due to incomplete mixing of hot and cold flow streams, thermal stratification or the presence of free surfaces and are usually a concern with regard to their potential to cause high thermal stresses and/or thermal fatigue in adjacent reactor components.

The following topics described in Volume 2 are also of relevance to LMFRs and are discussed in context in Section 2.3:

- Description of the modes of heat transfer (with thermal radiation being relevant to regions of an LMFR not containing liquid metal).
- Surface modifications.
- Solid material properties.
- The challenges of modelling solids and the application to structural integrity.
- The approaches to CHT modelling.

As with buoyancy influenced flow, there are additional considerations specifically relevant to liquid metals.

High Fluid-to-Wall Heat Transfer: The high thermal conductivity of liquid metals leads to high fluid-to-wall HTCs. This results in fluctuations in fluid temperature being transferred to the solid components with little attenuation. The risk that phenomena such as thermal striping will cause fatigue damage to reactor structures is, therefore, greater than it might be in a reactor containing a primary circuit fluid with a higher Prandtl number. The design of LMFRs needs to take this into account and minimise the impact of such phenomena where possible.

Thermal Field Length and Timescales: As for other fluids, a key challenge for CHT modelling is the ability to predict an unsteady flow field with sufficient accuracy. In liquid metals the reduced importance of small length-scale momentum field fluctuations on the fluid temperature field can make unsteady wall temperatures easier to predict than for higher *Pr* fluids. This is discussed further in the context of CFD modelling of liquid metals in Section 3.3.

2.3 Thermal Hydraulic Challenges

In addition to the consideration of generic phenomena, it is also useful to consider some key areas of a reactor and the specific challenges and combinations of phenomena that are present. It should be noted that this section does not constitute the results of a Phenomena Identification and Ranking Table (PIRT) analysis (as described in Volume 1) of any particular LMFR design. It is intended to highlight phenomena (with no ranking of their importance) that often occur in LMFR that have aspects that are unique to or in some way different from other reactor technologies. Depending on the specific design of the reactor and the purpose of a given study, it may not be necessary to predict all of these phenomena with a high level of accuracy. The examples given by Cheng (2018) and Liao *et al.* (2021) provide a useful starting point for those wishing to develop a PIRT.

2.3.1 Fuel Assembly and Core Thermal Hydraulics

As for other reactor technologies, flow within the core is characterised by the narrow passages and small scale features of the fuel assembly. Again, similarly to other technologies, the most important consideration is that the fuel cladding temperature is maintained within design parameters for all conditions. As described in Section 1.3, fuel channels within an LMFR are often designed to be compact. Where the gaps between the fuel pins within the assembly are very small they need to be maintained by wire wraps rather than spacer grids.

Many of the thermal hydraulic phenomena within the core of an LMFR are similar to those found within a LWR (for example, the occurrence of ‘hot spots’). However, differences in the reactor design and the material properties of the fluid result in some differences in the thermal hydraulic challenges.

2.3.1.1 Spacer Grids and Wire Wraps

When spacer grids are used to maintain the geometry of a fuel assembly, their thermal hydraulic considerations are very similar to those for other reactor technologies (where spacer grids are commonly used). The additional thermal hydraulic challenges for LMFRs specifically, are those relating to the general differences in low *Pr* fluids (as described in Sections 2.1 and 2.2).

However, a wire wrap spacer is an additional feature on the surface of the fuel pins, which is not present on the fuel in other reactor technologies. As described in Section 1.3 and Figure 1.4, a single wire is wound helically around each fuel pin, thereby providing support to the lattice and preventing the cladding of adjacent pins from touching. Wire wrap spacers are typically used when the desired gap size is similar to (or less than) 1 mm.

The presence of wire wraps introduces additional challenges for the thermal hydraulic modelling of the fuel. The velocity of the flow past the pins is influenced by the wire to a greater or lesser extent depending on the proximity of an adjacent pin. This affects the pressure loss through the assembly, the surface heat transfer and the transverse mixing of the flow between subchannels (the fluid gaps between each triplet of pins in a hexagonal array shown in Figure 1.4). The phenomenon is sometimes described as ‘flow sweeping’ although it should not be assumed that the flow direction is simply that of the helical wire (as illustrated in Jeong *et al.*, 2017). Roelofs (2019, Chapter

5) provides a more detailed description of flow sweeping with reference to recent studies in the context of subchannel analysis.

Figure 2.3 shows Large Eddy Simulation (LES) CFD predictions that were undertaken to support the design of a new 7-pin sodium test rig[5]. The streamwise velocity and temperature contours are normalised by the area-average streamwise velocity ($\overline{U}$) and local bulk temperature (T_b), which increases linearly along the pin, respectively. The results show the large change in surface temperature on the central pin upstream and downstream of the wire wrap and mixing that occurs in the channels.

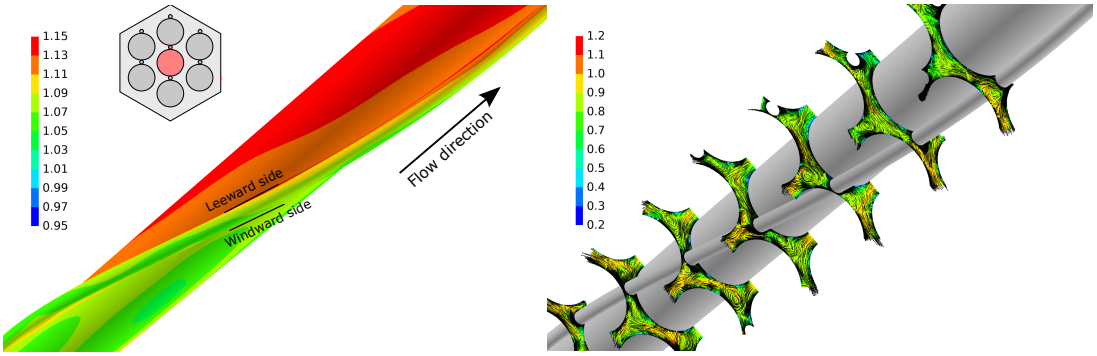

a: Normalised temperature contours (T/T_b) b: Normalised streamwise velocity contours ($U/\overline{U}$)

Figure 2.3: LES CFD results for 7-pin sodium test rig at Re = 50,000.

2.3.1.2 Inter-Wrapper Flow

In liquid metal cooled reactors, the fuel assembly is often hydraulically enclosed in a duct, called the 'wrapper', providing structural support to the assembly. The gap between each assembly is open for coolant and the heat transfer from the wrapper to/from the flow in the gap can be important, especially under fault recovery conditions. As a minimum, the inter-wrapper flow has a significant effect on the temperatures of, and therefore the thermo-mechanical loads on, the wrapper itself. Figure 2.4 illustrates the potential transverse flow through the inter-wrapper gaps.

One of the biggest challenges in the thermal hydraulic prediction of the inter-wrapper flow is that it can be highly coupled with the flow in the upper plenum as well as the temperature distribution within the core (as described in Tenchine *et al.*, 2012a). For example, under conditions where the inter-wrapper gaps are not fed by a bypass flow from the bottom of the core (or when this flow rate is low), a radial pressure profile at the top of the core could drive hot fluid down some of the gaps where it interacts with colder fluid.

Under passive decay heat removal conditions, flow within the inter-wrapper gaps can play an important role in the cooling of the core. Immersed decay heat removal heat exchangers located within the upper plenum result in local regions of cool fluid, which can flow down directly into the inter-wrapper gaps or down the periphery of the core and up the inter-wrapper gaps (Velusamy *et al.*, 2010) providing valuable cooling.

[5] These simulations were performed as part of the UK Government funded Project FAITH (Fuel Assembly Incorporating Thermal Hydraulics). This project was delivered by Cammell Laird with support from the National Nuclear Laboratory and Frazer-Nash Consultancy.

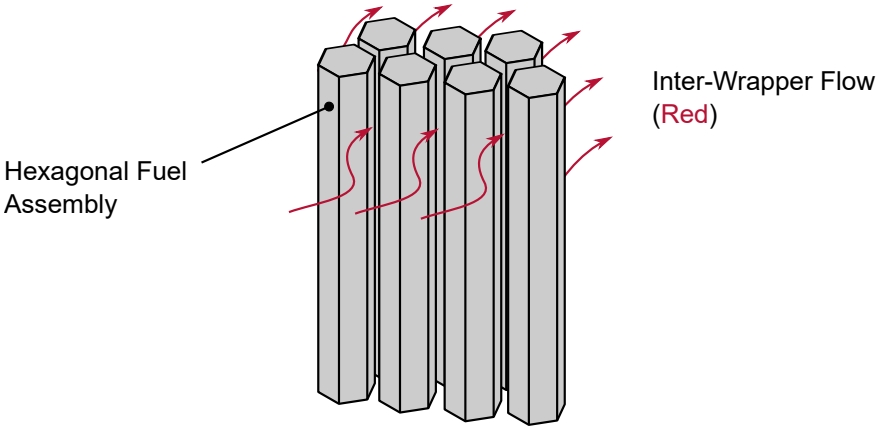

Figure 2.4: Inter-wrapper gaps under transverse flow conditions.

Under conditions where a local rise in temperature is seen within a single fuel assembly (for example due to a distortion or blockage as discussed below), the inter-wrapper flow can provide cooling to the assembly. It promotes the dissipation of heat within the core by both bulk movement of the flow within the inter-wrapper gap (the inter-wrapper flow is free to move vertically and transversely within the core) and by enabling the transport of heat to adjacent fuel assemblies. This cooling mechanism has been the subject of recent study, for example, the experimental work described by Pacio *et al.* (2019).

2.3.1.3 Fuel Distortion

Operational experience has demonstrated that, analogously with other reactor types, distortion of the 'as designed' geometry of fuel pins does occur in LMFRs (IAEA, 2008). There are a number of potential mechanisms including fuel cladding creep, fuel swelling and interaction of the cladding with wire wraps or spacer grids. Mechanisms such as cladding creep and swelling are more pronounced in LMFRs than LWRs due to the higher operating temperature and neutron fluence.

Prediction of the occurrence and effect of fuel distortion mechanisms is very much a multiphysics challenge but a number of the mechanisms are, at least in part, driven by thermal considerations. For example, the rate of fuel cladding creep is highly dependent on the temperature of the cladding. If fuel distortion does occur, the flow patterns through the core will be affected. In extreme cases a subchannel may become partially blocked. This will impact the fuel assembly pressure drops and the heat transfer from the surface of the fuel cladding.

In many ways the thermal hydraulic challenges associated with fuel distortion are similar to those seen in other reactor types but there are some additional considerations. In LMFRs a more tightly packed fuel assembly may mean that a small change in the geometry has a larger proportional effect on the flow distribution. Additionally, changes in the fuel geometry have a greater effect on the reactivity feedback in a fast spectrum reactor (discussed further in Section 3.2). However, the high thermal conductivity of liquid metals increases their ability to dissipate heat under reduced flow conditions.

A quantitative understanding of the fuel cladding temperature variation under both design (undistorted) conditions and a variety of distorted scenarios is often necessary to ensure safe, economical operation of a plant.

2.3.1.4 Fuel Surface Deposit

The build-up of surface deposits on fuel is of relevance across a range of technologies (as described in Volume 2). However, the nature of the deposit, the mechanisms for deposition and the impact on the cladding heat transfer varies. In SFRs surface deposits are not generally found to be a significant challenge. Within heavy liquid metal reactors the formation of a thin, stable oxide layer on the surface of the fuel cladding (and other hot components) is desirable to inhibit corrosion. The formation and control of this layer is closely linked to the coolant chemistry (Section 2.3.4) and represents a considerable challenge. From the perspective of thermal hydraulics there are two aspects of relevance:

- The formation and maintenance of the oxide layer is dependent on the oxygen concentration within the coolant local to the surface. Where the coolant flow is relatively fast moving and well mixed, the oxygen is continuously replenished. However, in areas of poor mixing or stagnation, the oxygen can become locally depleted. The thermal hydraulic challenge is, therefore, in the identification of such areas, such that they can be taken into consideration in the definition of the coolant chemistry and/or the design modified to mitigate the risk.
- The presence of an oxide layer on the surface of the fuel cladding represents a resistance to the transfer of heat from the fuel to the coolant. As this heat transfer is key to the successful operation of the reactor, it may be necessary to take this layer, and any uncertainty regarding its thickness, material properties or surface roughness into account when performing calculations.

The second of these is potentially relevant to all types of surface deposit (on the fuel and other surfaces within the reactor) and changes to the surface roughness can also affect the pressure loss characteristics of a component. The pressure loss through a region of the reactor may also be affected if a surface deposit accumulates to the point where it significantly restricts the open area available for flow and represents a partial blockage.

2.3.1.5 Fuel Assembly Blockage

The potential for partial blockage of a fuel assembly is common to all reactors with a solid, structured core. The primary concern associated with blockages is a local reduction in the flow of coolant and a subsequent over-heating of fuel in that region, causing serious damage and potential safety concerns. Blockages may occur due to a build up of particulates or, in the case of a more severe event, the migration of larger debris. The flow phenomena associated with a blockage are usually highly three-dimensional as the coolant diverts around the blockage and the peak fuel cladding temperature will depend on the size, shape and location of the blockage (Raj *et al.*, 2016 and Piazza *et al.*, 2017). Blockages due to large debris are often located at the bottom of the core, whereas blockages caused by the build up of particulates may occur in a wider variety of locations.

In heavy liquid metal reactors, an important source of particulate debris are oxides that are present on the surface of the fuel pins (and other components), in small quantities, by design. Excessive formation of oxides may lead to material becoming dislodged and being transported by the coolant (Roelofs, 2019). Other potential sources of particulates in the coolant include fuel material in the event of failure of the cladding and contamination by erosion or corrosion of reactor components.

The thermal hydraulic challenges of core blockages are largely similar to those of other reactor technologies, but the tight lattice of the fuel assemblies in many LMFRs renders them especially vulnerable. Where fuel spacer grids are present, blockages are usually located at the grid. In the case of wire-wrapped fuel, a blockage may occur anywhere in the fuel assembly where the gaps are narrowest (Pacio *et al.*, 2018).

Key to mitigating the consequences of a blockage, from a safety perspective, is understanding not only how a flow blockage affects the temperature of the local areas of fuel cladding, but how the blockage affects the temperatures of adjacent fuel pins or assemblies. For LMFRs with a fuel assembly wrapper, the inter-wrapper flow can be significant in cooling the blocked assembly (and also transferring heat to adjacent fuel assemblies) and so needs to be taken into account.

2.3.2 Above Core Thermal Hydraulics

The area immediately above the core in most reactors is geometrically complex, containing the above core structure supporting instrumentation and often control rod guide tubes. It is also often thermal hydraulically complex and characterised by steady and unsteady flow phenomena of differing scales interacting with each other and with solid components. The pool type design and compact core of LMFRs makes them especially susceptible to complex three-dimensional flow patterns. This, in combination with hot coolant temperatures, presents challenges for the design of components and instrumentation.

It should be noted that in LMFRs phenomena such as jets and thermal striping are not limited to the area immediately above the core. However, they are discussed in this section due to their particular significance within this region.

2.3.2.1 Temperature Monitoring Instrumentation

Thermocouples installed immediately above the core monitor the temperature of the flow exiting each of the fuel assemblies. These are often one of the only means of thermally monitoring the behaviour of the core and are therefore key to reactor safety and control. It is noted that this is true for all reactor technologies and the differences in this challenge for LMFRs are as a result of the material properties of the fluid and the specific design of this area of the reactor.

Hot liquid metals represent a challenging environment for many types of instrumentation, especially heavy liquid metals where the fluid is also corrosive. The development of appropriate instrumentation to work effectively in this environment for extended periods of time (i.e. those appropriate for long-term reactor operation rather than short duration tests) made considerable progress over the early years of LMFR development, and further work in this area is still ongoing.

Due to the variations in temperature of the flow exiting the core, the presence of the above core structure and the specific mounting arrangements for each thermocouple, the temperatures recorded may differ from the true temperature of the flow exiting each fuel assembly and it is important to understand and quantify any offsets that may be required. The main difficulty is that the aspects of importance to these offsets can be both small scale local effects (like a geometric offset in the mounting of a small number of thermocouples) and large scale ‘whole plenum’ effects (like radial flow over the top of the core) or a combination of both.

2.3.2.2 Jet Interaction

The presence of relatively high temperature and high velocity jets in the region above a reactor core is common across a range of technologies. The high shear forces at the periphery of a jet generates turbulence and causes local unsteadiness. This inherent unsteadiness has the potential to cause time varying temperature fluctuations in the coolant, even under nominally steady-state conditions. Although this is important in all reactor technologies, the high heat transfer between the coolant and the solid walls in LMFRs means that the temperature fluctuations seen by structural components can be higher.

When taken in the context of a pool type liquid metal reactor, jets of relatively fast fluid from the core are found to have a significant impact on the flow patterns in the wider upper pool domain (Tenchine, 2010). In particular, a jet can interact with any thermal stratification present and create unsteady temperature fluctuations at the interface of that stratified region with solid surfaces, potentially leading to thermal fatigue of the solid component. Adjacent jets of different temperatures can also interact with each other causing thermal striping (discussed below), which was investigated in the planar triple parallel jet sodium test (PLAJEST) experiment (Figure 2.5). A summary of fundamental jet experiments is provided in Roelofs *et al.* (2013b).

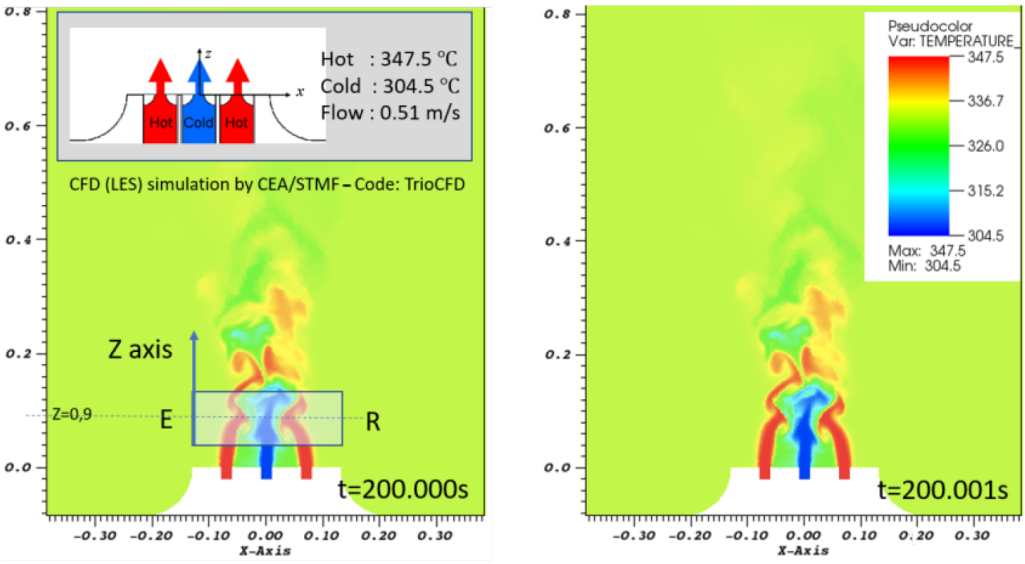

Figure 2.5: CFD results for the PLAJEST triple-jet experiment (Nagaso *et al.*, 2021).

2.3.2.3 Thermal Striping

Thermal striping is a phenomenon that encompasses damage caused by temperature fluctuations at the interface between non-isothermal flow streams, which are transmitted to structures in contact with these streams. Damage due to thermal striping has been seen in practice, for example on the Phénix and BN-600 reactors (IAEA, 2008) and can occur anywhere in a reactor where there is the introduction of fluid which is hotter or colder than its surroundings.

LMFRs are especially vulnerable to this phenomenon due to their high fluid-to-surface heat transfer coefficients, resulting in the potential for damage due to high cycle thermal fatigue. The flow that exits from the top of a LMFR core comprises hot flow from the fuel channels, but also flow streams

that have bypassed direct contact with the fuel, for example, from control sub-assemblies or inter-wrapper spaces. This creates an environment vulnerable to the effects of thermal striping and damage.

Thermal striping resulting from coaxial and planar jets of different temperatures has been studied both experimentally and numerically in the context of simple geometries (for example Kimura *et al.*, 2007 and Chacko *et al.*, 2011). The amplitude and frequency of the thermal fluctuations are the parameters of importance with regard to assessing the potential for damage. The thermal hydraulic modelling challenges relate to the need to use high-fidelity methods to capture the parameters of importance, in the context of a large and geometrically complex region of the reactor (an example of a more representative analysis is given in Choi *et al.*, 2015).

The design features used to prevent damage from thermal striping generally include the introduction of structures to enhance mixing. The above core structure, whilst being vulnerable to fatigue itself, can also be designed to include features of this type, potentially mitigating the problem of both thermal striping and stratification in the upper plenum. The ability to predict the mixing of flow streams of different temperatures is clearly important to the design of any such features.

2.3.3 Pool Thermal Hydraulics

As described in Section 1.3, the size, shape and layout of the 'pool' in a liquid metal cooled fast reactor shows significant variation from one design to another. Although this makes it more difficult to discuss the thermal hydraulics in a design-agnostic way, there are a number of similar challenges that occur to a greater or lesser extent in most designs. In all cases, the pools are characterised by complex three-dimensional flow patterns, which are hard to account for using simple modelling methods.

2.3.3.1 Pool Natural and Mixed Convection

As a consequence of the design of many LMFRs, the flow conditions in much of the pool are such that the influence of buoyancy is significant, even under nominally pumped flow conditions.

Additionally, most modern LMFR designs aim to be able to remove post-shutdown decay heat using primary circuit natural circulation. The thermal properties of a liquid metal coolant are such that heat can still be effectively removed from the core under very low flow velocity conditions. The thermal conductivity of liquid sodium is approximately 120 times higher than that for water. The conductivity of lead and LBE is only 20 to 30 times higher, but the high density of these heavy liquid metals leads to a high thermal mass and helps maintain lower fuel cladding temperatures for longer in the event of a fault. This, combined with the high boiling temperature, gives considerable grace time to establish effective natural circulation cooling, making it an attractive strategy (for more than just the most infrequent faults). Therefore, in a modern LMFR, the adequate prediction of flow distribution through the reactor and heat transfer from the fuel under these conditions is likely to be needed for the justification of the nuclear safety strategy.

Depending on the decay heat removal strategy, the flow distribution within the core of an LMFR can be quite different under natural circulation conditions than that seen during normal operation. For example, it is not unusual for the coolant to flow up channels in the middle of the core, but down those at the periphery and a number of different flow paths may be present for the removal of heat,

for example, as described in Gerschenfeld (2019) and illustrated in Figure 2.6. These differences mean that there will be a period of transition between normal operation flow patterns and natural circulation flow.

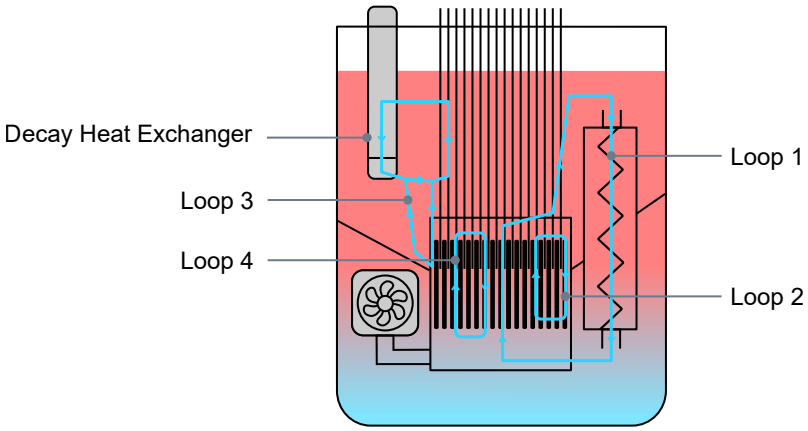

Figure 2.6: Example of potential decay heat removal paths in an LMFR.

If decay removal is partially via immersed decay heat exchangers at specific locations within the pool, then there is also potential for the development of large scale, possibly asymmetric, three-dimensional flows encompassing the pool and the core. Chellapandi and Velusamy (2015) and Parthasarathy *et al.* (2012) describe the decay heat removal strategy for a 500 MWe sodium-cooled Prototype Fast Breeder Reactor (PFBR) in India, which highlights the different long range and core natural circulation flow paths.

As for all buoyancy driven flows, the bulk flow rate is closely coupled to the heat transfer. The thermal hydraulic challenges (for computational modelling and experiment) are related to the need to predict three-dimensional, whole system flows driven by heat transfer which is affected by small scale flow features.

2.3.3.2 Stratification

A consequence of the low flow rates and influence of buoyancy in the plena of an LMFR is the potential for thermal stratification. These stratified regions are characterised by high vertical temperature gradients, which are experienced by adjacent structural components. The stratification is often unstable with respect to position and can lead to low frequency temperature oscillations of large amplitude. As in the case of thermal striping, the high heat transfer coefficients of liquid metals mean that these fluctuations are transmitted to the solid structures potentially causing damage by thermal fatigue.

Reactors are usually designed to minimise stratification but, even when the majority of the flow in an LMFR is well mixed, it is hard to completely eliminate it. The areas near the bottom of the hot plenum and the top of the cold plenum are often vulnerable.

Under primary circuit natural circulation conditions or low pumped flow rate, the likelihood of extensive stratification is increased and can result in severe thermal stresses on reactor components (IAEA, 2014a). For example, thermal stratification is predicted at the bottom of the cold plenum in Study C: Reactor Scale CFD for Decay Heat Removal in a Lead-cooled Fast Reactor (Figure 2.7).

The prediction of not only the general location of regions of high temperature gradient, but also the amplitude and frequency range of any oscillations represents a considerable challenge for all modelling methods.

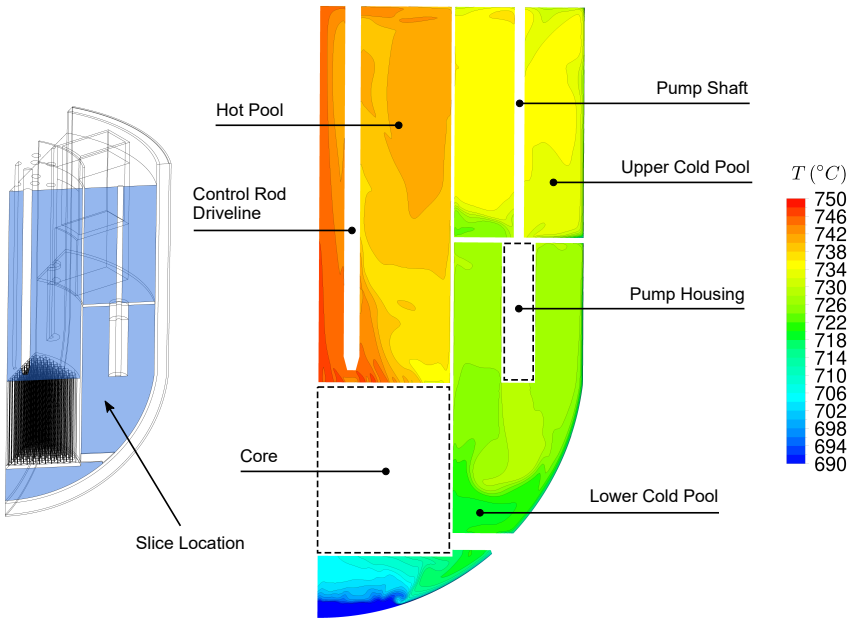

Figure 2.7: Thermal stratification in an LFR during natural circulation, taken from Study C.

2.3.3.3 Coolant Free Surface Movement

In pool type LMFRs a gas filled plenum is present above the pool, within the main vessel. This plenum allows for thermal expansion of the coolant and is filled with an inert gas to prevent contact of the coolant with oxygen and moisture.

Due to the size of the pool and the above core flows, the free surface of the coolant will be continuously fluctuating. These fluctuations result in a time varying temperature field for any structural components that pass through the free surface (for example the main vessel wall). In addition, vorticies or shearing at the surface may result in entrainment of the gas into the coolant (discussed further in Section 2.3.4).

For the purpose of determining the impact of the fluctuating free surface on the conjugate heat transfer to structural components, it is the location, magnitude and frequency of the fluctuations that are important (as for stratified flow). Determining the range of these parameters under normal operating conditions is necessary to ensure that the structural components are not subject to excessive damage by high and low cycle thermal fatigue.

The width of the pool in a typical LMFR design can lead to sloshing of the coolant in, for example, a seismic event. This is noted alongside other sources of mechanical loading in Section 2.3.4.

The thermal hydraulic modelling of the free surface requires a multiphase approach and the movement of the surface may be influenced by both the fluid below and the cover gas above. As with a number of other phenomena, it is the transient nature of the flow that effects the parameters of importance and makes predictions very challenging.

2.3.4 Other Aspects of Importance

The focus of the technical volumes in this series is primarily on single-phase flow and heat transfer. However, there are a number of other phenomena of importance to the design and substantiation of LMFRs and some overlap with the consideration of the thermal hydraulics. These are included briefly in this section for completeness, indicating relevant references for further learning.

Bubble Entrainment and Transport: The presence of a free surface and cover gas region above an LMFR leads to the possibility of gas bubble entrainment and transport within the reactor coolant. Gas may also enter the primary coolant in the event of a primary circuit heat exchanger tube rupture (if an intermediate liquid metal circuit is not employed). Gas bubbles within the coolant are of concern if they pass through the core because of the potential to cause an increase in reactivity. Possible mechanisms for gas entrainment include surface shearing, local vortices and liquid falling (especially where the design includes a difference in surface levels between the above core region and the main pool). Potential mechanisms are discussed further in Tenchine *et al.* (2014) and shown pictorially in Chellapandi and Velusamy (2015).

Melting and Solidification: All of the metal coolants considered for LMFRs are solids at room temperature, so (often electrical) heaters are required to heat the reactor at start-up with a new core and, depending on the design, to maintain the coolant as a liquid during refuelling or maintenance activities. The unplanned freezing of liquid metals is a problem with regard to blockage of flow paths and the potential for mechanical loads induced by freezing on adjacent structures. Lead-cooled reactors represent the most significant challenge due to the relatively high melting point of lead. The coldest regions in the primary systems, i.e. primary heat exchangers and decay heat removal systems, represent the highest risk areas for coolant freezing. IAEA (2013c) discusses this issue in more detail, including some operational experience relating to unplanned freezing in heavy liquid metal designs.

Sodium Boiling: The boiling temperature of heavy liquid metals is sufficiently high that coolant boiling is not deemed a credible scenario even under extreme conditions. However, for sodium, boiling is considered possible under a fault resulting in a loss of forced flow or water ingress. As for bubble entrainment, a concern is an increase in reactivity due to sodium voids within the core.

Current SFR designs are mitigating the risk of boiling in a number of ways. Passive decay heat removal strategies that are capable of maintaining a sufficient margin to coolant boiling help to prevent the possibility of prolonged boiling. The Advanced Sodium Technological Reactor for Industrial Demonstration (ASTRID) reactor has a core designed to achieve negative coolant void worth and a benchmark, aimed at improving computational methods, has been based on a similar concept (Bortot *et al.*, 2015a). IAEA (2008) reports work to support the development of boiling detection systems and the effect of voids on reactivity along with some experiments investigating the effects of sodium boiling carried out on the Dounreay Fast Reactor in 1977.

Mechanical Loading from Coolant: The density of sodium is similar to the density of water at reactor prototypical temperatures and pressures, so the mechanical loading on pumps or on structural components will be similar. However, LMFRs operate at a much lower pressure than LWRs, so thinner vessels are typically used and performance in the case of a seismic event (for example) can become one of the limiting factors for the design of the vessel (and of certain internal structures). Considerable effort has been expended in developing seismic isolation bases in countries where the risk of seismic activity is high, as described in IAEA (2013b). Lead and LBE have a density that is more than 10 times higher than sodium and therefore the challenges are greater, and where 'sloshing' 'of the fluid is an important consideration (Gopala and Roelofs, 2009 and Myrillas *et al.*, 2017). The size of the reactor pool in a LFR is often limited by seismic considerations.

Coolant Chemistry: The coolant chemistry is important (and complicated) in all reactor types. In liquid metal reactors, control of contaminants is important and previously operated sodium-cooled reactors include a sodium purification system as part of the design. For SFRs, the vigorous chemical reaction of sodium with water requires special design considerations (discussed further in IAEA, 2002).

In heavy liquid metal reactors, the corrosion of steel components is of particular concern. This can be mitigated by using oxygen within the coolant to maintain a protective oxide layer on vulnerable components. However, protecting the fuel cladding and other components from corrosive attack is considered a current challenge for these reactors, especially when their maximum coolant operating temperature is above approximately 550 °C.

Where liquid metal velocities are high, there is a risk of erosion to reactor components (especially if impurities are present in the circuit), sometimes resulting in the acceleration of corrosion. Erosion-corrosion damage to steel structures is a higher risk in lead and LBE and this mechanism is discussed further in IAEA (2002) and its references.

Further information on the chemistry of liquid metals can be found in IAEA (2012). Examples of studies of steel corrosion in heavy liquid metals include Deloffre *et al.* (2002) and Zhang (2009).

Flow Induced Vibration: Depending on the coolant velocities envisioned for operation, LMFRs can be as susceptible to Flow Induced Vibration (FIV) as other reactor technologies. As in these other technologies, the risks to the reactor include damage due to fretting (wear) and high cycle fatigue. Areas of a reactor vulnerable to flow induced vibration include the fuel assemblies (as described in Del Giacco *et al.*, 2014) and the above core structure (as described in Tenchine, 2010).

Cover Gas Thermal Hydraulics: An essential feature of all LMFRs is the presence of an inert cover gas layer above the liquid metal pool to isolate it from the surroundings and allow for coolant volume changes when the operating temperature varies. The heat transfer across the cover gas, and control of the thermal loading on the reactor cover, is of particular importance to the structural integrity of the reactor vessel.

Heat transfer across the cover gas region occurs via natural convection within the gas volume and radiation from the pool surface to the reactor cover. However, in the case of sodium, liquid metal can evaporate from the free surface of the pool into the cover gas region and forms an aerosol. The

evaporation and condensation of the aerosol droplets within the cover gas region further enhances the heat transfer across the cavity. In addition, the radiation flux across the cavity is mitigated by the aerosol due to scattering.

A summary of experiments on sodium surface emissivity and the heat transfer across a sodium aerosol-laden cover gas is given in Frazer-Nash (2019b). CFD modelling of the cover gas region behaviour in pool type sodium-cooled reactors has been validated against these experiments by Huang and He (2019).

Severe Accidents: In the context of LMFRs, severe accidents are often defined as Beyond Design Basis Accidents (BDBAs) involving core melt and potential significant relocation of the fissile core materials. Unlikely though this is, it may occur for a small portion of the core in the event of complete, undetected blockage of one or more fuel assemblies or for an unprotected loss of flow accident (i.e. the primary circuit pumps fail but for some reason the reactor does not shut down) or for an accidental reactivity increase. Under these circumstances it is important to be able to remove the heat generated by the fuel whilst maintaining the reactor vessel integrity. David *et al.* (2017) describes such a scenario, and the planned mitigations, in the context of the Indian PFBR. However, the strategy in the event of a severe accident can vary significantly with reactor design.

Neutronics: LMFRs operate with a fast (rather than thermal) neutron spectrum, and this influences the reactor physics of the core. Of particular relevance to thermal hydraulics are changes in the temperature of the fuel and reactor components (e.g. control rod drivelines) that lead to thermal expansion, which has a greater effect on the calculation of reactivity feedback than for thermal spectrum reactors. This is discussed further in Section 3.2.2 in the context of system code models. The modelling of neutronics and its coupling to thermal hydraulics is discussed in more detail in Volume 6, Sections 2.6 and 3.4.

3 Methodologies

In selecting and using a methodology for the analysis of thermal hydraulics, it is always recommended that the analyst should have sufficient understanding of the modelling method, the assumptions and the inputs to make effective engineering judgements, based on the results of their analysis.

For LWRs (and, in a UK context, AGRs) there is a large body of information resulting from or supported by operational experience. Analysts can use this to develop their understanding and, in some cases, short-cut the process by using established 'best practice' or codified guidance. For liquid metal cooled reactor analysis, a comparable depth of information is not available. This is not simply because no one has recorded it (in fact there are a number of extremely useful examples of where research groups have captured their own experiences for the benefit of others, e.g. Roelofs, 2019), rather that there has not been the sustained level of activity across multiple organisations to reach a robust consensus on as many issues. This is especially pertinent where analysis methodologies have made significant advances in the last 25 years, because a large amount of LMFR experimental activity across Europe and the US occurred before 1995.

In this context, it should be noted that the majority of references in this section (and throughout this document) are journal papers and/or consolidated research outputs, rather than outputs based on industrial experience. However, there are a number of more general reactor thermal hydraulic texts that contain some specific reference to where a different approach is needed for liquid metals. Much of the theory presented in Todreas and Kazimi (2021), for example, is applicable to the analysis of LMFRs.

For isothermal flow analysis, liquid metals behave similarly to other fluids. For example, the pressure drop across a component is driven by the geometry and the Reynolds number and correlations and closures developed for gases or water can often be applied (depending on the range of the correlation), as demonstrated in Section 15 of NSC (2015). Whilst correlations for pressure drop within simple geometries might be available in open literature, predicting the pressure drop across items such as reactor core components or a fuel assembly may need specific correlations to be developed. In many cases these will relate to individual reactor designs (and so cannot be covered here), however, Section 3.2 includes a number of correlations for pressure drop across wire-wrapped fuel bundles which form a useful starting point for calculations (although they do not account for the presence of surface deposits, for example).

It is the transport of heat, including the influence of temperature on the hydrodynamics (via buoyancy), where liquid metals require special treatment. An engineer undertaking thermal hydraulic modelling in liquid metals may need a higher level of expertise to achieve a useful and robust result than those working with more conventional fluids. For example, the level of expertise needed to

implement a new or modified turbulence model in a CFD code (Section 3.3) is considerably greater than that needed to use a standard model within the recommended range of flow parameters.

Although performing heat transfer analysis using liquid metals involves some different challenges, the overarching principles of good thermal hydraulic modelling practice are equally applicable. Volumes 1 and 4 contain the following relevant information that complements this volume:

- Phenomena Identification and Ranking Table (PIRT).
- Verification, Validation and Uncertainty Quantification (VVUQ).
- Introduction to overall modelling approach.
- Introduction to System and Subchannel codes.
- Introduction to CFD methods.
- Introduction to experimental methods.

3.1 Heat Transfer Correlations

In many engineering applications, the calculation of turbulent heat transfer between a solid surface and a fluid is performed by using experimentally derived, empirical correlations. These are used routinely by those performing calculations by hand and are also embedded into a range of modelling tools (e.g. system and subchannel codes as described in Section 3.2).

For commonly encountered fluids there are a large body of correlations for a wide range of flow conditions and applications. However, due to the dissimilarity of the thermal and momentum boundary layers (see Section 2.1.2) in a liquid metal, many correlations for other fluids are not applicable to liquid metals[1] and specific low Pr correlations must be used. Unsurprisingly, the maturity of these correlations for use in NPP design and substantiation is lower than in more established reactor technologies, but for a range of geometries correlations do exist. From as early as 1940 researchers have performed experiments and derived correlations for liquid metal flows. Generally, correlations have been developed within a specific research project, often with access to only a small number of experimental studies. However, more recently there have been a number of publications that present an overview of commonly studied flows.

As for other fluids, heat transfer correlations are usually expressed as functions of the Nusselt Number (Nu)

$$Nu = \frac{hL}{k}$$

where h is the HTC, L is an appropriate characteristic length scale and k is the thermal conductivity of the fluid.

As mentioned previously, laminar flow is not often present in practical LMFR applications. However, if required, of NSC (2015, Section 10.2) includes a description of correlations for laminar internal flow in a number of different geometries. The remainder of Section 3.1 of this document focuses on engineering heat transfer correlations for turbulent flow.

Specific correlations are included as examples throughout this section. It is strongly recommended

[1] Some correlations published in more general references (e.g. Kakaç *et al.*, 1987 and Incropera *et al.*, 2011) do have a range that extends to lower Prandtl numbers, but it is often unclear how extensively they have been derived from or validated by data in the low Pr range.

that the reader refers back to the stated sources of the correlations, and considers their relevance to the specific application of interest, before using them for reactor design or substantiation activities.

3.1.1 Forced Turbulent Flow in Circular Pipes

Pacio *et al.* (2015b) present data from 21 sources to perform an assessment of heat transfer correlations for fully developed turbulent flow in pipes. The study incorporates results for sodium, NaK eutectic, lead, LBE and mercury and includes correlations for both uniform heat flux and uniform temperature boundary conditions. Although the authors stress the challenges of examining a large body of experimental data, some of which is now very old, the study identifies the similarities and differences between a range of correlations and the findings for different metals. Additionally, the study performs statistical analysis and identifies the best performing correlations and the RMS error for different groups of metals.

For liquid metals, correlations for Nu tend to be of the form

$$Nu = a + bPe^{c}Pr^{d}$$

Although some correlations are found to also include the turbulent Prandtl number (explained in Section 3.3.2), these are less well developed and contain considerable variation and so are not considered in detail by Pacio *et al.* (2015b).

Based on this study, the following correlations were recommended in Pacio *et al.* (2015b) for use with Sodium (including NaK eutectic) and Lead (including LBE) respectively, assuming a constant wall heat flux:

$$\begin{aligned} Nu &= 5.6 + 0.0165Pe^{0.85}Pr^{0.01} && \text{for Na and NaK} \\ Nu &= 0.625Pe^{0.4} && \text{for Pb and LBE} \end{aligned}$$

for $Re > 10^4$ and $0.007 < Pr < 0.046$.

The same analysis is presented in Section 10.4 of NSC (2015), although with slightly different conclusions. In this reference the following correlations are recommended for use with Sodium (including NaK eutectic) and Lead (including LBE) respectively, assuming a constant wall heat flux for fully turbulent flow and $Pe > 300$:

$$\begin{aligned} Nu &= 5.0 + 0.0125Pe^{0.80} && \text{for Na and NaK} \\ Nu &= 5.9 + 0.015Pe^{0.80} && \text{for Pb and LBE} \end{aligned}$$

Although these two references disagree as to the best correlations, it is noted that the top performing two or three correlations in each case show very similar RMS errors, such that the choice of one rather than another is likely unimportant. Pacio *et al.* (2015b) and NSC (2015) also recommend alternative correlations for the assumption of a constant wall temperature, although there was insufficient data in this case for a statistical analysis.

When using heat transfer correlations for liquid metals, it should be noted that an RMS error of $\pm 20\%$ was not unusual in the context of those analysed. As discussed in Volume 4 (Confidence

and Uncertainty), care should be taken when using correlations derived from a single set of data. The degree to which the correlation matches the data from which it was derived is not a fully rigorous indication of its accuracy when applied for prediction, especially when used for conditions that are in some way different from the experiment.

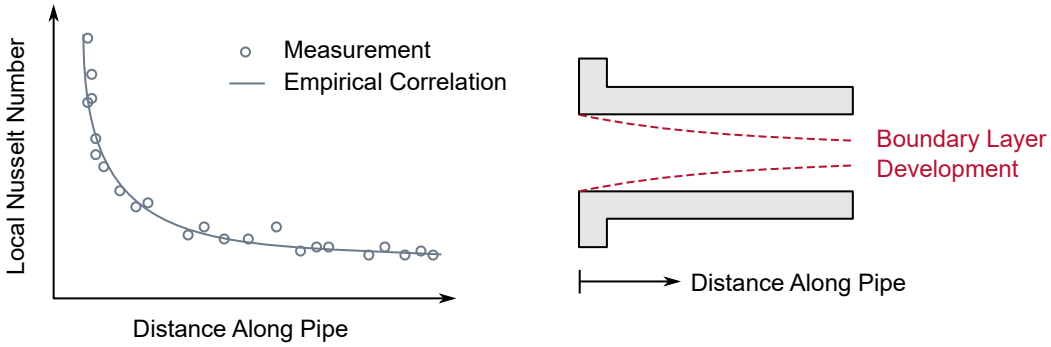

Figure 3.1: Sketch of the typical variation of the local *Nu* number in the entrance region of a circular pipe.

For flow that is not fully developed, there is far less data available, even for circular pipes. A sketch of the typical variation of the local Nusselt number in the entrance region of a circular pipe is shown in Figure 3.1. Jaeger (2017a) describes a recent review of liquid metal experimental data and correlations for developing flow in pipes and tube bundles. The study confirmed the findings of earlier work (e.g. Ching-Jen and Chiou, 1981) that the HTC at the entrance (within 2 diameters) of a circular pipe can be twice as large as that in the fully developed region. It also concludes that fully developed flow is established within 10 to 15 hydraulic diameters for 'combined' (thermal and hydraulically) developing flow and 20 to 30 hydraulic diameters for purely thermally developing flow (where the flow is already hydraulically fully developed)[2]. The higher heat transfer is of relevance to reactor design where the engineer wishes to realise the benefit of this enhancement for the design of components such as heat exchangers and also to assess the heat transfer to structural components located in a developing flow region.

Correlations are proposed within Jaeger (2017a) and NSC (2015) for both 'thermally' and 'combined' developing flow for use in system code analyses. However, the spread of experimental data (and challenges relating to detailed knowledge of the experimental conditions) makes the uncertainty large. This results in a degree of subjectivity in the recommendations for the 'best' correlation and different sources do not necessarily agree. However, both of the references above agree that

$$\frac{Nu_x}{Nu_\infty} = 1 + \frac{2.4}{x/D} - \frac{1}{(x/D)^2} \quad \text{for } x/D > 2.0 \text{ and } Pe > 500$$

(originally developed within Ching-Jen and Chiou, 1981) represents a reasonable fit to available data for combined developing flow, where x is the distance from the pipe entrance and D is the pipe diameter. Nu_x/Nu_∞ is the ratio of local (developing) to fully developed Nusselt number.

[2] However, the criteria for what is meant by 'fully' developed flow/temperature fields is not specified in Jaeger (2017a).

3.1.2 Forced Turbulent Flow in Channels

Circular pipes are the most studied geometry from the perspective of developing empirical turbulent heat transfer correlations, however, real LMFRs contain a much wider range of internal flow geometries. Additionally, as discussed in Section 2.1.3, the use of the hydraulic diameter to scale a correlation from one geometry to another is much less successful in liquid metals than for fluids with higher Prandtl numbers, so it is necessary to consider a range of specific geometries. Flow within rod or tube bundles is of particular relevance and is discussed separately in Section 3.1.3. This section describes a number of other channel flow configurations where reviews of experimental data and correlations are available.

3.1.2.1 Circular Annular Channels

Jaeger *et al.* (2015a) includes a review of available experimental data and correlations for heat transfer for forced flow within annular channels. The results of 19 experimental studies (including those with both alkali and heavy liquid metals) and 8 different correlations were considered. The author comments on each one, before considering the entire data set and developing a new correlation as a best fit to all available data. However, the majority of the experiments were carried out in the 1950s and 1960s and some concerns are expressed regarding the completeness of the reporting and the influence of uncertainties. Additionally, the studies were carried out with annuli of different diameters and different diameter ratios and there is little repetition with the same geometry. There is also some evidence (although not conclusive) that the heating of both the inner and outer surfaces of the annulus yielded higher HTCs than cases where only a single side was heated. With this level of variation, it is not surprising that the RMS error of the final correlation is high when comparing it to some of the sets of experimental data.

NSC (2015) also discusses HTCs in circular annular channels and a number of other examples are also included in the reference. However, unlike for some other geometries, it does not make any specific recommendations, instead stating that the variation in conditions for the available experimental data means that it is not possible to derive a general empirical formula from them.

It is recommended here that anyone wishing to use a correlation for a circular annular channel refers carefully to the experimental data reported in Jaeger *et al.* (2015a) and chooses the most appropriate correlation in the context of the metal type and geometry that they are interested in (noting that there is likely a high uncertainty associated with all of the correlations).

3.1.2.2 Rectangular Channels and Parallel Plates

In a study similar to that performed for annular channels, Jaeger *et al.* (2015b) summarises experiments relating to the flow of liquid metals in rectangular channels with cross-sections of various aspect ratios. The number of sets of experimental data published in open literature was found to be from just 8 experiments and the authors also chose to use analytical studies and DNS data (both relating to infinite parallel plates) to supplement the dataset.

The following correlations are recommended in Jaeger *et al.* (2015b), although it is noted that the spread of experimental data for lower aspect ratio rectangular channels increases the uncertainty. According to the authors, there is also inadequate data to fully determine if using one correlation

for all channels with an aspect ratio (AR) of less than 1:10 is reasonable.

$$Nu = 5.2686 + 0.00104 Pe^{1.171} \quad \text{parallel plates \& channels, AR > 1:10}$$
$$Nu = 7.833 + 0.0138 Pe^{0.8} \quad \text{channels, AR < 1:10}$$

Both of the above correlations are valid for $Pe < 3000$. The first of these correlations is very similar to that recommended in NSC (2015) for parallel plates (with some small differences in the coefficients). As for all correlations in this section, it is recommended that the references above are studied to determine the applicability of the correlations to the geometry of interest.

3.1.3 Axial Forced Turbulent Flow in Rod/Tube Bundles

3.1.3.1 Fully Developed Flow in Bare Bundles

The heat transfer associated with axial flow along lattices of circular rods is of interest to the design of both a reactor core and some heat exchangers. Mikityuk (2009) reviewed data from 4 experiments (using NaK eutectic or mercury) for flow within triangular lattices of heated rods and assessed the quality of a number of correlations with regard to predicting the experimental Nusselt number. More recently a similar, more substantial, review was performed within El-Genk and Schriener (2017), including consideration of the applicability of correlations for alkali metals to LBE.

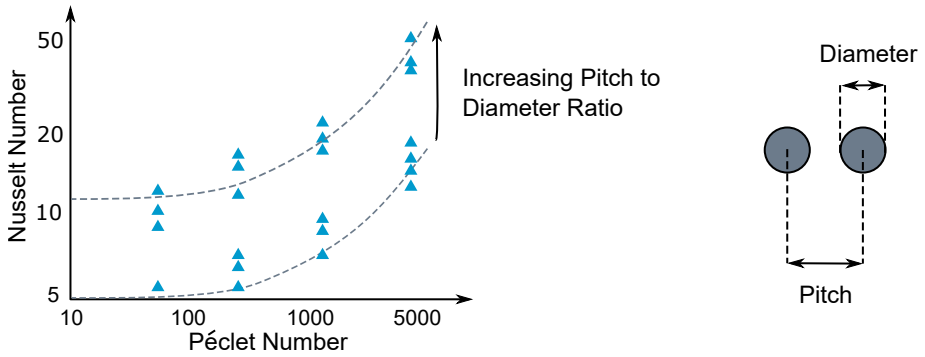

Figure 3.2: Sketch of the observed variation in Nusselt number with Péclet Number and pitch to diameter ratio of a lattice of circular rods (El-Genk and Schriener, 2017).

Correlations for Nu in rod bundles are typically functions of the Péclet Number and the pitch to diameter ratio of the bundle, but vary in functional form. A sketch of the Nusselt number variation observed by Mikityuk (2009) is shown in Figure 3.2. A useful table of correlations for heated rods bundles (assuming a constant heat flux) is included in Roelofs (2019). As an example, the correlation for Nu proposed by Mikityuk (2009) is

$$Nu = 0.047 \left(1 - e^{-3.8(p/D-1)}\right) \left(Pe^{0.77} + 250\right)$$

where p/D is the ratio of the bundle rod pitch to the rod diameter.

This correlation has a stated range of applicability of $1.1 < p/D < 1.95$ and $30 < Pe < 5000$ for triangular lattices (insufficient data was available for Mikityuk (2009) to draw clear conclusions for square lattices).

NSC (2015) also includes a similar table of correlations and recommends the equation above and a simplified correlation derived by Ushakov *et al.* (1977) for engineering use in triangular lattice arrays, with a range of applicability of $1.3 < p/D < 2.0$ and $1 < Pe < 4000$:

$$Nu = 7.55\frac{p}{D} - 20\left(\frac{p}{D}\right)^{-13} + \frac{3.67}{90}\left(\frac{p}{D}\right)^{-2} Pe^{0.56+0.19p/D}$$

However, when using these correlations for reactor design activities it should be noted that the uncertainty is likely to be greater than $\pm 20\%$ and, because the rod bundles in these studies include no spacers (wire wrap or grid), their applicability to a reactor core needs careful consideration.

3.1.3.2 Rod Bundles with Wire-Wraps and Spacers

A smaller number of experimental studies have been carried out considering triangular lattice rod bundles with either wire-wrapped or grid spacers, although not generally for the purpose of deriving empirical correlations.

Roelofs *et al.* (2013b) provide an overview of experimental studies for wire-wrapped assemblies carried out prior to 2012 (although it is noted that only 3 of these were actually performed using a liquid metal). More recently, Pacio *et al.* (2016) reported experimental work carried out at KALLA for the flow of LBE within a 19-rod bundle with wire wrap spacers. This work includes a comparison of the experimental results with a number of correlations and concluded that the average Nu was lower than that predicted by the majority of the correlations for bare rod bundles at the same Pe. It is noted that when considering wire-wrapped fuel pins (rods), the number of geometrical parameters of interest is increased to include the diameter of the wire and its helical wire 'pitch' (the axial distance for the wire to wrap once around a pin). This is likely to make the development of a universally applicable heat transfer correlation challenging.

Similar work was carried out by the same team (Pacio *et al.*, 2015a) for the flow of LBE in a 19-rod, triangular lattice bundle with grid spacers without mixing vanes. The focus of this work was more on the validation of 3D modelling tools (e.g. CFD), however a comparison was made with the correlation of Ushakov *et al.* (1977) given above. The correlation was found to under-predict the measured Nu (by around 20%) but, because the temperature measurement locations were on the spacers, this is not surprising.

The main purpose of the majority of recent heated rod bundle studies, including spacers, has been to assess the pressure drops and local variations in fuel cladding temperature due to the spacers (e.g. identification of 'hot spots'), rather than the development of a robust heat transfer correlation. In general, correlations for bare rod bundles are likely to be appropriate for use within fuel bundles with grid spacers, except for the region within 2 to 3 hydraulic diameters of the spacers themselves. For wire-wrapped fuel, the correlation of 'Kazimi and Carelli' referred to in Pacio *et al.* (2016) has been found to be a reasonable fit to available data. Its lower predictions of Nu, when compared with other bare bundle correlations, are likely because it is intended to be a conservative (rather than best estimate) correlation. However, as the original source of this correlation is not openly available, it is hard for a user to assess the applicability to their geometry and operating conditions.

The investigation of heat transfer using a validated three-dimensional CFD approach (despite its difficulties) is considered the best way forward in the absence of more extensive experimental data.

3.1.3.3 Developing Flow

As well as considering developing flow in circular pipes, Jaeger (2017a) also reviewed experimental data for developing flow in rod bundles. There were only 5 sources of experimental data identified, but all showed an increase in Nu in the developing region in a similar way to that observed in circular pipes. The maximum relative Nu reported was around 2.2, approximately 4 rod diameters downstream of the entrance (this was the measurement point closest to the pipe entrance, Nu may have been higher closer to the entrance). The following correlation was developed, but with so little data available it is difficult to estimate its potential uncertainty or the factors on which its accuracy depends.

$$\frac{Nu_x}{Nu_\infty} = 1 + \left(16.0 - 7.8571\frac{p}{D}\right) e^{-0.135x/D}$$

applicable for $1.2 < p/D < 2.0$ and $1 < Pe < 4000$, where x is the axial distance from the bundle entrance and Nu_∞ is the fully developed Nusselt number.

It is noted in NSC (2015) that bare rod bundles have been observed to have large development lengths (around 200 rod diameters, i.e. much larger than the ≈ 20 diameters implied by the correlation given above). However, the presence of grid spacers has been seen to reduce this significantly (to around 30 rod diameters) by enhancing mixing. For the wire-wrapped fuel tested in Pacio *et al.* (2016), it appears that the thermal development length was closer to 75 rod diameters (although it is hard to judge from the 3 measurement locations). The development length seen in any specific case will be highly dependent on geometrical features within and upstream of the area of interest.

The use of geometrically resolved modelling techniques that can take some account of these features is likely to offer more value if the heat transfer in areas of developing flow are of interest.

3.2 System Analysis

The use of 'system codes' (as described in Volume 1) for the analysis of nuclear reactor systems is universal across all reactor technologies. Even if it were possible to model the entire reactor using a geometrically resolved, meshed method, there will always be occasions when a simpler representation of the plant is useful. For example, the analysis of long transient accident scenarios, often involving control and instrumentation, back-up systems and other peripheral equipment does not lend itself well to an entirely high-fidelity approach. The main challenge of such codes is in the development and validation of the large (in-part design specific) input data set needed to characterise and validate all of the reactor components and physical processes of importance, such that the overall predictions of the model are adequate for their purpose.

In many respects, the advantages, limitations and challenges associated with system codes are the same for LMFRs as for other reactor technologies. As such, there has been considerable recent activity in extending the functionality of codes that are commonly used for LWR technologies to be suitable for liquid metal cooled reactors. However, there are a number of specific differences that need further consideration:

- The availability and accuracy of correlations (e.g. heat transfer correlations as described in Section 3.1) needed for a model is lower than for more commonly encountered fluids.

- The ‘pool type’ designs include large three-dimensional, poorly mixed bodies of fluid encompassing phenomena with a wide range of length and time scales. Such regions represent a considerable challenge for a modelling method that generally needs to assume fully mixed volumes of fluid with well defined boundary conditions.
- A fast neutron spectrum requires some changes to the neutronics modelling approach.
- High heat transfer between the liquid metal and the adjacent solid components requires careful consideration of ‘heat structures’ within the model.
- Some codes designed for other reactor technologies contain ‘hard coded’ (embedded) data or relationships that may not be applicable for liquid metals.
- The acquisition of experimental input and validation data is more challenging due to the additional complexities of performing experimental tests with liquid metals (see Section 3.4).

The remainder of this section examines these challenges and the availability and use of system codes for the modelling of liquid metal cooled reactors. It should be noted that this is an area of rapid ongoing development, so some of the information in this section may become out-of-date quickly.

3.2.1 Codes Used for Liquid Metals

The development of system codes for the modelling of LMFRs has been pursued by either constructing a code from scratch, addressing particular aspects of these reactors in the structure and implementation of the code, or by building upon a code developed and validated for water- or gas-cooled reactors.

In the latter case, the available framework may mean less effort is needed in terms of coding and validation of numerical approaches. On the other hand, care must be taken (in either case) that the code correctly represents phenomena that are unique for fast spectrum reactors, liquid metal coolants and alternative fuels – implementation of this may be more challenging in a code not designed for LMFRs. For example:

- Reactivity feedback from axial and radial expansion of the core is normally neglected in thermal spectrum reactors. In particular, the radial expansion in an LMFR may be governed by a core restraint system (not used in thermal spectrum reactors) and may be affected by subassembly bowing, which involves solving a complex coupled thermal hydraulic-mechanical problem. Similarly, axial expansion of control rod drivelines must be taken into account during transients. Moreover, the Doppler feedback has a different functional form in a fast spectrum (discussed further below).
- As seen above, the Nusselt numbers used for heat transfer may have a functionally different dependence on the Reynolds and Prandtl numbers compared with correlations for higher Pr fluids, which need to be accounted for in the model implementation. A similar issue is encountered in the parameterisation for the thermal conductivity of advanced fuels, preventing the use of some pre-existing/in-built functional forms for this property.
- When modelling fuel cladding performance, liquid metal embrittlement and high temperature helium embrittlement are phenomena that are not present in water-cooled reactors.

System codes that were written specifically for the purpose of modelling liquid metal cooled reac-

tors include SAS4A/SASSYS-1 developed by Argonne National Laboratory (Fanning *et al.*, 2017), SIMMER-IV (Yamano *et al.*, 2003), GRIF (Chvetsov and Volkov, 2000), DYANA-P (Natesan *et al.*, 2011), BELLA (Bortot *et al.*, 2015b) and the family of SIM-codes developed by KIT.

Examples of system codes originally developed for LWRs and later adapted for the modelling of LMFRs are RELAP, CATHARE, TRACE, SPECTRA, ATHLET and MARS. A short description of a selection of many of these codes and their application to LMFRs is given below.

ATHLET: ATHLET (Analysis of Thermal Hydraulics of LEaks and Transients)[3] is a liquid metal capable system code developed by GRS, Germany, which may be coupled to external 3D-kinetics and CFD codes. The code has been validated using experimental data from the TALL-3D, KASOLA and MYRRHA facilities.

BELLA: BELLA is developed by KTH[4], Sweden in collaboration with LeadCold, for the purpose of safety informed design of LFRs. It is a multipoint dynamics code relying on the point-kinetics approximation. Code-to-code benchmarks with respect to SAS4A/SASSYS-1 and SPECTRA have been performed. Its main strength is its simplicity, and adaptability to arbitrary configurations of fuel, cladding and coolant. A significant weakness is the lack of fuel thermo-mechanics and detailed gap conductance modelling.

CATHARE: CATHARE (Code for Analysis of THermalhydraulics during an Accident of Reactor and safety Evaluation)[5] is developed by CEA and is capable of modelling LMFRs based on point-kinetics and reactivity feedback from diagrid expansion, wrapper axial and radial expansion, and fuel cladding axial and radial expansion. Modifications to the original LWR code are described in Tenchine *et al.* (2012b). It has been validated with respect to the Phénix end-of-life tests (IAEA, 2013a) and was used for the EBR-II shutdown heat removal test benchmark coordinated by IAEA (2017).

MARS-LMR: MARS-LMR (Multidimensional Analysis for Reactor Safety) is an LMFR version of the MARS code, developed by Korea Atomic Energy Research Institute (KAERI). Point-kinetics is applied and reactivity feedback by structure expansion, fuel axial expansion, core radial expansion, and control rod drive line/reactor vessel expansion has been implemented. The code has been validated with respect to the Phénix end-of-life tests (IAEA, 2013a) and was used for the EBR-II shutdown heat removal test benchmark (IAEA, 2017).

RELAP5-3D: RELAP5-3D (Reactor Excursion and Leak Analysis Program)[6] is developed by Idaho National Laboratory (INL) in the USA and can model LMFRs with a multi-dimensional thermal hydraulic and kinetic modelling capability. It has been validated with respect to the Phénix end-of-life tests (Narcisi *et al.*, 2020) and was used for the EBR-II shutdown heat removal test benchmark (IAEA, 2017), as well as the CIRCulation Eutectic (CIRCE)-HERO integral test facility (Lorusso *et al.*, 2021) and European SCAled Pool Experiment (E-SCAPE) facility (Castelliti *et al.*, 2019).

SAM: SAM (System Analysis Module)[7] is a system analysis tool being developed at ANL in the USA for advanced reactor technologies including LMFRs. It includes a multi-dimensional

[3] www.grs.de/en/computer-code-athlet
[4] BELLA is open source and is available on request from KTH.
[5] cathare.cea.fr
[6] relap53d.inl.gov/SitePages/Home.aspx
[7] www.anl.gov/nse/system-analysis-module

flow model for thermal mixing and stratification phenomena in large enclosures, and can be coupled to other advanced simulation tools. The code has been validated against the EBR-II shutdown heat removal test (Mui *et al.*, 2019) and loss of flow without scram FFTF benchmark (Liu and Hu, 2020).

SAS4A/SASSYS-1: SAS4A/SASSYS-1 (Reactor Safety Analysis System)[8], developed by ANL, has been in continuous use and development for nearly five decades, primarily for the purpose of modelling power and flow transient in SFRs with metal alloy and oxide fuels. It has been validated against experimental data from EBR-II, FFTF and Phénix end-of-life tests. Capabilities for the modelling of lead-cooled reactors have been recently added. Its main strengths are the detailed thermo-mechanical modelling of metal alloy and oxide fuel systems, including axial expansion, and modelling of core disruptive events with coolant boiling and fuel melting and relocation. 3D-kinetics and fuel bowing modelling are available, but not in all versions of the code. The code does not permit detailed modelling of steam generators located in the primary system, as usually would be the case for lead-cooled reactors, so modifications to the modelling approach are needed to circumvent this.

SIMMER: SIMMER (S_N, Implicit, Multifield, Multicomponent, Eulerian, Recriticality) was originally developed by Los Alamos National Laboratory (LANL) for the purpose of modelling core disruptive events in SFRs. Currently, the code is owned by a consortium of Japan Atomic Energy Agency (JAEA), CEA and KIT and its use is restricted to members of the SIMMER consortium. It has been validated with respect to the CABRI and SCARABEE reactor tests. Capabilities for modelling LFRs have been added. Its main strength is the ability to model core disruptive events including fuel dispersion into the coolant. The code has been used for the EBR-II shutdown heat removal test benchmark (IAEA, 2017).

SIM-LFR/SFR: SIM-LFR/SFR is developed by KIT for the purpose of analysing unprotected and protected transients in LMFRs using point kinetics. Code-to-code benchmarking has been conducted for ASTRID and the Advanced Lead Fast Reactor European Demonstrator (ALFRED).

SPECTRA: SPECTRA (Sophisticated Plant Evaluation Code for Thermal-hydraulic Response Assessment)[9] is a thermal hydraulic system code coupled to a point kinetics model, developed at NRG, Netherlands. For liquid metal reactor applications, the fluid properties and heat transfer correlations are defined by the user. A radioactive particle transport package deals with release of fission products, aerosol transport, deposition and resuspension. The code validation work has included the EBR-II shutdown heat removal test benchmark (IAEA, 2017).

TRACE: TRACE (TRAC/RELAP Advanced Computational Engine)[10] has been extended at PSI, Switzerland to include sodium two-phase flow models in order to allow the simulation of boiling events in SFRs. Additionally, some development work has been undertaken to extend its capabilities to include lead and LBE. Validation of the sodium boiling model has been performed on the basis of past out-of-pile experiments. Further code validation has also included the Phénix end-of-life and EBR-II shutdown heat removal benchmarks.

[8] www.ne.anl.gov/codes/sas4a-sassys-1
[9] www.ensuringnuclearperformance.com/en/products/safe-operations/safety-analyses/spectra
[10] www.nrc.gov/about-nrc/regulatory/research/safetycodes.html

3.2.2 Model Build

When building a system code model for an LMFR there are several aspects that are different with respect to the case of a light-water or thermal spectrum gas-cooled reactor. Whereas some phenomena make the modelling task more complex, others allow the user to adopt a less detailed approach, without loss of accuracy. A discussion on the particular features of LMFRs that distinguish them from other systems is given below.

Neutron kinetics of LMFRs are, in general, less complicated than in thermal spectrum reactors. This is due to a considerably larger range of validity of the point-kinetics approximation. Specifically, since the neutron mean free path is of the order of several centimeters in a fast spectrum reactor, the neutron flux is almost constant within a fuel rod. During a transient, the point-kinetic approximation of a constant flux profile is therefore more valid than in a thermal spectrum reactor. Hence, the lack of accurate 3D-neutronic modelling in a system code is less of a drawback.

Coupled temperature-reactivity dynamics on the other hand, are more complex in an LMFR since, in addition to the coolant/moderator temperature coefficient and the fuel Doppler coefficient. Both axial expansion of the fuel (and control rod drivelines) and radial expansion of the fuel assembly diagrid must also be properly modelled. Whereas the fuel Doppler coefficient in a LWR is low compared to the moderator temperature coefficient, in an LMFR, it may be of the same magnitude. Therefore, a precise calculation of the fuel temperature is not only of importance for determining the margin to fuel cladding failure, but also to obtain the correct reactivity feedback from Doppler broadening and fuel axial expansion[11].

It is recommended that a user examines code documentation carefully to check that the code they are using is appropriate for modelling the dynamics of LMFRs. For example, it should be noted that the Doppler coefficient in a fast spectrum reactor is proportional to inverse temperature, whereas in thermal spectrum reactors it is often parametrised as proportional to the inverse square root of temperature. If the temperature dependence is ‘hard coded’ into a system code (as is the case in some versions of RELAP) it cannot be applied to the simulation of transients in an LMFR.

Thermophysical and irradiation properties are important to specify accurately for any reactor technology. For LMFRs this may be more difficult depending on the system code being used. For example, codes such as SPECTRA allow a high level of control regarding the material properties, with these being completely specified by the user. However, this is not always the case and some codes require changes to be made by the code developer to allow modelling of a fluid that was not part of its original design intent.

For advanced reactor technologies, another challenge is presented by the use of new types of fuel. For example, the fuel-cladding gap conductance for helium-bonded ceramic fuels must be carefully evaluated, which means that an adequate thermo-mechanical model of fuel swelling and gas release is important. Since swelling and gas release in nitride and carbide fuels is different from that in oxides (with a larger swelling rate, but a lower gas release rate) the model will need to be developed and validated for the specific fuel type being used.

[11] A particular challenge is the prediction of fuel assembly bowing resulting from the presence of a core pad restraining the movement caused by diagrid expansion.

Heat transfer from fuel cladding to the coolant in LMFRs is characterised by a Reynolds number of approximately 50,000, and a Prandtl number of approximately 0.01. As previously described, it is necessary to use heat transfer correlations specifically developed for liquid metal flow (due to their much lower Pr), and the system code used should be capable of applying those. Considering the correlation of Mikityuk (2009) (described in Section 3.1.3) as an example

$$Nu = 0.047\left(1 - e^{-3.8(p/D-1)}\right)\left(Pe^{0.77} + 250\right)$$

it should be noted that in some codes, Nu must use a specific functional form, for example

$$a + bPe^{c}$$

This means that a set of coefficients from the Mikityuk correlation (or a fit for another correlation with a different functional form) would have to be generated for the particular geometry (p/D) of the reactor core to be modelled. The error introduced by such a fit would need to be assessed and taken into account in the interpretation of the results (along with other sources of uncertainty). Other correlations may be used for bundles with wire-spacers, but again a fit to a different functional form may be required.

Channel pressure drop is a key prediction of a system code model, because a high proportion of the primary circuit pressure drop is usually across the core. For wire-wrapped fuel the correlation for friction factor (f) based on the work of Rehme (1973) is recommended by Bubelis and Schikorr (2008) and was found to be a good fit to experimental data and CFD by Jeong *et al.* (2017):

$$f = \left(\frac{64}{Re}\sqrt{F} + \frac{0.0816}{Re^{0.133}}F^{0.9335}\right)\frac{N_r\pi(D_r + D_w)}{P_w}$$

where D_r and D_w are rod and wire diameters, N_r is the number of rods in the bundle, and P_w is the total wetted perimeter of the fuel assembly. F is given by

$$F = \sqrt{\frac{P_r}{D_r}} + \left(7.6\frac{D_r + D_w}{H}\left(\frac{P_r}{D_r}\right)^2\right)^{2.16}$$

where H is the wire pitch and P_r is the rod pitch. Due to its complexity, some system codes may not permit a direct input of this form. For example, considering an input using the simple Blasius form for the friction factor

$$f = \frac{a}{Re^{b}}$$

which, when fitted to the correlation of Rehme for a particular geometry, will be adequate around nominal operating conditions, but may introduce a significant error in transition to natural convection (low Reynolds number) conditions.

Heat exchangers/steam generators vary with reactor design. In a sodium-cooled reactor there is normally an intermediate heat exchanging circuit containing sodium, whereas, in a heavy liquid metal cooled reactor, the steam generator would typically be located in the primary circuit. Different system codes allow the modelling of different configurations. For example, a system code primarily developed for LWRs might assume that the secondary circuit always contains steam. SAS4A/SASSYS-1 assumes that the secondary circuit contains a liquid metal (as would be the

case for an SFR). An experienced user may be able to work around the restrictions of a specific code using certain modelling 'tricks', but it is easier and clearer if the chosen code is intended to directly support an applicable design of secondary circuit.

Solid components within the reactor primary circuit can be important to the thermal performance of the system, and the temperature prediction of some components (for example the fuel cladding) is a key objective for many thermal hydraulic modelling tasks. Due to the high fluid-to-surface HTCs in liquid metals, CHT is likely to play an important role. For steady-state normal operation this is unlikely to cause difficulties (although needs to be taken into account), but for transients involving rapid changes of temperature, heat transfer to and from reactor components with significant thermal mass is likely to have an effect. It is therefore important to give attention to the appropriate modelling of solid reactor components in contact with the primary circuit flow.

Thermal stratification can be a significant issue in LMFRs due to the pool type configuration and lower primary circuit velocities, as discussed in Section 2.3.3. One of the key limitations of system codes is the ability to adequately predict multi-dimensional phenomena, such as buoyancy-driven flow and mixing in plena. As discussed in Volume 3, Section 3.1.1, some system codes may be able to represent pools using a multi-dimensional component or parallel (vertical) channels connected by cross-flow junctions. However, this is only intended to capture large-scale effects and further research and investigation is required to determine the level of confidence in the system code predictions by comparison against CFD or experimental results.

Heat losses to the environment may be larger than from an LWR, due to the higher operating temperatures of LMFRs, and may be deliberately introduced as part of safety systems. Such losses need to be accounted for as part of decay heat removal calculations, and assessments of thermal efficiency during operation.

3.2.3 Interpretation of Results

The numerical solution to the set of coupled differential equations describing the state of LMFRs in a system code can be obtained with a relatively high level of confidence, since the number of nodes required to obtain a converged solution is relatively low. This is due to the improved accuracy of the point kinetics approximation and prevalence of single-phase flow in the primary system. The main issue is whether all relevant physical phenomena, such as bypass-flow and stratification, have been properly taken into account when implementing the system code model, and whether the geometry is adequately described. Therefore, benchmarking the code using integral test facility experiments is important to establish confidence in the overall model (as for all reactor technologies).

A description of some useful LMFR benchmarking activities suitable for the validation of system code models is given in Section 3.4.5. It is noted that a general lesson learnt from these benchmarks is that the blind calculation results feature a high degree of variability, even in the qualitative trends of the predictions. This may be attributed to the user approach to implement the experimental set-up in their respective code, rather than to uncertainties in input data. Simulations informed by experimental data exhibit smaller variations, but are still of significance. It is recommended that the findings of these benchmarks (regarding the uncertainty in the modelling results) are taken into account, particularly when considering the use of system codes for supporting a safety case in the licensing of new reactors. Volume 4 discusses these issues in more detail.

3.2.4 Subchannel Analysis

For the analysis of LWRs, a system code is often used in conjunction with other 'nuclear codes' to determine the key parameters of importance. These additional codes typically either examine areas of the reactor of high importance at a greater level of geometrical resolution than a system code, or are used to predict the effect of phenomena only encountered in specific components or under specific fault conditions. For LWRs, subchannel codes are currently used to improve the resolution of system code predictions in the fuel channels (a number of commonly used subchannel codes are summarised in Volume 1). 'Containment codes' and 'Severe Accident codes' are examples of tools used to predict phenomena involving energy or mass transport across the primary system boundary and specific sets of conditions.

For the next generation of LMFRs, there is no reason why a similar overall approach could not be adopted (subject to the challenges and limitations described in the rest of Section 3), especially if appropriate codes are readily available to the organisation performing the analyses. An example of coupling between a system code and a containment code, aimed at supporting source term evaluations for dose analysis, is discussed in Hua *et al.* (2020). Analogously, for an LMFR containment design featuring water-based systems for decay heat removal, it would be practical to use an existing code and take the benefit of previous validation exercises.

However, where there is less embedded knowledge and investment in these codes for LMFRs, or where the approaches used are less applicable to LMFRs, it is also possible for reactor designers to chose a different path. Modern CFD, including coarse grid methods (as described in Section 4), could be used as a platform for the development of the equivalent to a subchannel code. Advantages of this approach include improved predictions of the complex flows and temperature distributions relevant to the performance of wire-wrapped fuel and the flexibility to model LMFR specific designs.

Given the large variation in methods (with many proprietary codes and bespoke tools), it is not possible to offer code-specific advice on subchannel, severe accident or containment analysis in the context of this volume. However, it is worth noting that a number of more commonly used LWR subchannel code sets (for example MATRA and COBRA) have been developed over the past 15 years to include versions aimed specifically at modelling LMFRs. Additionally, some organisations have been working on developing new subchannel codes, such as ANTEO+ described by Lodi *et al.* (2016).

As for all modelling tools, it is recommended that the user interrogates any methods carefully for aspects that may be invalid for low Pr fluids, or fast spectrum reactors, so that all models have the necessary level of applicability and validation.

3.3 CFD Methods

The role of CFD in the design and, most particularly, in the safety substantiation of nuclear power plants has been a relatively minor one and there are a number of good reasons for this.

1. At the time that much of the original design work was carried out for NPPs in Europe and North America, CFD (as we know it today) was not available. Alternative calculation methods (including the precursors to modern CFD) were used and these were built on and developed for specific applications over subsequent decades such that a large body of knowledge and expertise became embedded in the resulting tools. This investment has resulted in toolsets that are suitable for covering the vast majority of normal operation and fault scenarios for extant reactors. Even where the use of modern, flexible CFD methods offers a benefit, there is often little incentive to use them.
2. The importance of two-phase flow to LWR designs represents a considerable challenge to any modelling method. Even today, the detailed modelling of two-phase flow phenomena with CFD across the range of conditions and at the scales needed for LWR analysis is more of a research topic than industrial practice, which limits its wide application to these reactors at the current time.
3. The computational expense of CFD is much greater than that of simpler methods. The increase in computing power in recent years has made complex CFD modelling more accessible, but the analysis of long transient scenarios (important to predicting the performance of NPPs under many conditions) is still a time-consuming and costly exercise.
4. Although CFD includes fewer approximations and less empiricism than many more commonly used methods, 'industrial' CFD is by no means a perfect representation of the physics. The complexity of the modelling method, as well as size and complexity of computational domain, can make it very hard to quantify the impact of the underlying assumptions, and the flexibility of tools make it hard to control 'user effects' (as described in Volume 4). For these reasons it can be difficult to use CFD in safety substantiation[12].

The main drivers for the current use of CFD in NPP design are in the refinement and optimisation of components and the analysis of complex or novel geometries. It is used both during the design process and to reduce the amount of experimental work needed to substantiate the final performance. Additionally, CFD is used to visualise flow, develop an understanding of what phenomena are important and to characterise complex components or reactor regions as part of the development or validation of simpler models.

The design of modern LMFRs presents opportunities for CFD to play a more substantial role:

- The maturity of specific 'nuclear codes' to analyse the different regions and operating regimes of LMFRs is less than for LWRs, so model development based on a modern, state-of-the-art platform can be pursued without needing to discard as much previously gathered knowledge.
- Two-phase flow is less important in the analysis of LMFR reactor operation.
- A pool type design encompasses large regions of complex three-dimensional flow, which increases the benefits of CFD compared with simpler, less geometrically resolved methods.

[12] CFD can be used for NPP safety analysis under some circumstances as discussed in Volumes 1 and 4.

The CFD analysis of liquid metals introduces additional challenges compared to the analysis of more commonly employed engineering fluids. In particular, the low Prandtl number of the fluids means that many of the turbulence models and wall functions in CFD codes are not appropriate for the modelling of heat transfer and the development of new/modified approaches is the topic of ongoing research. It should be noted that for the CFD modelling of isothermal flow, liquid metals can be treated in the same way as $Pr \approx 1$ fluids. However, since isothermal flow is not present in the majority of important NPP calculations, this is of little advantage to the nuclear engineer.

The use of CFD as a design tool in NPPs has gained momentum over the past 10 years and CFD analysis is currently being used to provide useful insights for modern LMFR designs (for example, work described in Roelofs, 2019). However, it should be stressed that both the analysis and validation of liquid metal CFD are currently more challenging than that with more conventional fluids and so should not be attempted by inexperienced users without access to mentoring and support. It is recommended that a CFD practitioner working with liquid metals for the first time starts with basic flow geometries and boundary conditions before building up the complexity to their study of interest.

Volumes 1, 2 and 3 contain descriptions of the use of CFD in NPP design and safety substantiation, as well as an overview of the most commonly used codes and turbulence modelling methods. It is recommended that these are read in conjunction with the remainder of this section.

3.3.1 DNS and LES CFD Modelling

The challenges and benefits of using DNS methods are no different for liquid metals than for other fluids. Because the length and time scales of turbulent flow are fully resolved, the low Pr of the fluid is completely accounted for and no special modifications to the analysis method are needed. However, due to the computational expense, the extensive use of DNS in an industrial context is unlikely for the foreseeable future. The main benefits of DNS analysis for liquid metal thermal hydraulics are in validating less computationally expensive methods (a number of examples available in open literature are given in Section 3.4). It should be noted that undertaking DNS analysis is a specialist field and the modelling tools are not necessarily available in an industrialised, easy-to-use form.

LES represents a less computationally expensive method of achieving a high-fidelity solution than DNS. It achieves this by only resolving the larger scale turbulent eddies and accounting for the smaller scales using a Sub-Grid-Scale (SGS) model. In LES simulations, the Reynolds number of the flow, cell size and SGS model determine the portion of the turbulence spectrum that is resolved. This, in combination with the geometrical extent and complexity of the model, impacts how computationally expensive the analysis is.

In the context of liquid metal CFD modelling, it is the SGS model that is likely to contain assumptions that are less valid for low Pr fluids. As for RANS turbulence modelling, the impact of these assumptions will be associated with the dissipation of heat. However, the smallest length-scales associated with the temperature field are larger than those associated with the velocity field (a consequence of the low Pr). So for a given LES grid, the proportion of turbulent temperature field which is resolved will be higher than that of the velocity field, resulting in the SGS model having less effect on the temperature field. The result of this for the user is that (providing it is computationally feasible to use wall-resolved LES) it is often possible to achieve a high level of accuracy without

making any specific changes to the CFD tool to account for the low *Pr* of the fluid. Examples of the use of wall-resolved LES modelling in liquid metals can be found in Roelofs *et al.* (2013a) and Roelofs (2019).

In most cases it is not computationally feasible or necessary to model an entire fluid system with LES. The extent of the solution domain needs careful consideration to prevent excessive influence of inlet and outlet boundary conditions. For liquid metals, the larger length scales associated with thermal fluctuations need to be taken into account and may result in the need for a larger solution domain than for other fluids.

Due to the small near-wall mesh size needed to resolve the momentum boundary layer, modelling using an LES approach becomes much more computationally expensive in the presence of solid walls. In addition, the number of cells needed to resolve a high proportion of the turbulent energy increases with increasing *Re* and *Ra*. For these reasons wall-resolved LES modelling is often still computationally challenging for many industrial applications. The reduction in near-wall mesh resolution needed to capture the temperature field (discussed above), mitigates this to some extent in low *Pr* fluids. However, the resulting model may still be too expensive for routine use.

To address this issue a number of hybrid (RANS/LES) approaches have been developed (a number of examples are described in Volume 3). However, the RANS elements of these methods will be subject to the same deficiencies regarding the modelling of liquid metals as a purely RANS approach (discussed below). Wall Modeled Large Eddy Simulation (WMLES) represents a potentially good compromise for the modelling of internal flows, however it is a less mature approach and little evidence for the validation of the associated wall treatments for liquid metal flow has been found. Near-wall modelling is discussed further in Section 3.3.2.5.

3.3.2 RANS CFD Modelling

Extensive use of RANS CFD modelling is now made across many industries. The use of a common method has significant advantages in terms of the investment in tool development and the sharing of good practice and expertise across different engineering sectors. However, the degree of applicability of the experience gained from other industries depends on the similarities and differences in the thermal hydraulic phenomena and objectives of the analysis. NPP engineering presents some specific thermal hydraulic challenges, such as the high importance of heat transfer and complex internal flow. These are shared by engineers such as gas turbine designers, but not by those working in external aerodynamics, for example.

For LMFR designers, the use of a more unusual fluid is a disadvantage when it comes to using multi-purpose tools. As discussed in Section 2.1, low *Pr* prevents the application of common analogies between the turbulent transport of momentum and heat. Unfortunately, these analogies are extensively used in the development of RANS turbulence models and wall treatments, thereby reducing the accuracy of CFD predictions made with these models for liquid metal applications, where heat transfer is of importance.

It should be noted that no single RANS turbulence model is considered able to capture the effects of all phenomena under all conditions (for any fluid). A consequence of this is a large amount of choice for the CFD user. Even within a single code it is not unusual to have more than 10 different

RANS turbulence models and variants available, and the details of the implementation of nominally the same model can differ between codes, in a way that affects analysis results. For this reason the accuracy and usefulness of a RANS CFD analysis is highly dependent on the experience and rigour of the user. Guidance on which turbulence model is best to use for different types of flow can often be found in code user guides. However, this can be challenging for modelling domains containing a variety of thermal hydraulic phenomena, and under these circumstances it is considered best practice to perform turbulence model sensitivity tests. Further information on different types of turbulence model can be found in Volumes 1, 2 and 3, as well as CSNI (2015). This volume considers the additional considerations needed when modelling liquid metals specifically.

One of the simplest and most robust methods of modelling turbulence is by introducing the concept of 'eddy diffusivity' which is used for the calculation of the time-averaged transport of momentum due to the action of turbulent eddies[13]. The 'turbulent Prandtl number' is then used to relate the transport of heat to the transport of momentum and it is the nature of this relationship that is different for fluids with molecular Prandtl numbers that are significantly less than 1.

In the remainder of this section RANS and Unsteady Reynolds-Averaged Navier-Stokes (URANS) analyses are considered together as the differences between them are the same for liquid metals as for other fluids. A more complete description is given in Volumes 1 and 3.

3.3.2.1 Turbulent Prandtl Number

Just as the Prandtl number represents the ratio between the molecular diffusivity of momentum and heat, the turbulent Prandtl number is defined as the ratio between transport of momentum and heat due to turbulent eddies. Turbulent Prandtl number is relevant to linear eddy viscosity turbulence models as discussed below and and its use in turbulence modelling is described by Kays (1994). Considering a simple, two-dimensional, steady-state form of the Reynolds-averaged equations for momentum and energy[14] (without temperature varying material properties or viscous dissipation) for a boundary layer (from Kays, 1994):

$$\text{Momentum:} \quad u\frac{\partial u}{\partial x} + v\frac{\partial u}{\partial y} + \frac{1}{\rho}\frac{dP}{dx} = \frac{\partial}{\partial y}\left(\nu\frac{\partial u}{\partial y} - \overline{u'v'}\right)$$

$$\text{Energy:} \quad u\frac{\partial t}{\partial x} + v\frac{\partial t}{\partial y} = \frac{\partial}{\partial y}\left(\alpha\frac{\partial t}{\partial y} - \overline{t'v'}\right)$$

Where x and u are parallel to the solid surface and y and v are perpendicular. P is the pressure, ρ is the density and α is the thermal diffusivity. The eddy diffusivity for momentum and heat (ϵ_M and ϵ_H) are then defined to simplify the turbulent momentum and energy fluxes:

$$\overline{u'v'} = -\epsilon_M\frac{\partial u}{\partial y}$$

$$\overline{t'v'} = -\epsilon_H\frac{\partial t}{\partial y}$$

[13] See Volume 3, Section 3.2.6 for general information regarding RANS turbulence modelling.

[14] The Reynolds-averaged form of the Navier-Stokes equations (hence the term RANS) commonly used in CFD modelling and familiar to CFD practitioners. Those unfamiliar with these equations can refer to various text books (e.g. Versteeg and Malalasekera, 2007) for the theory, however, understanding these equations is not required for the majority of this section.

ϵ_M (also called the eddy or turbulent viscosity and given the symbol ν_t in many more recent publications[15]) is commonly evaluated by using, for example, a k - ε model and ϵ_H (often called α_t) is then found using the turbulent Prandtl number (Pr_t):

$$Pr_t = \frac{\epsilon_M}{\epsilon_H}$$

Use of the simplest form of the Reynolds analogy results in a Pr_t of 1. For the moderate and high Prandtl number fluids most commonly encountered, $Pr_t = 0.85$ has been determined to be an appropriate value for use outside of the laminar sublayer (by experiment and DNS modelling). However, Pr_t is only found to be a constant value over regions of the boundary layer where it can be assumed that the temperature profile is logarithmic. This only occurs when the contribution of conduction is negligible (see Kays, 1994 for a fuller explanation).

In liquid metals, conduction plays an important role in heat transfer in turbulent flows up to quite high Reynolds numbers. This complicates the shape of the temperature profile within the boundary layer (and in other regions that would otherwise have a high temperature gradient) and it can no longer be well represented by such a simple relationship. Therefore, whilst there is considerable evidence that a constant Pr_t of 0.85 is sufficient for modelling most fluids, for liquid metals, no such consensus exists and the most appropriate treatment of turbulent Prandtl number is the subject of ongoing research. The non-similarity of the thermal and momentum flow fields suggests that the use of a constant value can lead to large errors in some situations and more complex formulations are proposed (often functions of Reynolds number and molecular Prandtl number).

3.3.2.2 Eddy Viscosity Models

Eddy Viscosity Models (EVMs) are a class of RANS model that represent the turbulence using scalar quantities (including turbulent kinetic energy and a representation of length scale) which are solved for using transport equations. The most common are linear EVMs where the resulting turbulent viscosity is then used to relate the Reynolds stresses to the mean strain via a linear relationship. Linear EVMs come in a variety of forms, although it is variants of the two-equation k - ε and k - ω models that are most commonly used in analysis of internal flow with modern CFD. Different CFD codes contain different variations of these models and different corresponding input parameters. It is important to understand what is available in the code that is being used and theory guides supplied with the code often provide the information required. The use of these models for the analysis of buoyancy influenced flow (including more sophisticated non-linear EVMs) is discussed in Volume 3 and the associated advantages and shortfalls of these models are equally applicable to liquid metals.

For the modelling of liquid metals specifically, it is the use of the Reynolds analogy within these models that introduces additional challenges. Two-equation turbulence models make use of the Reynolds analogy – they formulate equations for the transport of heat due to the action of turbulence directly from those used for the momentum field, by using the turbulent Prandtl number (as described above). For most models, Pr_t is given a default value of 0.85, however, it is often possible for a user to modify this value or to insert an algebraic expression for Pr_t in its place (although this should not be done unless use of an alternative value or expression can be justified).

[15] The nomenclature within the field of turbulence modelling can be inconsistent between publications, for example the term 'turbulent viscosity' is also used for μ_t, where (as for the molecular kinematic and dynamic viscosity) $\nu_t = \mu_t/\rho$.

If a Re-Normalisation Group (RNG) k-ε model is available, then Pr_t is not assumed to be constant, rather it is calculated from the analytical derivation associated with this method. Kays (1994) proposed a simple empirical correlation that fits the RNG values of Pr_t closely and can therefore be used in combination with other turbulence models (where user input is available):

$$Pr_t = \frac{0.7}{Pe_t} + 0.85$$

where

$$Pe_t = \frac{\nu_t}{\nu} Pr$$

is the turbulent Péclet number.

The use of the 'Kays' correlation has been shown to improve the predicted temperature profile in a number of simple liquid metal test cases. However, the validation of this correlation has been for forced convective flow only and it is noted in a number of places (e.g. Roelofs, 2019 and Pacio *et al.*, 2015a) that this type of approach is not likely to be as successful in natural or mixed convective flow.

Manipulation of Pr_t (and other constants present in a two-equation turbulence model) can be used to change the magnitude of the turbulent diffusivity of heat in relation to the turbulent viscosity. However, this approach alone cannot change the limitation of the underlying turbulence model or the fact that the only inputs available for calculations of the eddy diffusivity of heat are those calculated for the eddy diffusivity of momentum. This approach therefore assumes that the length and timescales associated with the turbulent fluctuations in the temperature field are 'similar' to the turbulent fluctuations in the velocity field (i.e. the Reynolds analogy). Otić and Grötzbach (2007) discusses differences between the turbulent timescales for low Pr fluids and the implications for turbulence modelling in more detail. Section 3.3.2.4 describes potential advancements on the standard approach which, whilst not industrially mature, offer potential improvements for liquid metals.

3.3.2.3 Reynolds Stress Models

Reynolds Stress Models (RSMs) (often referred to as stress transport models or second-moment closures) are the most complex and computationally expensive of the RANS turbulence models. They work by solving a separate equation for each component of the Reynolds stress tensor, which do not need to be linearly related to the strain rate tensor. These models are therefore able to capture anisotropic effects that EVMs cannot.

From the perspective of liquid metal modelling, the most basic RSM models still generally employ the Reynolds analogy (via the use of the turbulent Prandtl number) for turbulent heat transport. Therefore, the same deficiencies in the modelling of turbulent heat transport are present as for EVMs. As for other RANS turbulence models it is often possible for a user to modify the value of Pr_t, but there is no single value or expression that is likely to be applicable for all flows.

A more sophisticated approach to the modelling of turbulent heat dissipation in RSM models employs the Generalized Gradient Diffusion Hypothesis (GGDH) which uses anisotropic eddy-diffusivity. This has been shown to give improvements for buoyancy influenced flow (as described in Volume 3), but still includes the concept of 'similarity' between the moment and thermal fields, which needs careful consideration for liquid metals.

3.3.2.4 Modified Approaches to RANS Turbulent Heat Transfer

In an attempt to overcome some of the limitations of common RANS turbulence models for a variety of applications, a number of other models have been developed. Those of most interest to the modelling of liquid metal heat transfer introduce additional scalar quantities to represent the turbulent transport of heat, resulting in either three or four turbulent parameter transport equations. This approach enables the effect of turbulence on the temperature field to be calculated separately and have been shown to improve predictions for liquid metal heat transfer compared with two-equation models (e.g. Otić and Grötzbach, 2007 and Manservisi and Menghini, 2014).

For example, the Algebraic Heat Flux Model (AHFM) is based on an algebraic simplification of the full transport equations for the turbulent heat fluxes (Hanjalić *et al.*, 1996), and retains all of the major generation terms (mean temperature gradients, mean velocity gradients and direct buoyancy effects). This approach (relevant to both EVM and RSM) has shown promising results and is an ongoing area of research (discussed further in Section 4).

However, the additional equations and more complex formulations for turbulent heat flux introduce additional empirical coefficients which need to be determined. Shams *et al.* (2019b) summarises the evolution of a specific example of an implicit AHFM developed during the Thermal Hydraulics of Innovative Nuclear Systems (THINS) and subsequent Simulations and Experiments for the Safety Assessment of MEtal cooled reactors (SESAME) projects in Europe. Successive studies have been undertaken to calibrate the coefficients for different flow phenomena and the work illustrates the challenges of calibrating a complex RANS model.

The majority of these more advanced heat transfer models have not found their way into mainstream CFD codes at this time. The example given in Shams *et al.* (2019b) has previously been implemented in both the commercial STAR-CCM+ code and the open source Code_Saturne, although is not currently available in the released versions[16].

Given the limited track record of all of these models in an industrial context and the variability in their performance, it is strongly recommended that anyone considering using them examines existing validation and calibration evidence in detail. Users may need to repeat or supplement this evidence with additional studies depending on the application of interest.

3.3.2.5 Near-Wall Treatment

For internal flow, the boundary layers adjacent to the solid walls often have a significant effect on the entire flow field. Furthermore, in nuclear thermal hydraulics, the prediction of heat transfer to and from solid surfaces is often an important objective, so appropriate modelling of the near-wall region of the flow in CFD is therefore of high importance.

As introduced in Volume 1, there are broadly two methods for modelling the near-wall region, which are shown in Figure 3.3. In wall-resolved approaches, the near-wall region is meshed with small cells all the way to the wall. For this to work well, the mesh must be sufficiently fine in the wall-normal direction to resolve all portions of the boundary layer, and the turbulence model needs

[16] It is noted that Code_Saturne contains an unusually large range of turbulence modelling options. However, the onus is on the user to validate these models for their application.

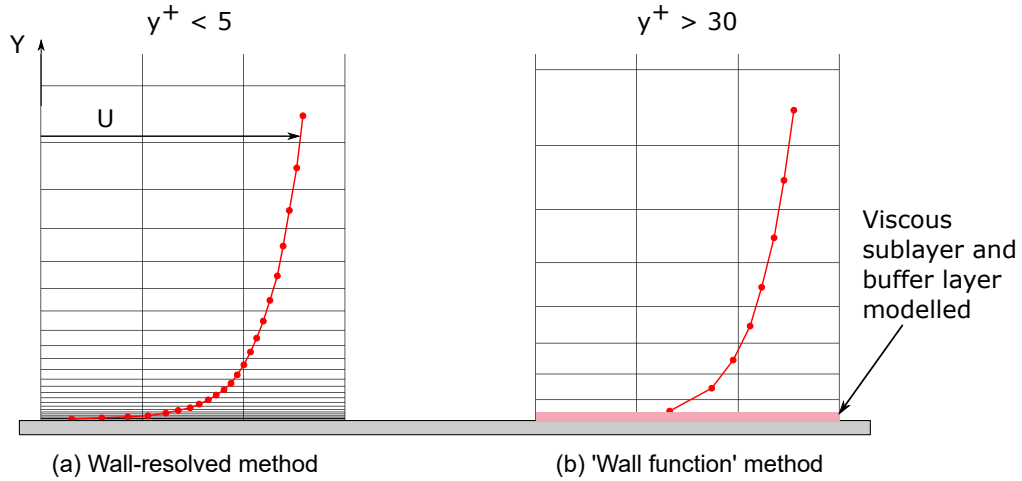

Figure 3.3: Illustration of near-wall treatment methods for a cell-centred CFD code.

to be suitable for near-wall modelling (or appropriately modified in the near-wall region)[17]. This approach generally yields the most accurate results, but depending on the size of the analysis domain and the flow characteristics (e.g. *Re*) it can be computationally expensive[18]. Alternatively, in wall-modelled approaches the boundary layer is not fully resolved (instead it is 'modelled') and a semi-empirical 'wall function' is used to represent the unresolved portion.

As with turbulence models, mainstream CFD codes offer a range of options for near-wall modelling, including combining the two methods described above by switching between them depending on the local mesh refinement and flow parameters. It should be noted that wall treatments are not only used for RANS modelling. LES modelling becomes less computationally expensive if the near-wall region is not fully resolved and LES that is used in an industrial context often employs a form of wall treatment. Like other empirical models, a wall function is only applicable for flow that is broadly in line with the assumptions made in its development (this is the same for all fluids).

Wall functions work by assuming a functional form for the variation in velocity (and temperature) near to the wall that is representative of a typical boundary layer. That is a velocity gradient that is linear in the viscous sublayer and logarithmic through the turbulent portion of the boundary layer. They act on the cells that are in contact with the wall. Away from the wall, the flow variables are calculated directly from the solution of the transport equations. For the cells in contact with the wall, the effect of the wall treatment on the momentum and energy equations depends on the height of the cell centroid (or node, depending on the code) normal to the wall.

In the context of liquid metal modelling, the use of a wall-resolved approach applies the same (or in the case of some models, a modified) turbulence modelling approach as in the mainstream flow, with the same strengths and limitations as previously discussed. However, when applying a wall function there is an extra complication as it is important that the selected wall treatment is able to represent a different thickness for the temperature linear sublayer compared with the velocity field viscous sublayer.

[17] For natural or mixed convection flows, care also needs to be taken regarding the aspect ratio of cells near the wall.
[18] Using a wall-resolved mesh in RANS modelling is often called a 'low Reynolds number' approach, because it is more computationally feasible at low *Re*, and alternative methods work less well at low *Re*.

A number of studies have been carried out to test the applicability of commonly used wall functions, in combination with RANS turbulence models, to modelling liquid metal flow and heat transfer. Maciocco (2002) includes a study examining standard wall functions in three commercial CFD codes and IAEA (2006) presents a number of analyses in which wall functions were used and their impact on the results is discussed[19]. It was found that models exist in mainstream CFD codes that can achieve different velocity and temperature distributions, but that the criteria for the thickness of the temperature linear sublayer (i.e. where the model assumes a switch from a linear temperature profile to a logarithmic one), is inconsistent between codes, and none of the switching points were very close to that predicted by more detailed approaches. The recommended pragmatic approach from Maciocco (2002) is to ensure that wall functions are only used over the region where the thermal boundary layer can be assumed to have an approximately linear profile (thereby avoiding the switching point). A maximum first cell y^+ of 70 (acceptable up to 100) was found to achieve this, but this value may vary for different types of flow and different wall functions.

In modern CFD codes implementing this recommendation is complicated by the use of more advanced wall functions. Some modern wall treatments not only enable switching from a wall function to a low Reynolds number approach depending on the near-wall mesh, but also blend the wall function linear and logarithmic profiles so that a smooth profile is calculated through the buffer layer for all cell sizes. As the approach is blended, rather than a discrete switch between models at a fixed value of y^+ (or $y^\star$), it is not possible to define an exact transition between viscous sublayer and logarithmic layer treatments. However, this does not necessarily make these wall functions unsuitable to use, and the relevant software documentation often provides specific information on how the wall treatments work. For example, in the ANSYS CFX Automatic Wall Treatment method the thermal profile blending (based on the work described in Kader, 1981) is a function of the dimensionless wall distance $y^\star$ and the molecular Prandtl number. When the molecular Prandtl number of the fluid is $\ll 1$, the blending function extends the linear temperature profile to larger cell sizes, thereby achieving an increased thickness of the conduction sublayer. In this particular case, therefore, the recommendation of Maciocco (2002) can still be achieved with a similar maximum y^+.

Many more recent investigations into the applicability of various turbulence models to liquid metals have not included investigations of wall functions (the analyses tend to use a wall-resolved approach). An exception was found in the work of Bieder *et al.* (2018) where both standard and scalable wall functions were used. The work showed little difference between the two approaches, although consideration of wall heat transfer specifically was not the focus of the work.

As for turbulence models, CFD users will need to carefully examine the options available in their code and consider which wall treatments are most appropriate for their study. If they are inexperienced with modelling liquid metals, it is recommended that preliminary basic studies (comparisons of simple cases with relevant benchmark data) are performed to check that the model is functioning as expected.

The implications for near-wall modelling of fluids with $Pr > 1$ are described in Volume 6.

[19] The publication dates of Maciocco (2002) and IAEA (2006) mean that the code specific information may be out of date.

3.3.2.6 Using RANS and URANS Turbulence Models for Liquid Metal Analysis

Despite the various limitations of RANS turbulence models, the computational cost of the alternatives means that they are likely to remain a major part of industrial CFD analysis for at least the next generation of NPPs. For all CFD, especially when using RANS turbulence models, the burden of demonstrating that the modelling approach employed is appropriate for the application of interest lies with the user. The 'best' model for any given application depends on many factors and no code documentation or best practice guide can foresee all circumstances. For the modelling of liquid metals, this is likely to be a more challenging task. It should be recognised at the outset that the level of guidance offered in mainstream code documentation and the level of validation of various models in a liquid metal context will be less than for more conventional fluids.

When selecting a turbulence model it is important to consider the purpose of the analysis. This includes defining the main results of interest and the level of confidence needed in the answers (see Volumes 1, 3 and 4 for CFD model development guidance and the assessment of confidence). In the context of liquid metals, the following general additional advice is offered to the industrial CFD user as a starting point.

1. If the main purpose of the analysis is the prediction of the velocity field, the flow is primarily driven by pressure differences (forced convection) and the temperature variation within the domain of interest is low, then a RANS turbulence model should be selected based on the same considerations as for a $Pr = 1$ fluid. If an EVM is chosen and there is concern that temperature variations may have an influence on the flow (i.e. via buoyancy), then a turbulent Prandtl number (Pr_t) of around 2 may improve the results (Roelofs, 2019), especially at lower Péclet numbers (less than 1000). A sensitivity study varying Pr_t between 0.85 and 5 should give an indication of how much the results of interest are being affected by the specific choice of Pr_t.
2. If the purpose of the analysis is the prediction of the velocity field but it is expected that the outputs of importance will be influenced by buoyancy then the selection of a RANS turbulence model is challenging in any fluid (the recommendations given in Volume 3 are also applicable to liquid metals). The implications for the modelling of liquid metals specifically depend on the nature of the flow field. Reasonable results can be obtained without any specific modifications if the turbulent viscosity throughout the domain is low (Maciocco, 2002). If it is not, then increasing Pr_t to 2 or higher will help to reduce excessive diffusivity of heat. For flow that is highly influenced by buoyancy, the use of an advanced approach to model the turbulent heat flux (such as an appropriately calibrated algebraic heat flux model) in combination with a turbulence model suited to buoyancy influenced flows (as demonstrated in Shams *et al.*, 2019b) or an increased fidelity of approach (i.e. LES) are considered the best ways forward.
3. If the purpose of the analysis includes the prediction of surface heat transfer (i.e. the Nusselt number) then the modelling of the thermal boundary layer is important. For internal liquid metal flow (in a pipe or channel) the thermal boundary layer may encompass the entire solution domain (unlike the momentum boundary layer). Use of the standard $Pr_t = 0.85$ in combination with a wall-resolved approach will usually result in a Nusselt number that is too high (Manservisi and Menghini, 2014). For relatively simple, forced flow the correlation of Kays for Pr_t, described above, has shown good agreement with DNS and experimental

results. Evidence of this can be found in open literature, for example Roelofs *et al.* (2015). However, no such simple correlation is readily available for cases where the surface heat transfer is influenced by buoyancy.

4. If the purpose of the analysis includes the prediction of surface heat transfer and the computational expense of a wall-resolved solution is too high, then wall functions can be used but need to be treated with caution as described in Section 3.3.2.5.
5. In all cases, supplementing a set of RANS and/or URANS studies with one or more LES studies will provide insight into the applicability of a turbulence model. An LES study performed early in a modelling task can be used for turbulence model and input parameter selection and a later study, of a case of high importance, can be used to increase confidence in all of the work.

3.4 Validation and Benchmarking

One of the biggest challenges in engineering analysis can be gaining confidence in the results of complex models. As all models are a mathematical approximation of reality, none of them provide perfectly accurate solutions. Even if the model itself is considered extremely accurate, in real engineering applications aspects of the model input data are often uncertain or unknown. Volume 4 (Confidence and Uncertainty) discusses confidence in nuclear thermal hydraulic analysis across all technologies and is equally applicable to liquid metal cooled reactors. For consideration of how analysis is used in nuclear safety substantiation, Volume 1, Section 2.2 is recommended reading.

This section describes information of value for the analysis of LMFRs. In particular the following types of information may be used to improve confidence in analysis results:

- Similar analysis work.
- High-fidelity analysis results.
- Experimental data from test facilities.
- Operational reactor data.

The published outputs of major projects in aspects of LMFR development often include several of the above. A number of examples of such projects are also included below.

3.4.1 Recent Major Projects

The GIF was established in 2001 to enable international collaboration for next generation reactors. Both SFRs and LFRs (including those cooled by both lead and LBE) are included in the reactor concepts under development within this community. The work of each nation is usually related to a specific reactor under development in that country with the GIF providing a framework of committees and working groups to enable effective collaboration (further description is included in GIF, 2014 and GIF, 2021).

In addition to a large number of specific supporting activities, current SFRs ‘design tracks’ under development listed in GIF (2021) include:

- The Japan Sodium-cooled Fast Reactor (JSFR), Japan.
- The Korea Advanced Liquid Metal Reactor (KALIMER), Korea.

- The European Sodium Fast Reactor (ESFR), Euratom.
- The BN-1200 reactor, Russia.
- The Advanced Fast Reactor-100 (AFR-100) reactor, United States.

Similarly for LFRs, GIF (2021) includes a number of supporting activities, private commercial reactors and reactors for space and/or marine propulsion, as well as national programmes:

- The BREST-OD-300 reactor, Russia.
- The ALFRED reactor, European reactor demonstrator.
- The MYRRHA reactor, Belgium.
- The Small, Sealed, Transportable, Autonomous Reactor (SSTAR), United States.
- The China LEAd-based Research Reactor (CLEAR) project, China.

In addition to the reactor development projects targeted under the GIF framework, other ongoing and historic reactor design activities also produce publications of value. Even those being carried out by specific commercial organisations often involve collaborations which lead to the publication of analysis work. Additionally, work supporting nuclear safety claims is sometimes publicly available once formally submitted to a regulator.

Older reactor programmes, such as those mentioned in Section 1.2, provide sources of test facility and reactor data along with operational experience, improved knowledge of thermal hydraulic phenomena and lower fidelity modelling methods. Current programmes are likely to also include examples of modern analysis. The Indian PFBR and the (recently cancelled) French ASTRID reactor project being notable examples.

Although most ‘major projects’ are focused around a single reactor design, there have also been a number of important initiatives considering thermal hydraulics in a more reactor generic context. For liquid metals, the recent SESAME and previous THINS European collaborative projects are an excellent source of published, state-of-the-art information (e.g. Roelofs (2019) and its references).

3.4.2 Examples of Analysis

When performing an analysis, it is often extremely helpful to learn from the experience of others. If an organisation has carried out similar work in the past, then sources of previous experience within it may be easy to find. However, when using a new method or performing analysis for a new application, this is more difficult. In a research environment it is common practice to start a project with a literature review, however, in an industrial environment this step is not often undertaken. The main reasons for this are usually time and/or budgetary constraints and the perception that little of significant use can be discovered without many weeks of effort. However, much can be achieved in a few days of targetted internet searching. Whilst comparison with examples of similar, published analyses cannot generally be considered as validation, it can assist learning and improve confidence.

A number of examples are provided in this section (and throughout Section 3) as a starting point for those wishing to see what others have done. However, they represent only a small proportion of what is available, and it is strongly recommended that examples that are specifically relevant to the purpose of any analysis are sought. The organisations who have carried out the work included in the sections below have, in many instances, published a variety of work relating to LMFRs.

When using the publications of others to inform your own activities there are few things that it is worth considering:

- Most publications are keen to demonstrate the success of what has been done, however, the most useful examples will also share where things have been tried which were less successful and why they believe this was the case.
- Publications where an author has drawn information from a number of sources and made use of this combined information to increase confidence in their work are of higher value.
- Basing modelling decisions on the findings of a single source (or work from a single organisation) should be avoided if possible. Try to find two or more examples from different organisations.
- Publications describing analysis where there has been no attempt (or acknowledgement of the need) to validate the results, or compare them with other studies, should be viewed with more caution.
- There are many publications that use analysis tools that are not readily available to all industrial engineers.
- Publications of analysis carried out by the developers of a code should be viewed accordingly; whist the analysis is likely to be of good quality, it is hard for the authors to be objective and they may have a commercial or reputational interest in not highlighting shortfalls and challenges.

3.4.2.1 Fuel Assembly and Core Flow Modelling

The fuel is one of the most analysed components in a nuclear reactor for obvious reasons. This is also true in LMFRs and there are a reasonably large selection of publications available containing both computational modelling and data from various test facilities (as described in Section 3.4.4).

The most common method used to analyse fuel assemblies in LWRs in a nuclear safety context is a subchannel code, especially when used in conjunction with a system code. Examples of the development and use of subchannel codes in LMFRs can be found in open literature. However, many subchannel codes are specific to various countries and/or organisations and are not publicly available for general use. A more general description of using subchannel codes in the context of LMFRs can be found in Roelofs (2019).

For more detailed analysis of fuel assemblies in a liquid metal environment, CFD has seen increasing use. In particular, wire-wrapped fuel designs are not employed in current LWRs and therefore many subchannel codes used for existing reactors would not be suitable without considerable modification. CFD provides a good alternative and/or a method to provide information to enable the improvement of subchannel and/or system codes. Recent examples of the modelling of hexagonal arrays of wire-wrapped fuel with RANS CFD:

- Merzari *et al.* (2016) describes a comparison of different RANS turbulence models with an LES benchmark case for a 7-pin bundle.
- Jeong *et al.* (2017) describes RANS modelling of a 127-pin bundle.
- Roelofs *et al.* (2019) and Dovizio *et al.* (2020) both present a summary of work aimed towards the validation of RANS turbulence models in the context of modelling wire-wrapped fuel.

Whilst many LMFRs intend to use closely spaced, wire-wrapped fuel, some (especially lead-cooled designs) are considering assemblies with fuel spacers. These have not received as much recent attention, however, due to their similarity with existing fuel designs; Pacio *et al.* (2015a) provides an example.

Examples of the analysis of fuel assemblies when blocked or distorted are less prevalent than those for normal operations, but Piazza *et al.* (2017) is one such example.

Another relevant aspect of the core flow in an LMFR is the inter-wrapper flow, especially under post-accident decay heat removal conditions. An example of a CFD analysis comparison with test rig data is included in Mathur (2019) and an example of including the inter-wrapper flow into a 'whole core' model is given in Tenchine *et al.* (2012a).

3.4.2.2 Pool and Above Core Modelling

As discussed in Section 2.3, modelling of the large plena in pool type LMFR designs presents particular challenges due to the large variation in the scale of thermal hydraulic phenomena and the potential for highly three-dimensional flow.

Three-dimensional thermal hydraulic modelling of the reactor pools (including the above core region) have been carried using CFD analysis. It is in the nature of a pool type design for the flow patterns in the different regions of the reactor to be influenced by each other, especially where buoyancy has a significant influence on the flow. For cases of interest, it is often necessary to model the entire primary circuit and therefore current CFD models usually incorporate a variety of simplifications. Helpful examples include:

- IAEA (2014a) describes a number of studies using different codes, benchmarked against data from the upper plenum of the Monju Reactor during a turbine trip test.
- Visser *et al.* (2019) describes CFD analysis of a forced flow within a reactor primary circuit and comparison with results from the E-SCAPE facility at SCK CEN, Belgium.
- Zwijsen *et al.* (2019) reports a comparison of CFD analyses with results from the CIRCE test facility (ENEA, Italy) including a natural circulation transient case.

There are fewer examples available of specific modelling of the detailed geometry in the above core region, but recent examples of upper plenum modelling (relating to two very different designs) can be found in Bieder *et al.* (2019) and Choi *et al.* (2015).

3.4.2.3 System Modelling

Although CFD analysis of reactor components has become more feasible in recent years, the analysis of LMFRs using system codes is still essential for the consideration of transient fault scenarios for the next generation of reactors. As described in Section 3.2, there has been considerable recent effort applied to improving the abilities of system codes, including benchmarking codes against historic reactor data. Examples of a number of benchmarks (including both experimental data and system code analysis) are given in Section 3.4.5. Further examples of system code analysis of LMFRs include:

- Stempniewicz *et al.* (2019) includes a comparison of two different system code models for steady-state and transient analysis of the SEALER reactor.

- Bandini *et al.* (2015) includes work to provide validation evidence for the use of RELAP5 and SIMMER-III by comparison with decay heat removal experiments using the CIRCE integral facility.
- Namala and Sumner (2019) describes system code analyses using the SAS4A/SASSYS-1 code with comparison to sodium stratification experiments and CFD results.
- Bubelis *et al.* (2017) describes a variety of different system codes and compares them when used to model an SFR core under steady-state and unprotected loss of flow accident conditions.

3.4.3 High-Fidelity Analyses

Due to the difficulties in gathering highly resolved experimental data in liquid metals, a number of studies have been undertaken using DNS and published as benchmark cases. These are of particular value for the validation of lower fidelity CFD methods, as many details relating to turbulence can be extracted from the DNS analysis. It is often not possible (or extremely expensive) to achieve a comparative level of detail by experiment especially considering the challenges of instrumentation in a prototypical LMFR environment. However, despite access to modern High Performance Computing (HPC) resources, it is still not feasible to perform a complex, high Reynolds number thermal hydraulic analysis with DNS. For this reason, high quality LES analyses are also produced as numerical benchmarking data.

Internationally there has been some effort to start to build a database of published, high quality DNS and LES data to enable the benchmarking of thermal hydraulic modelling tools with a lower computational cost (low Prandtl number examples for simple flow configurations are also included in more general databases). Notable recent examples for liquid metal thermal hydraulics:

- Shams *et al.* (2019c) summarises a set of high-fidelity data produced under the SESAME and MYRRHA Research and Transmutation Endeavour (MYRTE) European collaborative projects for seven different flow configurations designed to be used a numerical benchmark cases.
- Merzari *et al.* (2016) contains a high-fidelity LES analysis of a wire-wrapped fuel assembly.
- Doolaard *et al.* (2015) contains an example of using high-fidelity data as a benchmark for RANS CFD modelling.

As with all modelling, high-fidelity analyses (especially LES models) involve user choices. The quality of the output of these models and their utility as a benchmark is therefore dependent on the origins and original intent of the model. It is advised that anyone wishing to use a published high-fidelity analysis as a benchmark ensures that they have information regarding the context in which the model was produced and (if possible) makes contact with the model originator to check its suitability.

3.4.4 Experimental Data

Despite the increasing potential for the use of high-fidelity modelling methods, there is no better way to gain confidence in analysis results than by validation with suitable experimental data. The best way to achieve this is by a combined programme of specifically targeted analysis and experimentation. It is important to understand that doing the analysis and experiments in a disconnected or sequential manner is not nearly as valuable and performing them in parallel with regular exchanges of information. The benefits of experimental and analytical engineers working together have been highlighted within previous projects (for example in Moreau *et al.*, 2019).

A full description of experimental methods for liquid metals is beyond the scope of this document and, although experience with these fluids has been built up over many decades, the design and operation of liquid metal test facilities is still a specialist area. Instrumentation is a key challenge in a hot, possibly corrosive environment and the visual opacity of the fluids prevent the acquisition of data via windows and optical techniques. Therefore, it is often preferable to use an alternative, easier to handle, fluid for experiments. For isothermal tests, considering purely hydrodynamic phenomena, this has been found to work well (e.g. to determine the pressure drop over fuel bundles, as in Jeong *et al.*, 2017). However, if the focus of the investigation is heat transfer or the phenomena under investigation are influenced by buoyancy, then the low Pr of liquid metals has a significant influence and a fluid such as water is much more difficult to use as a substitute.

NSC (2015) contains a description of measurement techniques for liquid metals, Roelofs (2019) contains chapters on the design and operation of primarily heavy liquid metal facilities and IAEA (2018) contains a recent description of existing experimental facilities in support of LMFR. A summary of liquid metal test facilities is also provided in Frazer-Nash (2019a).

3.4.4.1 The Use of Third Party Experimental Data

When using the results of experimental studies there are a number of challenges that are common to all reactor technologies. For example, the scaling of the experimental data to the physical size and actual conditions of the case of interest is a branch of expertise in its own right (CSNI, 2017 presents detailed assessment of scaling for LWRs). The principles of scaling are the same for liquid metals as for other fluids (e.g. Van Tichelen *et al.*, 2011 and Shin *et al.*, 2021).

Using the results of previously conducted experiments, especially where no dialogue with the engineers who performed those tests is possible, can be very challenging. For example, in the measurement of surface heat transfer the following potential sources of error in the reported results have been identified in Pacio *et al.* (2015b) and Mikityuk (2009):

- Impurities in a liquid metal can result in the deposition of a film on surfaces due to chemical reactions between the impurities, fluid and surface material. Since this film will have a different (lower) conductivity than the fluid or the surface it will affect the heat transfer and the results of the test.
- Improper wetting of the surface and entrained gas will affect the measurement of surface heat transfer. This is more of problem when working with heavy liquid metals due to their higher surface tension.
- Experiments intending to investigate forced convection may in fact have been distorted by

buoyancy at higher heat fluxes. Although the quantitative results for the cases investigated will be correct, the conclusions drawn from the investigations might not be.

- Experimental studies often report derived parameters (such as Nusselt number). In addition to the measured values, these parameters contain fluid material properties and their value is therefore subject to the assumptions made by the author regarding these properties.

Despite the challenges, attempting to validate analysis results with published experimental data is sometimes the best that can achieved in a tight timescale (and is much better than making no attempt to validate the work). It should also be noted that, where a specific experiment has been recently completed, academic and research establishments are often happy to be approached to provide further information, providing their contribution is appropriately acknowledged.

3.4.4.2 Fuel Assembly and Core Experiments

Experiments studying liquid metal flow (especially sodium) in simple geometries have been carried out for research purposes since the early days of LMFR development and are too numerous to list here; a number of examples for pipe and channel flow are given in Section 3.1.

Considering LMFRs specifically, the most highly studied complex component is the fuel assembly. A large number of test facilities exist using either water (or an alternative transparent fluid)[20] as a working fluid or liquid metals. The use of substitute fluids (such as water) has the advantage of enabling optical measurement techniques to be used and isothermal operation at room temperatures. Work investigating specific designs of fuel assembly is often not openly available. However, two examples of recent/current test facilities that have published information using water (or an equivalent fluid) are:

- 61-pin wire-wrapped fuel assembly test facility at Texas A&M University as described in Goth *et al.* (2018) and its references. Additionally, Nguyen *et al.* (2020) describes experimental work investigating flow around local blockages.
- 37-pin wire-wrapped fuel assembly test facility at KAERI as described in Chang *et al.* (2016) and its references.

As previously discussed, experiments with water are good for the investigation of the hydrodynamics but are much less appropriate for determining heat transfer in a liquid metal environment. Due to the challenges of experimentation with liquid metals, fuel assembly test facilities that employ these fluids are less common. However, due to the importance of heat transfer from the core under a variety of circumstances, a number of historic and more recent experiments have been performed, for example:

- 19-pin fuel assembly installed in the NAtural CIrculation Experiment UPgrade (NACIE-UP) facility (ENEA, Italy) described in Di Piazza *et al.* (2016).
- The PLANt Dynamics Test Loop (PLANDTL) sodium test facility (JAEA, Japan) includes the inter-wrapper flow between several 7-pin fuel assemblies as described in Kamide *et al.* (2001).

[20] Alternatives to water are sometimes used to match their index of refraction to that of the solid transparent material used within the area of interest.

- The Technologies for HEavy metal SYStems (THESYS) facility at KALLA (KIT, Germany) also uses 7-pin fuel assemblies and includes inter-wrapper flow (as described in Mathur, 2019 and Uitslag-Doolaard *et al.*, 2019).

In addition to the examples above, Roelofs *et al.* (2013b) summarises a wider range of fuel assembly modelling and testing prior to 2012, including some historic tests from the 1970s and 1980s.

3.4.5 Reactor Data and Large Test Facility Benchmarks

Whereas experience from commercial operation of LMFRs is limited to the sodium-cooled BN-600 and BN-800 reactors in Russia, there is a set of valuable data from transient tests conducted in research and prototype reactors. In general, the findings of reactor transient tests are most suitable for the validation of system codes. This is because these are the most practical methods for predicting complex reactor transients, and prototype reactors lack the detailed instrumentation necessary to achieve robust validation of CFD models. However CFD codes have also been used in a number of examples below.

In particular, data from transient tests conducted in EBR-II, FFTF, Phénix and Monju have been made available to joint research projects coordinated by the IAEA. In such projects, a large number of organisations conduct independent simulations of the transient tests, using an analysis code of their choice under both 'blind' and 'open' conditions[21]. These benchmarks form a useful resource, providing both reactor data presented in a way to enable easy comparison to analytical results, as well as examples of the work of others.

A summary of the input data used by the participants of the benchmark, the relevant test results and the outcomes from the various analyses are collated and published, for example:

- IAEA (2013a) describes a benchmark study for system codes based on a sodium natural circulation test, carried out as part of the Phénix end-of-life testing programme.
- IAEA (2014a) used data from a Monju turbine failure test which involved the transient formation (and movement) of thermal stratification in the upper plenum (for validating CFD methods).
- IAEA (2014b) describes a power shape deformation due to an inadvertent control rod withdrawal from the Phénix end-of-life tests (focused on neutronics modelling).
- IAEA (2017) uses whole plant data from the EBR-II shutdown heat removal tests (from the 1980's) for the validation of system codes, neutronics codes and CFD modelling.
- An IAEA benchmark for system codes is currently underway based on an unprotected loss of flow test performed at the FFTF.

For lead and LBE-cooled systems, there are unfortunately no data from transients in operating power reactors. However, thermal hydraulic performance may be validated using data from large-scale loop and pool experiments. Data from various experiments have been published to different extents for the purposes of code development and benchmarking. For example:

[21] In benchmarks, blind predictions are performed with access only to the plant configuration and boundary conditions; open calculations are performed with the experimental data for the predicted quantities also available, which can be used to improve models.

- NSC (2012) and NSC (2018) describe benchmarking activities for system codes based on data from the Heavy Eutectic liquid metal Loop for the Investigation of Operability and Safety of PEACER (HELIOS) loop (NUTRECK, Korea) for both forced, isothermal flow (Phase 1) and non-isothermal natural convection (Phase 2) tests.
- Castelliti *et al.* (2019) describes the E-SCAPE pool facility (SCK CEN, Belgium) and an initial comparison of the test results with a RELAP5-3D model.
- Grishchenko *et al.* (2020) describes a benchmark aimed at validation of coupled system code and CFD approaches using data from the TALL-3D facility (KTH, Sweden).
- Lorusso *et al.* (2021) uses experimental data from the CIRCE-HERO (ENEA, Italy) integral test facility for the validation of system codes and coupled system code/CFD analyses.
- Forgione *et al.* (2019) details the results of a NACIE-UP benchmark for system codes that was undertaken as part of the SESAME project.
- The IAEA is launching a new benchmark for CFD, system and subchannel codes in 2022 to investigate the transition from forced to natural circulation using the NACIE-UP facility.

4 Future Developments

To conclude the present volume, this section considers how the aspects presented on the preceding pages may change in the future.

System codes are used extensively to specify and justify the design of LWRs based on the decades of development and breadth of validation, and general purpose CFD codes have reached a degree of maturity for the prediction of single-phase heat transfer for common fluids. However, there are currently limitations and uncertainties associated with applying these tools to liquid metal coolants.

Although there has been a resurgence in the design of LMFRs over the past ten years, further development and validation of system codes and CFD analysis is required to increase the level of confidence in these tools for liquid metal reactors. This is an area of active research, which is being strengthened by the requirement for CFD-grade experiments and integral effect tests to support the design of commercial reactors.

In the short term, research and development is required on system codes and turbulent heat transfer models for CFD analysis to improve heat transfer predictions for liquid metals. It is also expected that the use of coupled CFD and system code analyses will increase to better understand and predict the characteristics of areas of complex flow in parts of systems (Volume 2, Section 4).

4.1 System Code Development and Validation

A number of benchmarks have been completed over the past ten years (Section 3.4.5) to assess and validate the capability of system codes to simulate liquid metal natural circulation. These international validation exercises are ongoing through IAEA collaborative research projects, such as the FFTF and NACIE-UP benchmarks.

The benchmark results have demonstrated the improving capability of system codes to simulate liquid metal reactors under normal operation and natural circulation conditions. However, they have also confirmed the difficulty in accurately predicting the flow rate and peak temperatures during natural circulation, especially when thermal stratification occurs in hot pools.

These activities have highlighted the complexity associated with simulating real plants and the impact of user effects on the results. For example, the improvement in the accuracy of predictions from the initial blind solution phase to the final calculation, once the experimental results were made available, demonstrates the sensitivity of the results to modelling choices.

Development and validation of system codes for LMFRs is underway to address these issues and increase confidence in the predictions, which includes improved multiphysics coupling with neutronics due to the increased importance of reactivity feedback and core thermal expansion for

fast reactors. The inability of system codes to predict thermal mixing and stratification in hot pools of LMFRs is being investigated and addressed using a number of different techniques, such as:

- A multi-dimensional flow model is being implemented in some system codes, which is based on a 3D coarse-grid CFD approach with simple models to account for the effects of turbulence (e.g. SAM, Zou *et al.*, 2020).
- Most system codes allow multiscale coupling with CFD codes (Volume 2, Section 3.1), which provides more accurate simulation of 3D buoyancy driven effects but with significantly increased computational expense and transient solution timescales. This multiscale coupling process has been validated against liquid metal experimental data (Li *et al.*, 2019, Grishchenko *et al.*, 2020 and Lorusso *et al.*, 2021) and is part of the NACIE-UP benchmark being launched in 2022 by IAEA.
- Coarse grid CFD tools (Volume 2, Section 4.2) are being developed that combine the advantages of modern CFD and traditional subchannel codes. The novel SubChCFD method (Liu *et al.*, 2019 and Liu *et al.*, 2022) uses well-validated industry standard correlations, similar to those used in subchannel codes, to improve the reliability of the prediction without using a fine near-wall mesh. SubChCFD has the potential to model the whole primary circuity with resolved CFD regions, as required.

The increased use of CFD models within system code simulations for LMFRs puts increased pressure on developing turbulence models and the need for confidence in simulating heat transfer in liquid metals.

4.2 Turbulent Heat Transfer Models

Turbulent heat transfer models (Section 3.3.2.4 and Volume 3, Sections 2.2.4.4 and 3.2.6.5) simulate the turbulent heat transport. The development of algebraic expressions for the turbulent heat flux has shown promising results and is an active area of research that is particularly relevant for low-Prandtl number fluids.

The turbulent heat transfer model options available in most CFD tools are limited. Examples include the implementation of the Simple Gradient Diffusion Hypothesis (SGDH) and GGDH models in Fluent using User Defined Functions (UDFs) (Kumar and Dewan, 2013), and development of an explicit AHFM model in OpenFOAM (Manservisi and Menghini, 2014). Much of the recent development has been undertaken on implicit AHFMs within the SESAME project Roelofs (2019). This includes the AHFM-2005 version that has been implemented in STAR-CCM+, and NRG's new variant of the model called AHFM-NRG+ (Shams *et al.*, 2019a).

It is expected that these models will become more widely available within standard CFD analysis tools (Volume 1, Section 4.5.4) over the next few years. Further validation will then be required to understand and assess their potential benefits for forced, mixed and natural convection heat transfer in low-Prandtl number fluids.

5 References

Bandini G, Polidori M, Meloni P, Tarantino M, Di Piazza I (2015) RELAP5 and SIMMER-III Code Assessment on CIRCE Decay Heat Removal Experiments. *Nuclear Engineering and Design*, 281, 39–50, dx.doi.org/10.1016/j.nucengdes.2014.11.005.

Bieder U, Maillard J, Gorsse Y, Guenadou D (2019) CFD Analysis of the Flow in the MICAS Experimental Facility, a Water Model of the Hot Pool of a Sodium Cooled Fast Reactor. *Nuclear Engineering and Design*, 350, 67–77, dx.doi.org/10.1016/j.nucengdes.2019.04.033.

Bieder U, Ziskind G, Rashkovan A (2018) CFD Analysis and Experimental Validation of Steady State Mixed Convection Sodium Flow. *Nuclear Engineering and Design*, 326, 333–343, dx.doi.org/10.1016/j.nucengdes.2017.11.028.

Bortot S, Mikityuk K, Panadero A, Pelloni S, Alvarez-Velarde F, Lopez D, Fridman E, Cruzado I, et al. (2015a) European Benchmark on the ASTRID-like Low-Void-Effect Core Characterization: Neutronic Parameters and Safety Coefficients. In *Proceedings of ICAPP 2015*.

Bortot S, Suvdantsetseg E, Wallenius J (2015b) BELLA: A Multi-Point Dynamics Code for Safety-Informed Design of Fast Reactors. *Annals of Nuclear Energy*, 85, 228–235, dx.doi.org/10.1016/j.anucene.2015.05.017.

Bubelis E, Schikorr M (2008) Review and Proposal for Best Fit of Wire-Wrapped Fuel Bundle Friction Factor and Pressure Drop Predictions Using Various Existing Correlations. *Nuclear Engineering and Design*, 238(12), 3299–3320, dx.doi.org/10.1016/j.nucengdes.2008.06.024.

Bubelis E, Tosello A, Pfrang W, Schikorr M, Mikityuk K, Panadero A L, Martorell S, Ordóñez J, et al. (2017) System Codes Benchmarking on a Low Sodium Void Effect SFR Heterogeneous Core under ULOF Conditions. *Nuclear Engineering and Design*, 320, 325–345, dx.doi.org/10.1016/j.nucengdes.2017.06.015.

Castelliti D, Tichelen K V, Mirelli F (2019) LBE-Cooled Scaled Pool Facility E-SCAPE: Results and Applications for Code Validation. In *Proceedings of 18th International Topical Meeting on Nuclear Reactor Thermal Hydraulics (NURETH-18)*.

Chacko S, Chung Y M, Choi S K, Nam H Y, Jeong H Y (2011) Large-Eddy Simulation of Thermal Striping in Unsteady Non-Isothermal Triple Jet. *International Journal of Heat and Mass Transfer*, 54(19), 4400–4409, dx.doi.org/10.1016/j.ijheatmasstransfer.2011.05.002.

Chang S K, Euh D J, Choi H S, Kim H, Choi S R, Lee H Y (2016) Flow Distribution and Pressure Loss in Subchannels of a Wire-Wrapped 37-Pin Rod Bundle for a Sodium-Cooled Fast Reactor. *Nuclear Engineering and Technology*, 48(2), 376–385, dx.doi.org/10.1016/j.net.2015.12.013.

Chellapandi P, Velusamy K (2015) Thermal Hydraulic Issues and Challenges for Current and New Generation FBRs. *Nuclear Engineering and Design*, 294, 202–225, dx.doi.org/10.1016/j.nucengdes.2015.09.012.

Cheng L Y (2018) Phenomena Important in Liquid Metal Reactor Simulations. BNL–207816-2018-INRE, Brookhaven National Laboratory, dx.doi.org/10.2172/1460705.

Ching-Jen C, Chiou J S (1981) Laminar and Turbulent Heat Transfer in the Pipe Entrance Region for Liquid Metals. *International Journal of Heat and Mass Transfer*, 24(7), 1179–1189, dx.doi.org/10.1016/0017-9310(81)90167-8.

Choi S K, Kim D E, Ko S H, Lee T H (2015) Large Eddy Simulation of Thermal Striping in the Upper Plenum of the PGSFR. *Journal of Nuclear Science and Technology*, 52(6), 878–886, dx.doi.org/10.1080/00223131.2014.990532.

Chvetsov I, Volkov A (2000) 3-D Thermal Hydraulic Analysis of Transient Heat Removal from Fast Reactor Core Using Immersion Coolers. IAEA-TECDOC-1157, International Atomic Energy Agency.

CSNI (2015) Best Practice Guidelines for the Use of CFD in Nuclear Reactor Safety Applications - Revision. NEA/CSNI/R(2014)11, OECD NEA Committee on the Safety of Nuclear Installations.

CSNI (2017) A State-of-the-Art Report on Scaling in System Thermal-Hydraulics Applications to Nuclear Reactor Safety and Design. NEA/CSNI/R(2016)14, OECD NEA Committee on the Safety of Nuclear Installations.

David D K, Mangarjuna Rao P, Nashine B, Selvaraj P (2017) Numerical Simulation of Post Accident Heat Removal in a Typical Pool-Type SFR under Severe Core Relocation Scenario. *Progress in Nuclear Energy*, 101, 224–234, dx.doi.org/10.1016/j.pnucene.2017.07.011.

De Bruyn D, Abderrahim H A, Baeten P, Leysen P (2015) The MYRRHA ADS Project in Belgium Enters the Front End Engineering Phase. *Physics Procedia*, 66, 75–84, dx.doi.org/10.1016/j.phpro.2015.05.012.

Del Giacco M, Weisenburger A, Mueller G (2014) Fretting Corrosion of Steels for Lead Alloys Cooled ADS. *Journal of Nuclear Materials*, 450(1), 225–236, dx.doi.org/10.1016/j.jnucmat.2013.07.005.

Deloffre P, Terlain A, Barbier F (2002) Corrosion and Deposition of Ferrous Alloys in Molten Lead–Bismuth. *Journal of Nuclear Materials*, 301(1), 35–39, dx.doi.org/10.1016/S0022-3115(01)00724-3.

Di Piazza I, Angelucci M, Marinari R, Tarantino M, Forgione N (2016) Heat Transfer on HLM Cooled Wire-Spaced Fuel Pin Bundle Simulator in the NACIE-UP Facility. *Nuclear Engineering and Design*, 300, 256–267, dx.doi.org/10.1016/j.nucengdes.2016.02.008.

Doolaard H, Shams A, Roelofs F, Van Tichelen K, Keijers S, De Ridder J, Degroote J, Vierendeels J, et al. (2015) CFD Benchmark for a Heavy Liquid Metal Fuel Assembly. In *NURETH-16*.

Dovizio D, Mikuž B, Shams A, Roelofs F (2020) Validating RANS to Predict the Flow Behavior in Wire-Wrapped Fuel Assemblies. *Nuclear Engineering and Design*, 356, 110376, dx.doi.org/10.1016/j.nucengdes.2019.110376.

El-Genk M S, Schriener T M (2017) A Review of Experimental Data and Heat Transfer Correlations for Parallel Flow of Alkali Liquid Metals and Lead-Bismuth Eutectic in Bundles. *Nuclear Engineering and Design*, 317, 199–219, dx.doi.org/10.1016/j.nucengdes.2017.03.028.

Fanning T H, Brunett A J, Sumner T (2017) The SAS4A/SASSYS-1 Safety Analysis Code System, Version 5. ANL/NE–16/19, Argonne National Laboratory, dx.doi.org/10.2172/1352187.

Fink J, Leibowitz L (1995) Thermodynamic and Transport Properties of Sodium Liquid and Vapor. ANL/RE–95/2, 94649, Argonne National Laboratory, dx.doi.org/10.2172/94649.

Forgione N, Martelli D, Barone G, Giannetti F, Lorusso P, Hollands T, Papukchiev A, Polidori M, et al. (2019) Post-Test Simulations for the NACIE-UP Benchmark by STH Codes. *Nuclear Engineering and Design*, 353, 110279, dx.doi.org/10.1016/j.nucengdes.2019.110279.

Frazer-Nash (2019a) Project FORTE - Nuclear Thermal Hydraulics Research & Development Review of Thermal Hydraulic Test Facilities. FNC 53798/46969R Issue 1, Frazer-Nash Consultancy.

Frazer-Nash (2019b) Project FORTE - Nuclear Thermal Hydraulics Research Development: University of Manchester Research on the Aerosol-Laden Argon Cover Gas Region above the Sodium Pool of an LMFBR. FNC 53798/48652R Issue 1, Frazer-Nash Consultancy.

Gerschenfeld A (2019) Multiscale and Multiphysics Simulation of Sodium Fast Reactors: From Model Development to Safety Demonstration. In *Proceedings of 18th International Topical Meeting on Nuclear Reactor Thermal Hydraulics (NURETH-18)*.

GIF (2014) Technology Roadmap Update for Generation IV Nuclear Energy Systems. Generation IV International Forum.

GIF (2021) 2020 Annual Report. Generation IV International Forum.

Gopala V, Roelofs F (2009) Numerical Simulation of Liquid Lead Sloshing in the ELSY Reactor Vessel. In *5th International Workshop on Materials for HLM-Cooled Reactors and Related Technologies (HeLiMeRT)*.

Goth N, Jones P, Nguyen D, Vaghetto R, Hassan Y, Obabko A, Merzari E, Fischer P (2018) Comparison of Experimental and Simulation Results on Interior Subchannels of a 61-Pin Wire-Wrapped Hexagonal Fuel Bundle. *Nuclear Engineering and Design*, 338, 130–136, dx.doi.org/10.1016/j.nucengdes.2018.08.002.

Grishchenko D, Papukchiev A, Liu C, Geffray C, Polidori M, Kööp K, Jeltsov M, Kudinov P (2020) TALL-3D Open and Blind Benchmark on Natural Circulation Instability. *Nuclear Engineering and Design*, 358, 110386, dx.doi.org/10.1016/j.nucengdes.2019.110386.

Grötzbach G (2013) Challenges in Low-Prandtl Number Heat Transfer Simulation and Modelling. *Nuclear Engineering and Design*, 264, 41–55, dx.doi.org/10.1016/j.nucengdes.2012.09.039.

Hanjalić K, Kenjereš S, Durst F (1996) Natural Convection in Partitioned Two-Dimensional Enclosures at Higher Rayleigh Numbers. *International Journal of Heat and Mass Transfer*, 39(7), 1407–1427, dx.doi.org/10.1016/0017-9310(95)00219-7.

Hua T Q, Lee S J, Liao J, Moisseytsev A, Ferroni P, Karahan A, Paik C Y, Tentner A M, et al. (2020) Development of Mechanistic Source Term Analysis Tool SAS4A-FATE for Lead- and Sodium-Cooled Fast Reactors. *Nuclear Technology*, 206(2), 206–217, dx.doi.org/10.1080/00295450.2019.1598715.

Huang X, He S (2019) Numerical Modelling of Cover Gas Thermal Hydraulics in Sodium-Cooled

Fast Reactors. *Nuclear Engineering and Design*, 355, 110347, dx.doi.org/10.1016/j.nucengdes.2019.110347.

IAEA (2002) Comparative Assessment of Thermophysical and Thermohydraulic Characteristics of Lead, Lead-Bismuth and Sodium Coolants for Fast Reactors. IAEA-TECDOC-1289, International Atomic Energy Agency.

IAEA (2006) Theoretical and Experimental Studies of Heavy Liquid Metal Thermal Hydraulics. IAEA-TECDOC-1520, International Atomic Energy Agency.

IAEA (2008) Liquid Metal Cooled Reactors: Experience in Design and Operation. IAEA-TECDOC-1569, International Atomic Energy Agency.

IAEA (2012) Liquid Metal Coolants for Fast Reactors Cooled by Sodium, Lead and Lead-Bismuth Eutectic. Nuclear Energy Series NP-T-1.6, International Atomic Energy Agency.

IAEA (2013a) Benchmark Analyses on the Natural Circulation Test Performed during the PHENIX End-of-Life Experiments. IAEA-TECDOC-1703, International Atomic Energy Agency.

IAEA (2013b) Challenges Related to the Use of Liquid Metal and Molten Salt Coolants in Advanced Reactors. IAEA-TECDOC-1696, International Atomic Energy Agency.

IAEA (2013c) Status of Fast Reactor Research and Technology Development. IAEA-TECDOC-1691, International Atomic Energy Agency.

IAEA (2014a) Benchmark Analyses of Sodium Natural Convection in the Upper Plenum of the Monju Reactor Vessel. IAEA-TECDOC-1754, International Atomic Energy Agency.

IAEA (2014b) Benchmark Analyses on the Control Rod Withdrawal Tests Performed during the PHÉNIX End-of-Life Experiments. IAEA-TECDOC-1742, International Atomic Energy Agency.

IAEA (2017) Benchmark Analysis of EBR-II Shutdown Heat Removal Tests. IAEA-TECDOC-1819, International Atomic Energy Agency.

IAEA (2018) Experimental Facilities in Support of Liquid Metal Cooled Fast Neutron Systems. Nuclear Energy Series NP-T-1.15, International Atomic Energy Agency.

Incropera F P, DeWitt D P, Bergman T L, Lavine A S (2011) Fundamentals of Heat and Mass Transfer. Seventh edition, John Wiley & Sons.

Jackson J (1983) Turbulent Mixed Convection Heat Transfer to Liquid Sodium. *International Journal of Heat and Fluid Flow*, 4(2), 107–111, dx.doi.org/10.1016/0142-727X(83)90011-5.

Jackson J D, Axcell B P, Walton A (1994) Mixed-Convection Heat Transfer to Sodium in a Vertical Pipe. *Experimental Heat Transfer*, 7(1), 71–90, dx.doi.org/10.1080/08916159408946473.

Jaeger W (2017a) Empirical Models for Liquid Metal Heat Transfer in the Entrance Region of Tubes and Rod Bundles. *Heat and Mass Transfer*, 53(5), 1667–1684, dx.doi.org/10.1007/s00231-016-1929-8.

Jaeger W (2017b) Heat Transfer to Liquid Metals with Empirical Models for Turbulent Forced Convection in Various Geometries. *Nuclear Engineering and Design*, 319, 12–27, dx.doi.org/10.1016/j.nucengdes.2017.04.028.

Jaeger W, Hering W, Lux M (2015a) On the Liquid Metal Heat Transfer in Annular Channels: Review, Proposal and Validation of Empirical Models. In *Proceedings of 16th International Topical Meeting on Nuclear Reactor Thermal Hydraulics (NURETH-16)*.

Jaeger W, Hering W, Lux M, Portes F (2015b) Liquid Metal Thermal Hydraulics in Rectangular Ducts: Review, Proposal and Validation of Empirical Models. *The Proceedings of the 23rd International Conference on Nuclear Engineering (ICONE-23)*, 2015.23, dx.doi.org/10.1299/jsmeicone.2015.23._ICONE23-1_56.

Jeong J H, Song M S, Lee K L (2017) CFD Investigation of Three-Dimensional Flow Phenomena in a JAEA 127-Pin Wire-Wrapped Fuel Assembly. *Nuclear Engineering and Design*, 323, 166–184, dx.doi.org/10.1016/j.nucengdes.2017.08.008.

Kader B A (1981) Temperature and Concentration Profiles in Fully Turbulent Boundary Layers. *International Journal of Heat and Mass Transfer*, 24(9), 1541–1544, dx.doi.org/10.1016/0017-9310(81)90220-9.

Kakaç S, Shah R K, Aung W (1987) Handbook of Single-Phase Convective Heat Transfer. Wiley.

Kamide H, Hayashi K, Isozaki T, Nishimura M (2001) Investigation of Core Thermohydraulics in Fast Reactors—Interwrapper Flow during Natural Circulation. *Nuclear Technology*, 133(1), 77–91, dx.doi.org/10.13182/NT01-A3160.

Kays W M (1994) Turbulent Prandtl Number—Where Are We? *Journal of Heat Transfer*, 116(2), 284–295, dx.doi.org/10.1115/1.2911398.

Kimura N, Miyakoshi H, Kamide H (2007) Experimental Investigation on Transfer Characteristics of Temperature Fluctuation from Liquid Sodium to Wall in Parallel Triple-Jet. *International Journal of Heat and Mass Transfer*, 50(9), 2024–2036, dx.doi.org/10.1016/j.ijheatmasstransfer.2006.09.030.

Kumar R, Dewan A (2013) Assessment of Buoyancy-Corrected Turbulence Models for Thermal Plumes. *Engineering Applications of Computational Fluid Mechanics*, 7(2), 239–249, dx.doi.org/10.1080/19942060.2013.11015467.

Li S, Gerschenfeld A, Bernard O, Sageaux T (2019) Onset of Natural Convection in a Sodium-Cooled Fast Reactor during a Station Black-out: Blind Benchmark of Safety Assessment Using Multi-Scale Coupled Thermal- Hydraulics Codes. In *Proceedings of 18th International Topical Meeting on Nuclear Reactor Thermal Hydraulics (NURETH-18)*.

Liao J, Ferroni P, Wright R F, Bachrach U, Scobel J H, Sofu T, Tentner A M, Lee S J, et al. (2021) Development of Phenomena Identification and Ranking Table for Westinghouse Lead Fast Reactor's Safety. *Progress in Nuclear Energy*, 131, 103577, dx.doi.org/10.1016/j.pnucene.2020.103577.

Liu B, He S, Moulinec C, Uribe J (2019) Sub-Channel CFD for Nuclear Fuel Bundles. *Nuclear Engineering and Design*, 355, 110318, dx.doi.org/10.1016/j.nucengdes.2019.110318.

Liu B, He S, Moulinec C, Uribe J (2022) A Coarse-Grid Sub-Channel CFD Modelling for the Flow in a 5x5 Rod Bundle. In *Proceedings of 19th International Topical Meeting on Nuclear Reactor Thermal Hydraulics (NURETH-19)*.

Liu Y, Hu R (2020) Benchmark Modeling and Simulation of the FFTF LOFWOS Test #13 Using SAM. ANL/NSE-20/8, Argonne National Laboratory, dx.doi.org/10.2172/1671789.

Lodi F, Grasso G, Mattioli D, Sumini M (2016) ANTEO+: A Subchannel Code for Thermal-Hydraulic Analysis of Liquid Metal Cooled Systems. *Nuclear Engineering and Design*, 301, 128–152, dx.doi.org/10.1016/j.nucengdes.2016.03.001.

Lorusso P, Del Nevo A, Narcisi V, Giannetti F, Caruso G, Zwijsen K, Breijder P, Hamidouche T, et al. (2021) Total Loss of Flow Benchmark in CIRCE-HERO Integral Test Facility. *Nuclear Engineering and Design*, 376, 111086, dx.doi.org/10.1016/j.nucengdes.2021.111086.

Maciocco L (2002) Assessment of Turbulence Models for Heavy Liquid Metals in Computational Fluid Dynamics (WP 7 of the ASCHLIM Project). Centre for Advanced Studies, Research and Development in Sardinia, Italy.

Manservisi S, Menghini F (2014) A CFD Four Parameter Heat Transfer Turbulence Model for Engineering Applications in Heavy Liquid Metals. *International Journal of Heat and Mass Transfer*, 69, 312–326, dx.doi.org/10.1016/j.ijheatmasstransfer.2013.10.017.

Marth W (1993) The Story of the European Fast Reactor Cooperation. KfK 5255, Kernforschungszentrum Karlsruhe.

Mathur A (2019) Inter-Wrapper Flow CFD Approach. SESAME D2.15, NRG.

Merzari E, Fischer P, Yuan H, Van Tichelen K, Keijers S, De Ridder J, Degroote J, Vierendeels J, et al. (2016) Benchmark Exercise for Fluid Flow Simulations in a Liquid Metal Fast Reactor Fuel Assembly. *Nuclear Engineering and Design*, 298, 218–228, dx.doi.org/10.1016/j.nucengdes.2015.11.002.

Mikityuk K (2009) Heat Transfer to Liquid Metal: Review of Data and Correlations for Tube Bundles. *Nuclear Engineering and Design*, 239(4), 680–687, dx.doi.org/10.1016/j.nucengdes.2008.12.014.

Moreau V, Profir M, Alemberti A, Frignani M, Merli F, Belka M, Frybort O, Melichar T, et al. (2019) Pool CFD Modelling: Lessons from the SESAME Project. *Nuclear Engineering and Design*, 355, 110343, dx.doi.org/10.1016/j.nucengdes.2019.110343.

Mui T, Hu R, Zhang G (2019) Uncertainty Quantification on SAM Simulations of EBR-II Loss-of-Flow Tests. In *Proceedings of 18th International Topical Meeting on Nuclear Reactor Thermal Hydraulics (NURETH-18)*.

Myrillas K, Planquart P, Simonini A, Buchlin J M, Schyns M (2017) CFD and Experimental Investigation of Sloshing Parameters for the Safety Assessment of HLM Reactors. *Nuclear Engineering and Design*, 312, 317–326, dx.doi.org/10.1016/j.nucengdes.2016.06.042.

Nagaso M, Moysan J, Lhuillier C, Jeannot J P (2021) Simulation of Fluid Dynamics Monitoring Using Ultrasonic Measurements. *Applied Sciences*, 11(15), 7065, dx.doi.org/10.3390/app11157065.

Namala S, Sumner T (2019) Modelling Thermal Stratification in Upper Plenum of Sodium Fast Reactor Using Systems Code SAS4A/SASSYS-1 and Using CFD. In *Proceedings of 18th International Topical Meeting on Nuclear Reactor Thermal Hydraulics (NURETH-18)*.

Narcisi V, Giannetti F, Subioli A, Del Nevo A, Caruso G (2020) RELAP5-3D Three-Dimensional Analysis Based on PHÉNIX Dissymmetric Transient Test. *Journal of Nuclear Engineering and Radiation Science*, 6(1), 011301, dx.doi.org/10.1115/1.4044847.

Natesan K, Kasinathan N, Velusamy K, Selvaraj P, Chellapandi P, Chetal S C (2011) Dynamic Simulation of Accidental Closure of Intermediate Heat Exchanger Isolation Valve in a Pool Type LMFBR. *Annals of Nuclear Energy*, 38(4), 748–756, dx.doi.org/10.1016/j.anucene.2010.12.005.

Nguyen T, Vaghetto R, Hassan Y (2020) Experimental Investigation of Turbulent Wake Flows in a Helically Wrapped Rod Bundle in Presence of Localized Blockages. *Physics of Fluids*, 32(7), 075113, dx.doi.org/10.1063/5.0008589.

NSC (2012) Benchmarking of Thermal-Hydraulic Loop Models for Lead-Alloy-Cooled Advanced Nuclear Energy Systems. Phase I: Isothermal Forced Convection Case. NEA/NSC/R(2012)17, OECD NEA Nuclear Science Committee.

NSC (2015) Handbook on Lead-Bismuth Eutectic Alloy and Lead Properties, Materials Compatibility, Thermal-Hydraulics and Technologies. 7268, OECD NEA Nuclear Science Committee.

NSC (2018) Benchmarking of Thermal-Hydraulic Loop Models for Lead-Alloy-Cooled Advanced Nuclear Energy Systems. Phase II: Natural Convection. NEA/NSC/R(2018)1, OECD NEA Nuclear Science Committee.

Otić I, Grötzbach G (2007) Turbulent Heat Flux and Temperature Variance Dissipation Rate in Natural Convection in Lead-Bismuth. *Nuclear Science and Engineering*, 155(3), 489–496, dx.doi.org/10.13182/NSE07-A2679.

Pacio J, Daubner M, Fellmoser F, Litfin K, Wetzel T (2016) Experimental Study of Heavy-Liquid Metal (LBE) Flow and Heat Transfer along a Hexagonal 19-Rod Bundle with Wire Spacers. *Nuclear Engineering and Design*, 301, 111–127, dx.doi.org/10.1016/j.nucengdes.2016.03.003.

Pacio J, Daubner M, Fellmoser F, Litfin K, Wetzel T (2018) Heat Transfer Experiment in a Partially (Internally) Blocked 19-Rod Bundle with Wire Spacers Cooled by LBE. *Nuclear Engineering and Design*, 330, 225–240, dx.doi.org/10.1016/j.nucengdes.2018.01.034.

Pacio J, Daubner M, Wetzel T, Uitslag-Doolaard H, Mathur A, Roelofs F (2019) Inter-Wrapper Flow: LBE Experiments and Simulations. In *Proceedings of 18th International Topical Meeting on Nuclear Reactor Thermal Hydraulics (NURETH-18)*.

Pacio J, Litfin K, Batta A, Viellieber M, Class A, Doolaard H, Roelofs F, Manservisi S, et al. (2015a) Heat Transfer to Liquid Metals in a Hexagonal Rod Bundle with Grid Spacers: Experimental and Simulation Results. *Nuclear Engineering and Design*, 290, 27–39, dx.doi.org/10.1016/j.nucengdes.2014.11.001.

Pacio J, Marocco L, Wetzel T (2015b) Review of Data and Correlations for Turbulent Forced Convective Heat Transfer of Liquid Metals in Pipes. *Heat and Mass Transfer*, 51(2), 153–164, dx.doi.org/10.1007/s00231-014-1392-3.

Parthasarathy U, Sundararajan T, Balaji C, Velusamy K, Chellapandi P, Chetal S (2012) Decay Heat Removal in Pool Type Fast Reactor Using Passive Systems. *Nuclear Engineering and Design*, 250, 480–499, dx.doi.org/10.1016/j.nucengdes.2012.05.014.

Piazza I D, Marinari R, Forgione N, Magugliani F, Borreani W, Lomonaco G, Doolaard H, Roelofs F, et al. (2017) CFD Analyses of the Internal Blockage in the NACIE-UP Fuel Pin Bundle Simulator. In *Proceedings of 17th International Topical Meeting on Nuclear Reactor Thermal Hydraulics (NURETH-17)*.

Raj M, Velusamy K, Maity R K (2016) Thermal Hydraulic Investigations on Porous Blockage in a Prototype Sodium Cooled Fast Reactor Fuel Pin Bundle. *Nuclear Engineering and Design*, 303, 88–108, dx.doi.org/10.1016/j.nucengdes.2016.04.008.

Rehme K (1973) Pressure Drop Correlations for Fuel Element Spacers. *Nuclear Technology*, 17(1), 15–23, dx.doi.org/10.13182/NT73-A31250.

Roelofs F (2019) Thermal Hydraulics Aspects of Liquid Metal Cooled Nuclear Reactors. Woodhead.

Roelofs F, Gopala V, Van Tichelen K, Cheng X, Merzari E, Pointer W D (2013a) Status and Future Challenges of CFD for Liquid Metal Cooled Reactors. In **Keijers S** (editor) *International Conference on Fast Reactors and Related Fuel Cycles: Safe Technologies and Sustainable Scenarios (FR13)*.

Roelofs F, Gopala V R, Jayaraju S, Shams A, Komen E (2013b) Review of Fuel Assembly and Pool Thermal Hydraulics for Fast Reactors. *Nuclear Engineering and Design*, 265, 1205–1222, dx.doi.org/10.1016/j.nucengdes.2013.07.018.

Roelofs F, Shams A, Otic I, Böttcher M, Duponcheel M, Bartosiewicz Y, Lakehal D, Baglietto E, et al. (2015) Status and Perspective of Turbulence Heat Transfer Modelling for the Industrial Application of Liquid Metal Flows. *Nuclear Engineering and Design*, 290, 99–106, dx.doi.org/10.1016/j.nucengdes.2014.11.006.

Roelofs F, Uitslag-Doolaard H, Dovizio D, Mikuz B, Shams A, Bertocchi F, Rohde M, Pacio J, et al. (2019) Towards Validated Prediction with RANS CFD of Flow and Heat Transport in a Wire-Wrap Fuel Assembly. *Nuclear Engineering and Design*, 353, 110273, dx.doi.org/10.1016/j.nucengdes.2019.110273.

Rogers G F C, Mayhew Y (1992) Engineering Thermodynamics: Work and Heat Transfer. Fourth edition, Prentice Hall.

Romatoski R, Hu L (2017) Fluoride Salt Coolant Properties for Nuclear Reactor Applications: A Review. *Annals of Nuclear Energy*, 109, 635–647, dx.doi.org/10.1016/j.anucene.2017.05.036.

Shams A, De Santis A, Koloszar L, Villa Ortiz A, Narayanan C (2019a) Status and Perspectives of Turbulent Heat Transfer Modelling in Low-Prandtl Number Fluids. *Nuclear Engineering and Design*, 353, 110220, dx.doi.org/10.1016/j.nucengdes.2019.110220.

Shams A, De Santis A, Roelofs F (2019b) An Overview of the AHFM-NRG Formulations for the Accurate Prediction of Turbulent Flow and Heat Transfer in Low-Prandtl Number Flows. *Nuclear Engineering and Design*, 355, 110342, dx.doi.org/10.1016/j.nucengdes.2019.110342.

Shams A, Roelofs F, Niceno B, Guo W, Angeli D, Stalio E, Fregni A, Duponcheel M, et al. (2019c) Reference Numerical Database for Turbulent Flow and Heat Transfer in Liquid Metals. *Nuclear Engineering and Design*, 353, 110274, dx.doi.org/10.1016/j.nucengdes.2019.110274.

Shin Y H, Park J, Hur J, Jeong S, Hwang I S (2021) PILLAR: Integral Test Facility for LBE-Cooled Passive Small Modular Reactor Research and Computational Code Benchmark. *Nuclear Engineering and Technology*, 53(11), 3580–3596, dx.doi.org/10.1016/j.net.2021.05.024.

Sobolev V (2011) Database of Thermophysical Properties of Liquid Metal Coolants for GEN-IV. SCK-CEN-BLG-1069, Belgian Nuclear Research Center SCK CEN.

Stempniewicz M M, Zwijsen K, Roelofs F, Wallenius J, Bortot S, Mickus I (2019) Thermal-Hydraulic Analysis of SEALER under Steady-State and Accidental Scenarios. In *SESAME International Workshop*, p. 14.

Tashlykov O L, Dolgii Y F, Sesekin A N (2021) Optimization of Refueling Times in Fast Neutron Reactors. *IOP Conference Series: Materials Science and Engineering*, 1089(1), 012006, dx.doi.org/10.1088/1757-899X/1089/1/012006.

Tenchine D (2010) Some Thermal Hydraulic Challenges in Sodium Cooled Fast Reactors. *Nuclear Engineering and Design*, 240(5), 1195–1217, dx.doi.org/10.1016/j.nucengdes.2010.01.006.

Tenchine D, Barthel V, Bieder U, Ducros F, Fauchet G, Fournier C, Mathieu B, Perdu F, et al. (2012a) Status of TRIO_U Code for Sodium Cooled Fast Reactors. *Nuclear Engineering and Design*, 242, 307–315, dx.doi.org/10.1016/j.nucengdes.2011.10.026.

Tenchine D, Baviere R, Bazin P, Ducros F, Geffraye G, Kadri D, Perdu F, Pialla D, et al. (2012b) Status of CATHARE Code for Sodium Cooled Fast Reactors. *Nuclear Engineering and Design*, 245, 140–152.

Tenchine D, Fournier C, Dolias Y (2014) Gas Entrainment Issues in Sodium Cooled Fast Reactors. *Nuclear Engineering and Design*, 270, 302–311.

Todreas N E, Kazimi M S (2021) Nuclear Systems Volume I: Thermal Hydraulic Fundamentals. Third edition, CRC Press, dx.doi.org/10.1201/9781351030502.

Uitslag-Doolaard H, Roelofs F, Pacio J, Batta A (2019) Experiment Design to Assess the Inter-Wrapper Heat Transfer in LMFR. *Nuclear Engineering and Design*, 341, 297–305, dx.doi.org/10.1016/j.nucengdes.2018.11.019.

Ushakov P A, Zhukov A V, Matyukhin N M (1977) Heat Transfer to Liquid Metals in Regular Arrays of Fuel Elements. *High Temperature*, 15(5), 868–873.

Van Tichelen K, Vanderhaegen M, Jayaraju S, Keijers S, Roelofs F, Greco M (2011) Scaling Analysis for the European Heavy Liquid Metal Scaled Pool Facility Escape. In *The 14th International Topical Meeting on Nuclear Reactor Thermalhydraulics*.

Velusamy K, Chellapandi P, Chetal S C, Raj B (2010) Overview of Pool Hydraulic Design of Indian Prototype Fast Breeder Reactor. *Sadhana*, 35(2), 97–128, dx.doi.org/10.1007/s12046-010-0022-0.

Versteeg H K, Malalasekera W (2007) An Introduction to Computational Fluid Dynamics: The Finite Volume Method. Second edition, Pearson Education.

Visser D C, Roelofs F, Mirelli F, Tichelen K V (2019) Validation of CFD Analyses against Pool Experiments E-SCAPE. In *Proceedings of 18th International Topical Meeting on Nuclear Reactor Thermal Hydraulics (NURETH-18)*.

Wagner W, Cooper J R, Dittmann A, Kijima J, Kretzschmar H J, Kruse A, Mareš R, Oguchi K, et al. (2000) The IAPWS Industrial Formulation 1997 for the Thermodynamic Properties of Water and Steam. *Journal of Engineering for Gas Turbines and Power*, 122(1), 150–184, dx.doi.org/10.1115/1.483186.

Waltar A E, Todd D R, Tsvetkov P V (editors) (2012) Fast Spectrum Reactors. Springer.

Yamano H, Fujita S, Tobita Y, Kondo S, Morita K, Sugaya M, Mizuno M, Hosono S, et al. (2003) SIMMER-IV: A Three-Dimensional Computer Program for LMFR Core Disruptive Accident Analysis. Version 2. A Model Summary and Program Description. JNC-TN–9400-2003-070, Japan Nuclear Cycle Development Inst.

Zhang J (2009) A Review of Steel Corrosion by Liquid Lead and Lead–Bismuth. *Corrosion Science*, 51(6), 1207–1227, dx.doi.org/10.1016/j.corsci.2009.03.013.

Zou L, Nunez D, Hu R (2020) Development and Validation of SAM Multi-Dimensional Flow Model for Thermal Mixing and Stratification Modeling. ANL-NSE-20/19, Argonne National Laboratory, dx.doi.org/10.2172/1671335.

Zrodnikov A, Chitaykin V, Gromov B, Grigoryv O, Dedoul A, Toshinsky G, Dragunov Y, Stepanov V (2000) Use of Russian Technology of Ship Reactors with Lead-Bismuth Coolant in Nuclear Power. IAEA-TECDOC-1172, International Atomic Energy Agency.

Zwijsen K, Dovizio D, Moreau V, Roelofs F (2019) CFD Modelling of the CIRCE Facility. *Nuclear Engineering and Design*, 353, 110277, dx.doi.org/10.1016/j.nucengdes.2019.110277.

6 Nomenclature

Latin Symbols

A	Area, m^2
At	Atwood number ($At = (\rho_1 - \rho_2)/(\rho_1 + \rho_2)$)
Bi	Biot number ($Bi = hL/k_s$)
c_p, c_v	Specific heat at constant pressure or volume, $\mathrm{J\,kg^{-1}\,K^{-1}}$
d or D	Diameter ($D_h = 4A_{cs}/p_{cs}$ for hydraulic diameter), m
f	Darcy-Weisbach friction factor
Fo	Fourier number ($Fo = \alpha_s t/L^2$)
Gr	Grashof number ($Gr = gL^3\Delta\rho/\nu^2\rho = gL^3\beta\Delta T/\nu^2$, using the Boussinesq approximation $\Delta\rho/\rho \approx -\beta\Delta T$, where ΔT is often taken as $T_w - T_{s,\infty}$)
g	Acceleration due to gravity, $\mathrm{m\,s^{-2}}$
h	Specific enthalpy, $\mathrm{J\,kg^{-1}}$, Heat Transfer Coefficient (HTC), $\mathrm{W\,m^{-2}\,K^{-1}}$ or height, m
I	Radiative intensity, $\mathrm{W\,m^{-2}\,sr^{-1}}$ or $\mathrm{W\,m^{-2}\,sr^{-1}\,\mu m^{-1}}$ for a spectral density, where sr (steradian) is solid angle
J	Radiosity, $\mathrm{W\,m^{-2}}$
k	Thermal conductivity, $\mathrm{W\,m^{-1}\,K^{-1}}$
L	Length or wall thickness, m
M	Molar mass of a species, $\mathrm{kg\,kmol^{-1}}$
Ma	Mach number ($Ma = U/a$, where a is the speed of sound)
n	Refractive index
Nu	Nusselt Number ($Nu = hL/k_f$)
p	Perimeter, m
P	Pressure (P_s = static pressure, P_T = total pressure), $\mathrm{N\,m^{-2}}$ or Pa
Pe	Péclet number ($Pe = RePr$)
Pr	Prandtl number ($Pr = c_p\mu/k_f$)
q	Heat flux (rate of heat transfer per unit area, $q = Q/A$), $\mathrm{W\,m^{-2}}$
Q	Rate of heat transfer, W
r	Radius, m
R	Gas constant (for a particular gas, $R = \tilde{R}/M$), $\mathrm{J\,kg^{-1}\,K^{-1}}$
$\tilde{R}$	Universal gas constant, $8314.5\,\mathrm{J\,kmol^{-1}\,K^{-1}}$
R_{th}	Thermal resistance, $\mathrm{K\,W^{-1}}$
Ra	Rayleigh number ($Ra = GrPr$)
Re	Reynolds number ($Re = \rho UL/\mu$, or for an internal flow $Re = WD_h/A_{cs}\mu$)
Ri	Richardson number ($Ri = Gr/Re^2$)
Sr	Strouhal number ($Sr = fL/U$, where f is frequency)

St	Stanton number ($St = Nu/RePr$)
t	Time, s
T	Temperature (T_s = static temperature, T_T = total temperature), K
u_τ	Wall friction velocity ($u_\tau = \sqrt{\overline{\tau_w}/\rho}$), $\mathrm{m\,s^{-1}}$
U	Velocity, $\mathrm{m\,s^{-1}}$ or thermal transmittance, $\mathrm{W\,m^{-2}\,K^{-1}}$
v	Specific volume, $\mathrm{m^3\,kg^{-1}}$
V	Volume, $\mathrm{m^3}$
W	Mass flow rate, $\mathrm{kg\,s^{-1}}$
y	Wall distance, m
y^+	Non-dimensional wall distance ($y^+ = y u_\tau/\nu$)

Greek Symbols

α	Thermal diffusivity ($\alpha = k/\rho c_p$), $\mathrm{m^2\,s^{-1}}$
β	Volumetric thermal expansion coefficient ($\beta = -(1/\rho)(\partial\rho/\partial T)$), $\mathrm{K^{-1}}$
γ	Ratio of specific heats ($\gamma = c_p/c_v$)
ϵ	Emissivity or surface roughness height, m
κ	Absorption coefficient, $\mathrm{m^{-1}}$
λ	Wavelength, m
μ	Viscosity, $\mathrm{kg\,m^{-1}\,s^{-1}}$
ν	Kinematic viscosity and momentum diffusivity ($\nu = \mu/\rho$), $\mathrm{m^2\,s^{-1}}$
ρ	Density, $\mathrm{kg\,m^{-3}}$
σ	Stefan Boltzmann constant, $5.67 \times 10^{-8}\,\mathrm{W\,m^{-2}\,K^{-4}}$
τ	Shear stress, $\mathrm{N\,m^{-2}}$
ϕ	Porosity or void fraction

Subscripts and Modifications

b	Bulk (mass-averaged) quantity
cs	Cross-sectional quantity
f	Quantity relating to a fluid
i	Quantity relating to a particular species
T	Total (stagnation) quantity
t	Turbulent quantity
s	Static quantity or quantity relating to a solid
w	Quantity relating to a wall or surface
∞	Quantity far from a wall or in free-stream
$\overline{\square}$	Average quantity
$\tilde{\square}$	Molar quantity
$\square'$	Varying quantity

7 Abbreviations

AGR	Advanced Gas-cooled Reactor
AHFM	Algebraic Heat Flux Model
ALFRED	Advanced Lead Fast Reactor European Demonstrator
AMR	Advanced Modular Reactor
ANL	Argonne National Laboratory
ARDP	Advanced Reactor Demonstration Program
ARIS	Advanced Reactor Information System
ASTRID	Advanced Sodium Technological Reactor for Industrial Demonstration
BDBA	Beyond Design Basis Accident
CEA	Commissariat à l'énergie atomique et aux énergies alternatives
CFD	Computational Fluid Dynamics
CHT	Conjugate Heat Transfer
CIRCE	CIRCulation Eutectic
DNS	Direct Numerical Simulation
E-SCAPE	European SCAled Pool Experiment
EBR	Experimental Breeder Reactor
EFR	European Fast Reactor
EVM	Eddy Viscosity Model
FFTF	Fast Flux Test Facility
FIV	Flow Induced Vibration
GGDH	Generalized Gradient Diffusion Hypothesis
GIF	Generation IV International Forum
GRS	Gesellschaft für Anlagen- und Reaktorsicherheit
HPC	High Performance Computing
HTC	Heat Transfer Coefficient
IAEA	International Atomic Energy Agency
INL	Idaho National Laboratory
JAEA	Japan Atomic Energy Agency
KAERI	Korea Atomic Energy Research Institute
KALLA	KArlsruhe Liquid Metal LAboratory
KASOLA	KArlsruhe SOdium LAboratory
KIT	Karlsruhe Institute of Technology
KTH	Royal Institute of Technology
LANL	Los Alamos National Laboratory
LBE	Lead-Bismuth Eutectic
LES	Large Eddy Simulation
LFR	Lead-cooled Fast Reactor
LMFR	Liquid Metal-cooled Fast Reactor
LWR	Light Water Reactor
MYRRHA	Multipurpose hYbrid Research Reactor for High-tech Applications

Abbreviations

NACIE-UP	NAtural CIrculation Experiment UPgrade
NPP	Nuclear Power Plant
NRG	Nuclear Research and Consultancy Group
PFBR	Prototype Fast Breeder Reactor
PFR	Prototype Fast Reactor
PIRT	Phenomena Identification and Ranking Table
PSI	Paul Scherrer Institute
RANS	Reynolds-Averaged Navier-Stokes
RMS	Root Mean Square
RNG	Re-Normalisation Group
RSM	Reynolds Stress Model
RVACS	Reactor Vessel Auxiliary Cooling System
SCK CEN	Studiecentrum voor Kernenergie Centre d'Étude de l'énergie Nucláire
SEALER	Swedish Advanced Lead Reactor
SESAME	Simulations and Experiments for the Safety Assessment of MEtal cooled reactors
SFR	Sodium-cooled Fast Reactor
SGDH	Simple Gradient Diffusion Hypothesis
SGS	Sub-Grid-Scale
TALL-3D	Thermal-hydraulic ADS Lead-bismuth Loop with 3D flow test section
THINS	Thermal Hydraulics of Innovative Nuclear Systems
UDF	User Defined Function
URANS	Unsteady Reynolds-Averaged Navier-Stokes
WMLES	Wall Modeled Large Eddy Simulation


Volume 5